A MODEL TO PREDICT THE EFFECT OF THE RADIATOR CORE AND AMBIENT CONDITIONS ON THE PERFORMANCE OF THE COOLING SYSTEM OF A RALLY CAR

by

Franciscus Xavierus Laubscher

Dissertation presented in partial fulfilment
of the requirements for the degree of

MASTER OF ENGINEERING

In the faculty of Engineering
University of Pretoria
Pretoria

April 2005

A MODEL TO PREDICT THE EFFECT OF THE RADIATOR CORE AND AMBIENT CONDITIONS ON THE PERFORMANCE OF THE COOLING SYSTEM OF A RALLY CAR

by

Franciscus Xavierus Laubscher

Promoter:	Prof. J.A. Visser
Department:	Mechanical and Aeronautical Engineering
Degree:	Master of Engineering

SUMMARY

The cooling systems of production vehicles are usually over designed to operate over a wide range of road and ambient conditions. This over design is usually achieved by higher water- and airflow rates through the heat exchanger than required under normal ambient conditions. Unfortunately these flow rates demand power directly or indirectly from the engine and thereby reduce the available drive train power. In some applications such as rally cars, it is possible to modify the configuration of the vehicle for specific ambient conditions on the day of the race. Such changes have to be made within the rules for the competition and in this case changes between races are limited to the heat exchanger and water pump. With knowledge of the conditions predicted for the day of the race, it should be possible for a team to select a heat exchanger that will dissipate the required heat as well as minimise the power used by the cooling system.

The purpose of this study is to develop a methodology that can be used to predict the performance of the cooling system of a rally car based on the characteristics of the heat

exchanger and the coupled effect of the heat exchanger on the cooling system. For this purpose, two commercially available heat exchangers were characterised over a range of ambient conditions in a controlled environment. Using the modified Wilson plot method, an iterative process was followed by manipulating recorded data to obtain the thermal resistance for both the water and air for each heat exchanger.

Information concerning the heat generated by the engine and the influence that the vehicle has on the flow rates of fluids through the exchanger were supplied by the rally team and incorporated into a simulation model to predict the performance of the cooling system as a function of the heat exchanger core, engine speed and vehicle speed. The final model takes into account the effect of ambient conditions on the heat generated by the engine and the characteristics of the cooling system by identifying all the ambient dependent variables in the model and expressing them as a function of individual ambient components.

The model derived and populated with actual data is able to:

- Identify the suitability of a specific heat exchanger core for prevailing conditions,
- Establish whether a reduction in water flow rate for a certain heat exchanger core is feasible.

The mathematical model discussed in this study is successful in serving as a tool to a rally team for prediction of the most appropriate heat exchanger core to be used under specific ambient conditions.

Keywords:

Automotive heat exchanger
Vehicle cooling system
Cooling performance prediction
Wilson plot method
Heat generation
Ambient conditions
Radiator
Windtunnel experiments
Heat dissipation
Fluid flow rates

ACKNOWLEDGEMENTS

I would like to acknowledge the following for their contributions during the course of this study:

- God, for giving me the opportunity to study and complete what I have started, without whom the study would not have been a success.

- My wife, Ethel Laubscher, who has been my pillar of support during the course of this study. Words cannot describe her contribution with emotional support.

- My parents, F.X. and Suekie Laubscher, who have been by my side since the first day, understanding and supporting me until the end.

- My father and mother in law, who always bring things into perspective. Thanks for your contribution and for proof reading the final document.

- Kobie Botha, who played an immense role in encouraging me to persevere and complete this study.

- Toyota Motorsport South Africa for making a vehicle available for the study.

- Last but not least, Prof. J.A. Visser for assisting and giving the good advice that was required to make the study a success.

INDEX

CHAPTER 1
INTRODUCTION, LITERATURE AND SCOPE

1.1 The problem considered

The cooling systems of modern passenger cars can operate under almost any reasonable ambient condition. The heat exchanger for a vehicle will be designed according to the heat to be dissipated, core characteristics, layout in the automobile and assumed operating conditions. After the initial design phase, the cooling system is tested in the specific car under severe environmental conditions in order to determine the suitability of the system. Although the individual components of the cooling system are optimised, the range of operating conditions that the vehicle will be subjected to, requires an over designed cooling system to ensure that the engine will be sufficiently cooled under any reasonable ambient condition.

In contrast to normal passenger vehicles, the cooling system of a rally car has a significant impact on the competitive performance of the vehicle. The weight and position of the heat exchanger filled with water will affect the handling of the car, while the power used by the cooling system will have a direct impact on the power delivered to the wheels. Knowledge about the prevailing ambient conditions on the day creates the opportunity to optimise the cooling system for a particular race. Such an optimisation process will require the ability to simulate the effect that different components and ambient conditions have on the performance of the cooling system.

Predicting the most appropriate cooling system for specific ambient conditions is not an easy task. Such a model will have to include the effect to changes in the ambient conditions on all the components of the cooling system. Of these, the two most important contributing factors are the dissipation of heat and the heat generated by the engine.

It is important to note that the objective of this study is not to design a heat exchanger for each application, but rather have the ability to simulate the effect of a particular heat exchanger on the overall performance of the cooling system. The primary objective is thus to be able to *select a heat exchanger based on prevailing conditions*, while the secondary objective is to *identify* whether *opportunities* exist *to reduce the power consumed* to drive the water pump in the cooling system.

1.2 Literature

The evaluation of an energy balance for the prediction of the cooling system performance consists of a number of sub-problems. The sub-problems and their components to be considered are:

- The heat transfer performance of the heat exchanger core that includes:
  - The selection of an appropriate heat exchanger for the application,
  - A methodology to characterise a heat exchanger core.
- The influence that the vehicle has on the cooling system which includes:
  - The relationship between fluid flow rates and vehicle characteristics,
  - The heat generated by the engine,
  - The operating conditions that will serve as input to the heat generation problem.

Literature that addresses the sub-problems and their components are discussed in this section.

1.2.1 Characterising the performance of a heat exchanger

Prior to developing a methodology to characterise the heat exchanger for this simulation model, it is important to select the best possible standard heat exchanger fin geometry. A few basic parameters that influence the performance of the different core geometries will be discussed briefly to explain the selection of the core used during this project. Aiding in

the selection process is the extensive research that was done in the last century in an effort to optimise the core performance of compact heat exchangers. This has resulted in various core designs being available, each with advantages and disadvantages.

Automotive heat exchangers fall in the category of compact heat exchangers due to the restricted space in the vehicle available to the heat exchanger. From the literature it can be concluded that an effective automotive heat exchanger will have a high heat transfer rate per surface area exposed to the air stream, a high heat transfer rate per frontal area and a high heat transfer rate per unit volume of the heat exchanger [1-5]. Various heat exchanger designs have been documented in literature that meet these objectives to a greater or lesser extent. Differences between the designs that are included in this category are mostly marked by variations in the airflow channel, water flow channel and fin designs. Although different variations are reported to have benefits at certain flow rates and applications, most variations were introduced to obtain a single goal - to reduce the formation of boundary layers on the heat transfer surface exposed to the air stream.

With the growth of a boundary layer on a surface, the convection heat transfer coefficient reduces in the flow direction of the passing fluid when the fluid has a laminar flow profile. The coefficient remains fairly constant and generally has a higher value in a turbulent flow profile [6]. Increasing heat transfer coefficients and the advantage gained when increasing the heat transfer area are constantly being investigated in order to obtain higher heat transfer rates. Two common heat exchanger geometries were identified in published literature due to their high heat transfer rates per frontal area, surface area and volume:

- Offset strip fin geometry [7]
- Louver fin geometry [8]

The *offset strip fin* geometry consists of a number of fins spaced in such a manner that the forming boundary layer is disturbed. Webb [7] describes the offset strip fin method as a surface enhancement technique that dissipates the boundary layer in the wake region

behind the strip. The efficiency with which this can be done is dependent on the length and thickness of the strip, the fin pitch (as shown in figure 1.1) as well as the Reynolds number of the flow over the surface.

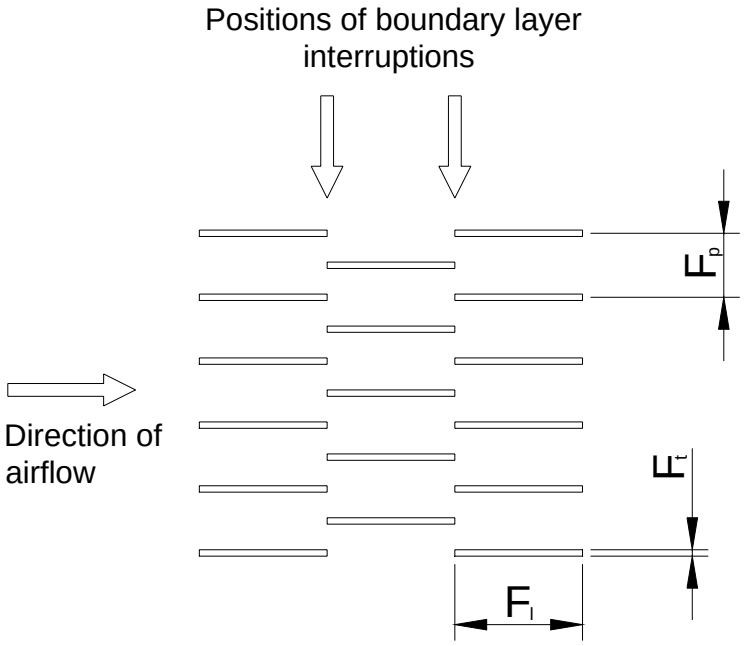

Figure 1.1 - Schematic of offset strip fin geometry

During manufacturing of the *louver fin* geometry, the louvers are punched into the fin material causing a flow disturbance in the flow channel as shown in figure 1.2. In this case the flow is disturbed by the angled geometry as well as the air stream entering the channel from the neighbouring channel. Similar to the offset strip fin, this enhancement technique is also Reynolds number dependent for a specific fin and louver pitch.

Greater care has to be taken with the manufacture and assembling of the offset strip fin, as the fins must have an offset relative to each other within a certain tolerance. On the other hand, the louvers on the louver fins are punched into the fin material using high speed manufacturing processes and a larger tolerance on the end product is permissible resulting in a less expensive heat exchanger surface, hence it's popularity in the

commercial market [8]. Further to this advantage, it is found in literature that the louver fin geometry has superior heat transfer properties compared to the offset strip fin [9–10].

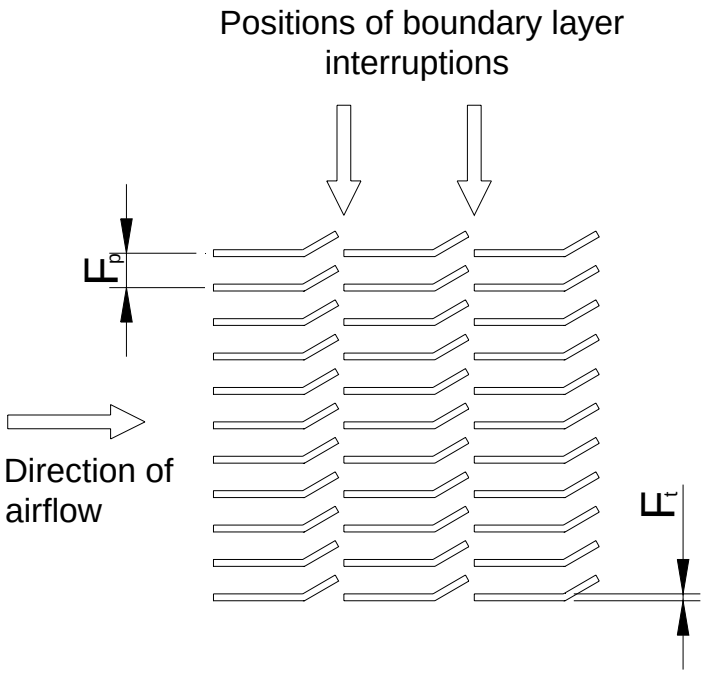

Figure 1.2 - Schematic of louver fin geometry

Both the mentioned heat exchanger fin geometries affect the pressure drop over a heat exchanger which is an important parameter that needs to be considered [11]. An increase in pressure drop reduces the flow rate that in turn reduces the heat transfer coefficient. The trade-off between increasing the heat transfer and the resulting increase in pressure drop is therefore an important parameter that needs to be balanced at all times [12]. As the forming boundary layer which has a huge impact on the heat transfer rate is Reynolds number dependent, it can be expected that a perfect balance will only be obtained for a specific core at a certain flow rate.

The water tube design in a heat exchanger is a contributing factor to the pressure drop characteristics over the air side of a heat exchanger. Chang, Wang, Shyu and Hu [13] investigated louver fin heat exchanger cores with flat and round tubes. Comparing these exchangers using augmentation techniques such as the volume goodness factor and the

area goodness factor, it was found that the flat tube geometry offered significant advantages when compared to the round tube heat exchanger configuration.

Webb and Jung [14] as well as Zang [15] ascribed the advantages to:

- the airflow being normal to the louvers,
- a reduction in wake area behind the tube which has a positive effect on the heat transfer on downstream fins, and
- a lower form drag associated with the design.

Based on the advantages found in the literature with regards to the performance and manufacturing cost of the louver fin compared to the offset strip fin geometry, the louver fin heat exchanger was selected as the surface geometry to be used for the rally car.

Having identified the heat exchanger that will be used in this application, a *method* is required *to characterise the performance of a specific heat exchanger*. The various characterisation methods found in the literature where the heat exchanger performance is isolated from external factors through testing of the exchanger in a controlled environment can globally be divided into two methods [16]:

- Transient heat exchanger test techniques
- Steady state heat exchanger test techniques

Transient test techniques rely on the response of one of the fluids in the exchanger when a controlled change of temperature is imposed on the other fluid. Through real time monitoring of the temperatures of both fluids, the transient temperature reaction of the heat exchanger is recorded. The characterisation of the heat exchanger is performed through the evaluation of the temperature gradients of the fluids as functions of time. Manipulating the data using documented equations [16], an overall heat transfer coefficient is obtained, characterising the heat exchanger at the specific flow rate at which the experiment was conducted.

Steady state test techniques on the other hand, rely on constant temperatures and fluid flow rates being maintained during the evaluation process. By recording the thermal energy change of the fluids, the heat transfer rate can be calculated. Although this is the oldest technique used to characterise heat exchangers, it is still the most commonly used method. The steady state test technique is particularly successful when a high heat capacity flow rate can be established on one side of the heat exchanger. The heat transfer rate on the other side of the heat exchanger should either be known, or the thermal resistance should be extremely small compared to the tested side. In the case of a water to air heat exchanger, the air side of the heat exchanger is usually the unknown side as the heat capacity flow rate for the air is usually much lower compared to the water side [16]. To characterise the automotive heat exchanger using this method, a specialised test facility is required that can supply warm water at a constant temperature and flow rate, and the airflow through the heat exchanger can be established in a wind tunnel. After steady state conditions are met, the fluid flow rates are recorded, as well as the parameters that determine the mass flow rate of the fluids. The typical experimental set-up required for such tests is shown in figure 1.3.

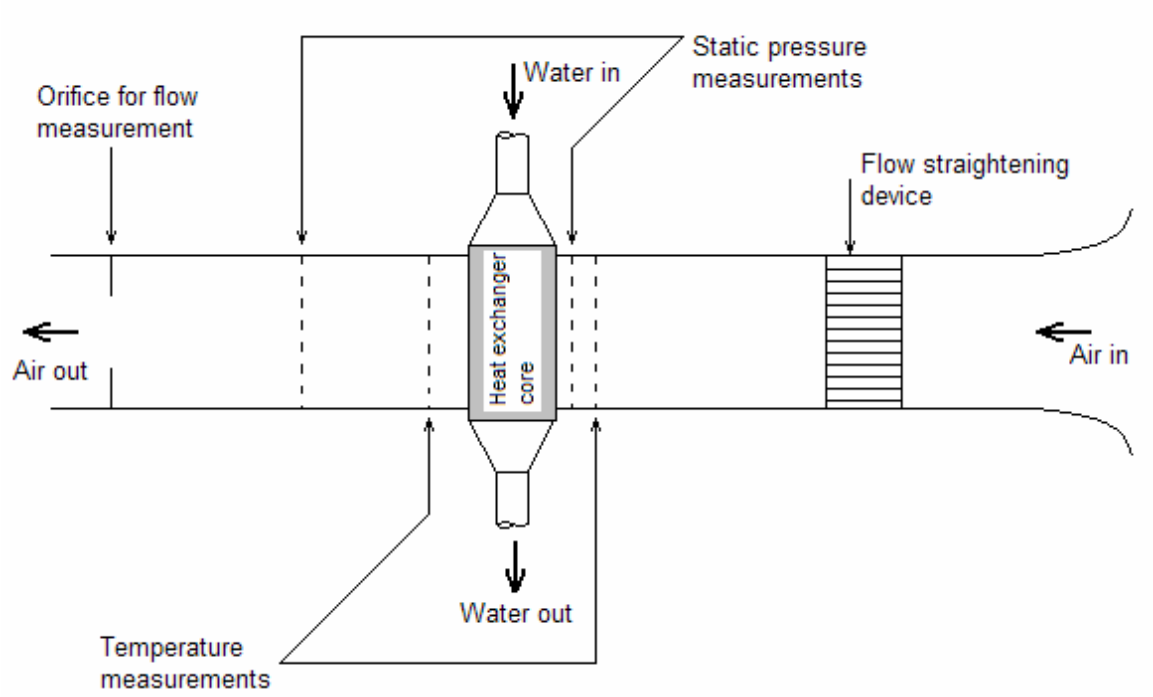

Figure 1.3 - Simplified heat exchanger test facility [16]

Using the data obtained in the experimental tests, a number of variables are defined to assist in characterising the heat transfer at specific fluid flow rates. The first being the effectiveness (ε) of the heat exchanger, indicating the performance of the heat exchanger at the specific fluid flow rates through the use of equation 1.1.

$$\varepsilon = \frac{\dot{Q}_{dissp}}{\dot{Q}_{\max}} \tag{1.1}$$

The maximum heat transfer rate is defined as the product of the minimum flow stream heat capacity rate as shown in equation 1.2 and the inlet temperature difference of the fluids. Classic water to air heat exchangers have shown that the minimum flow stream heat capacity rate is normally found on the air side of the exchanger, largely due to the lower mass flow rate of air available through the heat exchanger of a vehicle.

$$\dot{Q}_{\max} = C_{\min}\left(T_{w,in} - T_{a,in}\right) \tag{1.2}$$

Furthermore, a heat capacity ratio is defined as the ratio of the flow stream heat capacity rates as shown in equation 1.3.

$$R_c = \frac{C_{\min}}{C_{\max}} \tag{1.3}$$

Finally a fourth variable is defined as the Number of Transfer Units (*NTU*) shown in equation 1.4. Effectively, the *NTU* defines the overall heat transfer rate per degree Kelvin for the heat exchanger as a function of the mass flow rate and specific heat of the fluid having the lowest flow stream heat capacity.

$$NTU = \frac{UA}{C_{\min}} \tag{1.4}$$

Relationships between ε and the *NTU* exist in published literature, and selection of the most appropriate relationship has a direct impact on the accuracy with which the characterisation can be performed [17-18]. Having calculated the effectiveness (ε) from the recorded data in the experiments using equation 1.1, it now becomes possible to determine the value of *NTU* using these documented relationships.

Selection of the most suitable ε-*NTU* relationship for the heat exchanger configuration under evaluation is sometimes confusing. Documented relationships for the cross-flow heat exchanger configuration differ with regard to the air side of the exchanger being mixed or unmixed as it passes through the heat exchanger. Mixing of the air stream can best be explained through the visualisation of the flow through the perforated air ducts of a louver fin geometry. Shanoun and Webb [19] used the visualisation performed by Kajino and Hiramatso [20] to explain this effect as shown in figure 1.4.

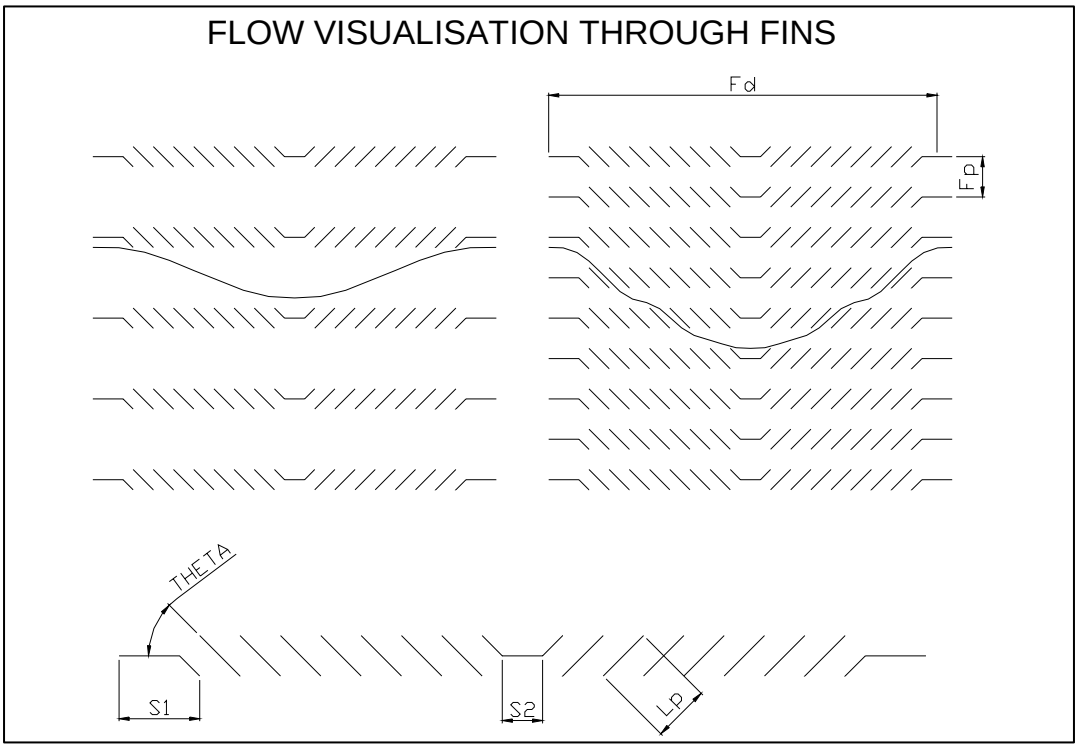

Figure 1.4 - Flow visualisation through fins

The fin pitch (F_p) is found to be the governing variable in determining if the flow will be duct-directed or louver-directed. A large fin pitch will promote duct-directed flow patterns as illustrated on the left hand side of figure 1.4, letting most of the air stream bypass the louvers. Louver-directed flow on the other hand, results from a smaller fin pitch as shown on the right hand side, forcing air through the louvers and promoting turbulent airflow patterns. This flow pattern enhances the surface by causing high airflow disturbances in the channel, limiting the formation of boundary layers on the fin surface [15][21-22]. Although louver-directed flow has a positive influence on the overall heat transfer coefficient of a heat exchanger, it is associated with a higher pressure drop over the heat exchanger.

The dependence of the flow path and mixing of the air stream causes uncertainties in the *ε-NTU* relationship that should be used to describe the heat exchanger. Wang, Webb and Chi [23], recommend the use of duct-directed flow, i.e. unmixed airflow of the heat exchanger, for use in calculations pertaining to cross-flow louver fin heat exchangers used in the automotive industry. The standard definition of the *ε-NTU* equation for unmixed flow is given by Kays and London [18] as:

$$\dot{Q}_{dissp} = \dot{m}_a c_{pa}(T_{w,in} - T_{a,in})\left(1 - \exp\left(\frac{(UA)^{0.22}\,\dot{m}_w c_{pw}}{\left(\dot{m}_a c_{pa}\right)^{1.22}}\left(\exp\left(-\frac{\left(\dot{m}_a c_{pa}\right)^{0.22}(UA)^{0.78}}{\dot{m}_w c_{pw}}\right)-1\right)\right)\right) \tag{1.5}$$

Further investigation into the *ε-NTU* relationship has shown that the relationship is also dependent on the number of water tube rows in a heat exchanger core. Equation (1.5) gives the relationship for heat exchangers with an infinite number of water tube rows, and is recommended for use when more than four water tube rows are found in the depth of the heat exchanger [23]. In cases of four rows and less, equations documented by the Engineering Science Data Unit (ESDU) [24] should be used for more accurate results.

Table 1.1 shows the equations applicable to the selected heat exchangers where C_{min} is found on the air side of the exchanger.

Table 1.1 – ESDU recommended ε-NTU equations [24]

No. tube rows	*ε-NTU* definition [24]	
1	$\varepsilon = \frac{1}{R_c}\left(1-\exp\left(-R_c\left(1-\exp\left(-NTU\right)\right)\right)\right)$	(1.6)
2	$\varepsilon = \frac{1}{R_c}\left[1-\left(\exp\left(-2KR_c\right)\right)\left(1+R_cK^2\right)\right]$ where, $K = 1-\exp\left(\frac{-NTU}{2}\right)$	(1.7)
3	$\varepsilon = \frac{1}{R_c}\left[1-\left(\exp\left(-3KR_c\right)\right)\left(1+R_cK^2\left(3-K\right)+\frac{3R_c^2K^4}{2}\right)\right]$ where, $K = 1-\exp\left(\frac{-NTU}{3}\right)$	(1.8)
4	$\varepsilon = \frac{1}{R_c}\left[1-\left(\exp\left(-4KR_c\right)\right)\left(1+R_cK^2\left(6-4K+K^2\right)+4R_c^2K^4\left(2-K\right)+\frac{8R_c^3K^6}{3}\right)\right]$ where, $K = 1-\exp\left(\frac{-NTU}{4}\right)$	(1.9)

Identifying and using the correct equation to describe the *ε-NTU* relationship is imperative. Blindly using equation 1.5 for any heat exchanger will lead to huge inaccuracies. In order to illustrate the error that can be made through deployment of the

incorrect relationship, figure 1.5 was generated, showing the different dependence of effectiveness (ε) on the *NTU* for the various equations [23] [25].

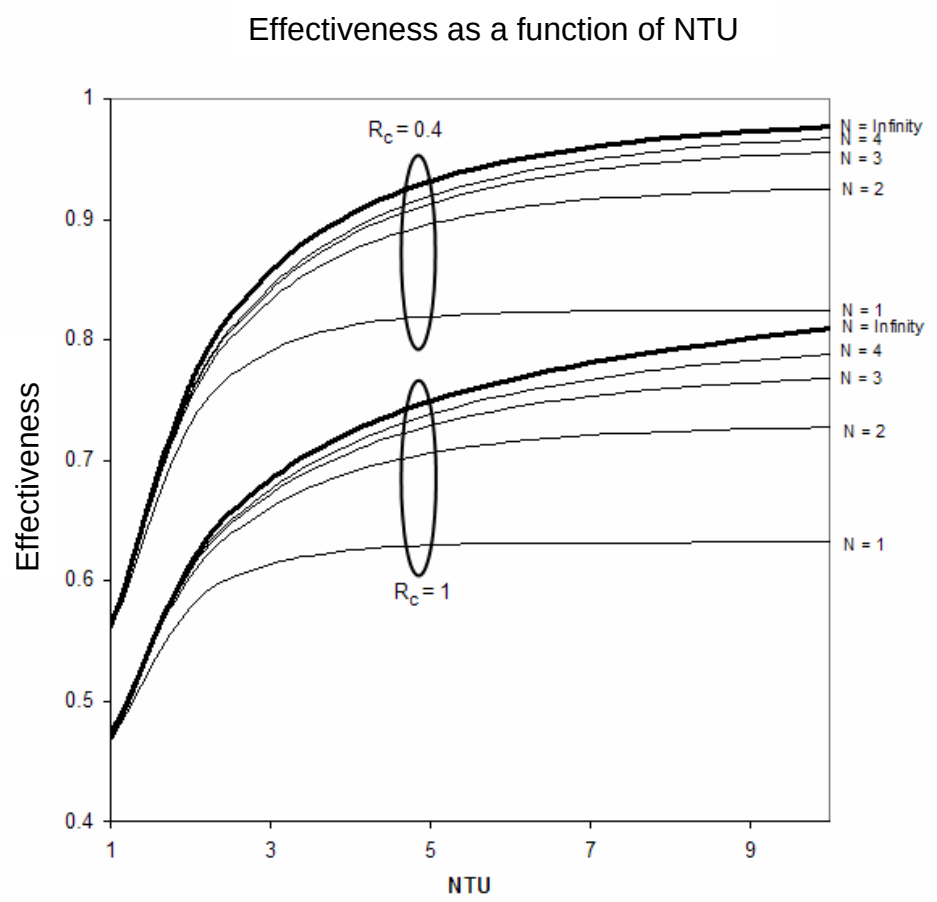

Figure 1.5 - Effectiveness as a function of NTU [23][25]

The value of *UA* can now be determined by selecting the appropriate ε-*NTU* equation for the given heat exchanger. It should be noted that a single value of *UA* will not suffice as part of the characterisation of an automotive heat exchanger, as *UA* will vary with changes in the fluid flow rates. The dependence of *UA* on fluid flow rates should be investigated in order to obtain a characteristic equation for the heat exchanger, making it possible to predict the heat transfer at various fluid flow rates.

The basic equation, from which the dependency of *UA* on fluid flow rates can be deduced, is based on the thermal resistance equation for a heat exchanger. Shah [26] gives this equation as shown in equation 1.10

$$\frac{1}{UA} = \frac{1}{(\eta_{oa} h_a A_a)} + R_{fa} + R_w + R_{fw} + \frac{1}{(\eta_{ow} h_w A_w)} \tag{1.10}$$

The second and fourth terms on the right hand side of the equation represent the thermal resistance due to fouling on the transfer surfaces. Fouling on both surfaces is associated with a reduction in the total heat transfer rate of the heat exchanger, decreasing the efficiency of the heat exchanger over time. It is found to be common practice to ignore the fouling factors when new heat exchangers are tested [16][18][23][26].

Further development of equation 1.10 stems from the Nussult number for fully developed turbulent flow through a constant cross section duct shown in equation 1.11 [27].

$$Nu = C_1 \, \mathrm{Re}^a \, \mathrm{Pr}^{0.4} \left(\frac{\mu_w}{\mu_m} \right)^{-0.14} \tag{1.11}$$

C_1 is a constant dependent on the duct, while a is approximated in this instance. The Dittus-Boelter equation gives a the value of 0.8, while Wilson [28] approximated a to a value of 0.82 in the process of deriving the original Wilson Plot method. Noticeably, the viscosity relationship is added to ensure that the variation in the properties between the fluids attached to the walls and the bulk fluid is taken into account when determining the true Nussult number.

Using an approximation of a and substituting the definition of Nu, Re and Pr into equation 1.11, the convection heat transfer coefficient for fully developed turbulent flow is derived as a function of the fluid velocity. Multiplying this relationship on both the left and right side with the heat transfer area, and assuming that the variation in the fluid properties will have a negligible effect on the heat transfer coefficient, the heat transfer coefficient multiplied by the heat transfer area reduces to the following:

$$\frac{1}{h_a A_a \eta_{oa}} = \frac{1}{\left(C_1 k_a^{0.6} \rho_a^{0.82} c_{p_a}^{0.4} \mu_a^{-0.42} D_{ha}^{-0.18}\right) V_a^{0.82} A_a \eta_{oa}} = \frac{1}{C_2 V_a^{0.82}} \tag{1.12}$$

where

$$C_2 = \left(C_1 k_a^{0.6} \rho_a^{0.82} c_{p_a}^{0.4} \mu_a^{-0.42} D_{ha}^{-0.18}\right) A_a \eta_{oa}$$

Further reduction in the number of variables in equation 1.10 can be made possible by carefully designing the experimental test procedure. Using data for which the thermal resistance on the water side of the heat exchanger remains constant, the third and fifth terms on the right of equation 1.10 are reduced to a constant value. The overall thermal resistance can thus be expressed as a first order polynomial function as presented in equation 1.13.

$$\frac{1}{UA} = \frac{1}{C_2 V_a^{0.82}} + C_3 \tag{1.13}$$

The values for C_2 and C_3 can now be determined by plotting a line through the physical data obtained from the steady state experiment. The intercept of the line plotted with the y-axis represents the value of C_3, while the slope of the line results in the inverse value of C_2. Figure 1.6 shows the method of approximation.

The original Wilson-plot method serves as a good first order test technique and basis for comparisons, but is unfortunately flawed with the assumption that the constant *a* is known prior to the test. Shah and Johnson [29] documented that *a* is actually a function of the Prandtl and Reynolds numbers as well as the geometry of the duct through which the fluid passes and will differ from one heat exchanger core configuration to the next. A further flaw in the original Wilson-plot technique stems from the assumption that the thermal resistance for one side of the heat exchanger is known. In most cases the thermal resistance on one side of a heat exchanger will however not be known when automotive

heat exchangers are tested. In these cases and cases where the airflow does not show a dominant heat transfer resistance, the *modified Wilson plot technique* is deployed to determine the heat transfer characteristics. This is usually found in cases where high airflow rates are maintained through the heat exchanger or when performance enhancement techniques such as fins and louvers are included in the heat exchanger geometry [28].

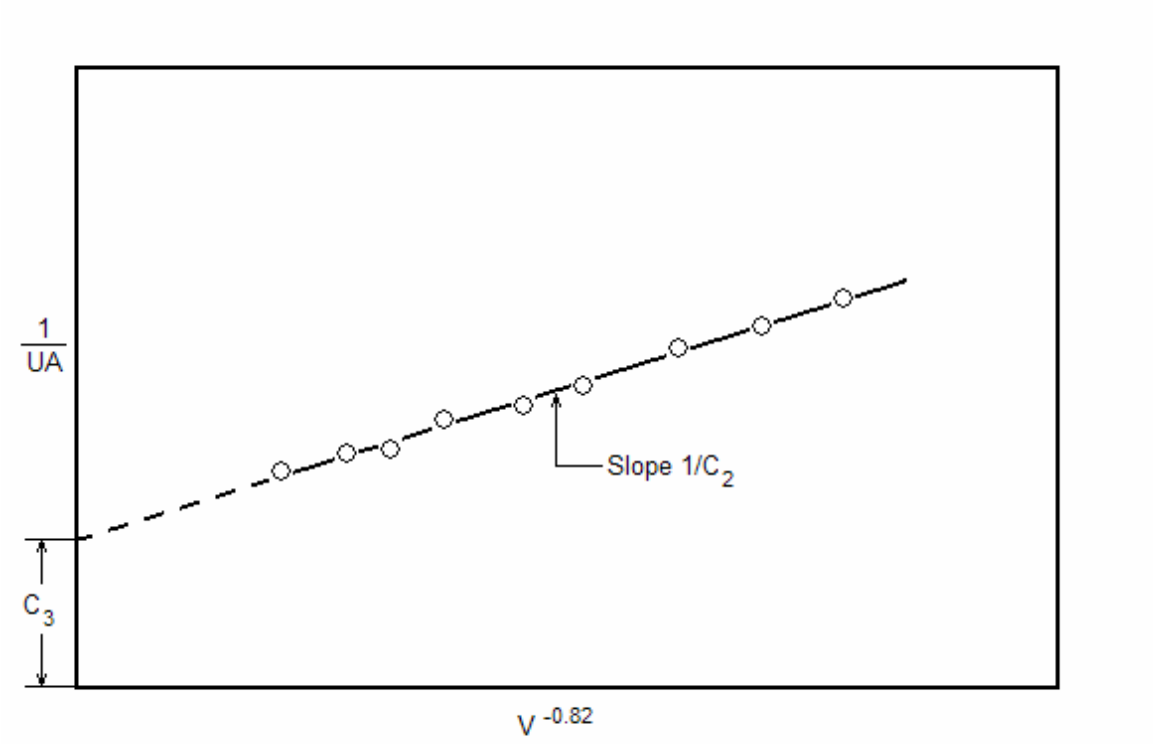

Figure 1.6 - Visualisation of original Wilson plot method

Having identified the shortcomings of the original Wilson plot technique, Shah [26] documented a method through which exponents and the constants in the Dittus-Boetler equation can be calculated for both the water and air sides of the heat exchanger. Neglecting the fouling resistances for the air and water side heat exchange surfaces, the new relationship is expressed in equation 1.14.

$$\frac{1}{UA} = \frac{1}{\left(C_4 \left(\frac{\mathrm{Re}_w^a \, \mathrm{Pr}_w^{0.4} \, A_w k_w}{D_{hw}} \right) \left(\frac{\mu_{ww}}{\mu_{mw}} \right)^{-0.14} \right)} + R_w + \frac{1}{\left(C_5 \left(\frac{\mathrm{Re}_a^d \, \mathrm{Pr}_a^{0.4} \, A_a k_a}{D_{ha}} \right) \left(\frac{\mu_{wa}}{\mu_{ma}} \right)^{-0.14} \right)} \tag{1.14}$$

Assuming that the thermal resistance R_w is negligible as commonly found on thin tube wall aluminium heat exchangers, 4 unknowns can be identified in equation 1.15:

a, d, C_4 and C_5.

$$\frac{1}{UA} = \frac{1}{\left(C_4 \left(\frac{\mathrm{Re}_w^a \, \mathrm{Pr}_w^{0.4} \, A_w k_w}{D_{hw}} \right) \left(\frac{\mu_{ww}}{\mu_{mw}} \right)^{-0.14} \right)} + \frac{1}{\left(C_5 \left(\frac{\mathrm{Re}_a^d \, \mathrm{Pr}_a^{0.4} \, A_a k_a}{D_{ha}} \right) \left(\frac{\mu_{wa}}{\mu_{ma}} \right)^{-0.14} \right)} \tag{1.15}$$

Through the careful design of an experimental procedure, it now becomes possible to isolate either the first or second term in equation 1.15 during the data manipulation stage of the characterisation. By ensuring that the airflow rate is kept at a constant predetermined value, it is possible to calculate the values of the constant C_4 and a. The first step in this calculation is done by rewriting equation 1.15 as shown in equation 1.16.

$$\left[\frac{1}{UA} - R_w \right] \left[\frac{\mu_{wa}}{\mu_{ma}} \right]^{-0.14} = \frac{1}{C_4} \left[\frac{\left(\frac{\mu_{wa}}{\mu_{ma}} \right)^{-0.14} \Big/ \left(\frac{\mu_{ww}}{\mu_{mw}} \right)^{-0.14}}{\left[\frac{\mathrm{Re}_w^a \, \mathrm{Pr}_w^{0.4} \, A_w k_w}{D_{hw}} \right]} \right] + C_a \tag{1.16}$$

where

$$C_a = \frac{1}{C_5 \left[\frac{\mathrm{Re}_a^d \, \mathrm{Pr}_a^{0.4} \, A_a k_a}{D_{ha}} \right]}$$

Equation 1.16 now has the form of a first order polynomial when the value of a is guessed. Plotting the results obtained through equation 1.16, as shown in figure 1.7, the value for the constant C_4 is determined for the associated constant a.

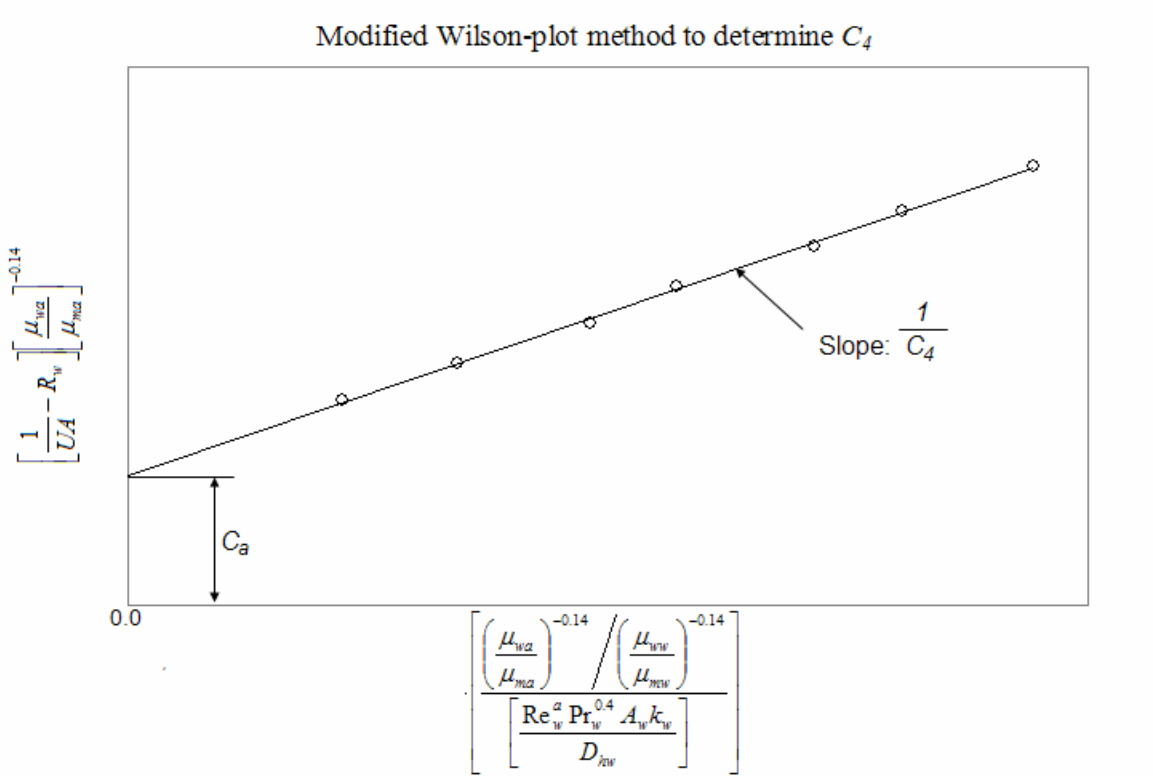

Figure 1.7 - Modified Wilson plot method to determine C_4 for a guessed value of a

Validation of the value for a needs to be obtained, as it was guessed in the previous calculation. This is done by rewriting equation 1.15 as follows:

$$\left[\frac{1}{UA} - R_w - \frac{C_a}{\left(\frac{\mu_{wa}}{\mu_{ma}}\right)^{-0.14}}\right]\left[\frac{\mathrm{Pr}_w^{0.4} A_w k_w}{D_{hw}}\right]\left(\frac{\mu_{ww}}{\mu_{mw}}\right)^{-0.14} = \frac{1}{C_4 \mathrm{Re}_w^a} \qquad (1.17)$$

An equation for a straight line is achieved by substituting y_w with the left-hand term in equation 1.17, and taking logarithms for the equation as per equation 1.18.

$$\ln\left(\frac{1}{y_w}\right) = a\ln(\mathrm{Re}_w) + \ln(C_4) \tag{1.18}$$

where

$$y_w = \left[\frac{1}{UA} - R_w - \frac{C_a}{\left(\frac{\mu_{wa}}{\mu_{ma}}\right)^{-0.14}}\right]\left[\frac{\mathrm{Pr}_w^{0.4} A_w k_w}{D_{hw}}\right]\left(\frac{\mu_{ww}}{\mu_{mw}}\right)^{-0.14}$$

Figure 1.8 shows the plotted graph for equation 1.18, from which the value for *a* can be determined. An iteration process now follows where a new value for *a* is selected and used in equation 1.16, resulting in a value for C_4. Once this is calculated, C_4 is used in equation 1.18 to validate the guessed value of *a* through a plot similar to that found in figure 1.8.

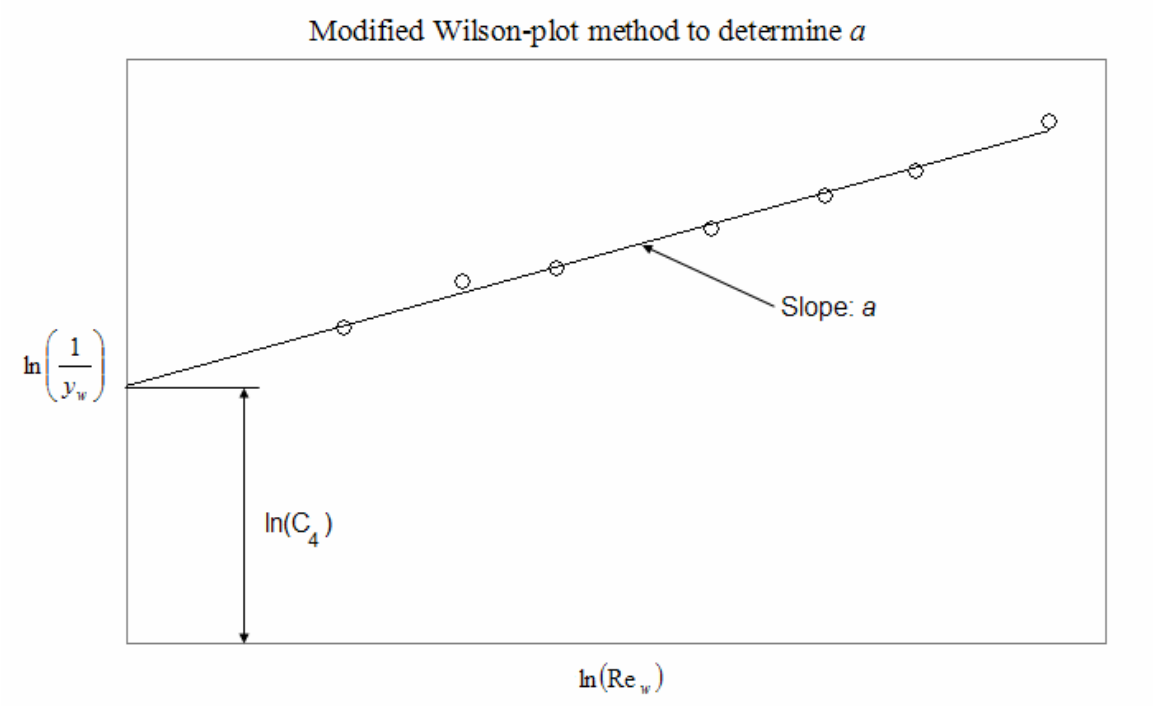

Figure 1.8 - Modified Wilson plot method to validate the value of a

Once the difference between the guessed and resultant values for a is found to be within a desired tolerance, a similar procedure is followed to obtain the values for d and C_5. In this analysis, data is used where the thermal resistance of the water is kept constant through testing at a single waterflow rate whilst varying the airflow rates. It should be noted that the success in determining the constants accurately will be totally dependent on the experimental data and the accuracy with which either the water- or airflow rates can be maintained at constant values. A number of cautions were found in the literature, and are discussed in the remainder of this section.

The contact resistance between fin and tube will be included in the air side thermal resistance when experimental data is used. Wang, Webb and Chi [23] cautioned that different fin-tube bonding techniques will have an effect on the heat transfer characteristics. It should thus be noted that once the constant values for equation 1.15 have been obtained through the modified Wilson-plot method, the results cannot be applied to any heat exchanger with the same geometry without investigating similarities in the manufacturing process.

When using the modified Wilson plot method to characterise an exchanger, as was successfully done by many authors [31-33], the potential sources of errors should be taken into consideration when selecting the heat exchanger and test facility. Knowing that the thermal resistance due to the convectional heat transfer from the heat exchanger surface to air will be dominant, a reduction in the uncertainties of the characterisation can be achieved by minimising the following two variables:

- Thermal resistance through the heat exchanger water tube wall.
  Minimisation of the thermal resistance through the heat exchanger surface cannot be controlled in an experimental evaluation as it is dependent on the material used for the heat transfer surface. Thin tube wall and fin heat exchangers manufactured from either copper or aluminium ensures low thermal resistance through the tube wall, and will increase the accuracy with which the experiments can be performed.

- Thermal resistance from the water to the heat transfer surface.
  Minimisation of the thermal resistance due to convection heat transfer from the water to the heat transfer surface can be controlled through the experimental test procedure. In the case where the thermal resistance is to remain constant to determine the values for d and C_5, the waterflow rate should be kept constant at the maximum possible flow rate through the exchanger.

Further limitations of this method are found in the possible *NTU* range for which tests can be performed. Shah [26] recommends a maximum *NTU* measurement of 3 for a test using air and water as fluids, as the accuracy of both the temperature and flow rate measurements become questionable at low airflow rates.

A second uncertainty at low airflow rates is the *heat transferred to the ambient* due to the lack of complete insulation of the heat exchanger test section from ambient temperatures. Although most heat exchanger test sections can be insulated fairly well, the influence of heat loss due to incomplete insulation is amplified at low airflow rates.

Further inaccuracies in determining the heat transfer surface performance is caused by *inaccurate airflow rate measurements* due to air leaks from the wind tunnel behind the airflow sensor on the inlet side of the heat exchanger. Depending on the pressure drop through the heat exchanger, this phenomenon is not necessarily highlighted at low airflow rates, but in combination with the previously mentioned influences, could lead to even higher inaccuracies at low airflow rates.

In addition to the effect that measurement errors can have on the heat transfer calculation for a surface, the effects of ill-constructed heat exchangers are also great [26]. When tests are performed on a specific heat exchanger, and the results used for heat exchangers that are of the same design but with small deviations from the tested exchanger, differences in performance can be expected. Poor thermal bonding between the fins and the primary surface, fluid flow blockages in the channels, and differences in material surface finishes will have an effect on the heat transfer characteristics of the fluids. The steady state

method is however reported to be accurate within ± 5% when the temperatures are measured within ± 0.1°C while none of the uncertainties discussed are present, and is one of the reasons for its popularity in the industry [26].

1.2.2 Influence of vehicle configuration on the cooling system

The vehicle itself has a huge effect on the performance of the cooling system. Three areas were identified where the vehicle has a direct impact on the cooling system characterisation model:

- Dependence of the waterflow rate on the engine speed,
- Dependence of the airflow rate on the vehicle speed,
- Heat generated by the engine to be dissipated through the cooling system.

The *water circuit* in a vehicle is isolated from any external influences on the system as a known mass/volume of water is used in a closed circuit to transfer the heat from the engine to the heat exchanger. The pump performance in terms of the mass flow rate will only change if additional restrictions are placed in the water system which will usually be associated with water system component changes.

On the other hand, the *airflow through the heat exchanger* is not only dependent on components that are directly related to the cooling system and it is therefore essential to consider the factors influencing airflow through the system. It is widely accepted in published literature that the flow rate through an automotive heat exchanger is generally the most important parameter that will dictate the heat transfer rate of the heat exchanger [34-36]. Furthermore, it is known that the flow rate is dependent on the flow path through the engine compartment and not only the heat exchanger. In an optimal flow circuit, the air passing through the heat exchanger needs to be channelled through the compartment in such a manner that a minimum back pressure is induced behind the heat exchanger, to maximise flow rate. Changes to components or the configuration not directly related to

the cooling system will thus also have an influence on the flow rate, as it will either increase or decrease the restriction in the flow path. For this reason it is important to be aware of factors that will increase or decrease airflow through the heat exchanger core. General findings in literature on case studies performed in this field give some indication of the effect that certain components have on the flow stream.

Quantifying the influence of individual components on the airflow rate through a heat exchanger will be dependent on the specific vehicle evaluated. Nevertheless, common trends are found in the literature. El-Bourini [37] investigated the effects of the front-end components on the airflow through the engine compartment. By measuring the airflow rate at various positions on the heat exchanger frontal surface, and calculating the mean airflow through the heat exchanger, a relationship between the vehicle speed and the air speed through the exchanger was obtained as shown in figure 1.9a and 1.9b. It was concluded that the total assembly of all the front-end components reduced the possible airflow by 84% in the case of his test vehicle. Only 48% of the reduction was caused by components involved in the cooling system of the vehicle while the remainder was due to other vehicle components.

In a similar experiment, Bahnsen [38] evaluated a vehicle for which the drag coefficient could be reduced by approximately 7% through covering the underbody of the vehicle. A large reduction in fuel consumption was noticed with this configuration. An alarming restriction in the airflow through the heat exchanger core was however noted, and the need to re-evaluate the cooling system was listed as a field for further investigation.

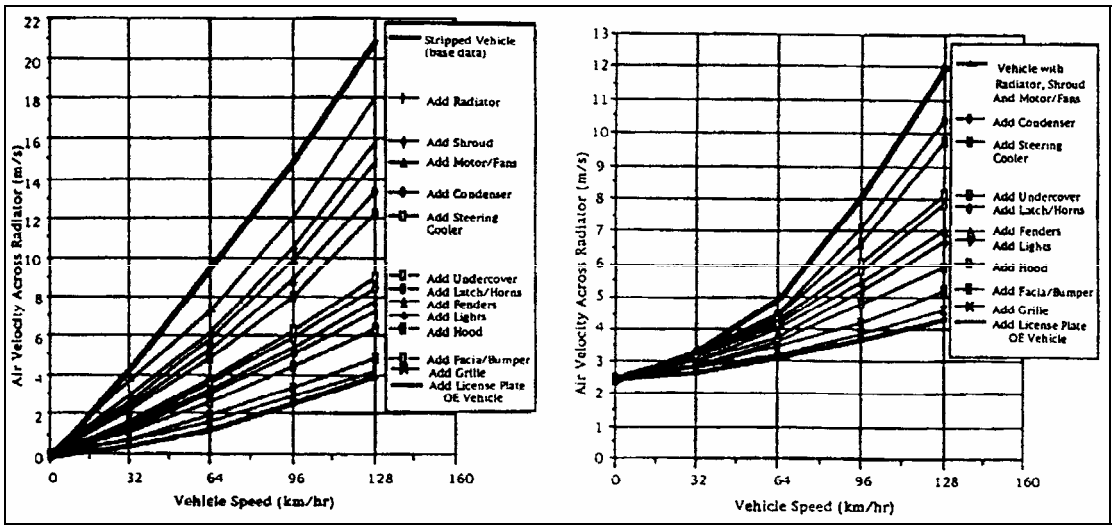

Figure 1.9a and 1.9b - Front end component effects on air velocity on heat exchanger with fan switched off (a) and fan switched on (b) [37]

Configuration changes in the engine bay of highly competitive rally vehicles are inevitable. The question is if the restriction of the standard configuration tested, can be expressed in such a manner as to benchmark it. This will make it possible to compare the restriction of different configurations, and determine the most suitable configuration to maximise airflow through the system.

In order to benchmark and compare the restriction in flow through heat exchanger cores, reference can be made to studies on the airflow in front of a porous wall which is analogous to that of a heat exchanger in a vehicle without shroud baffling on the air exit side of the heat exchanger [39]. Using equation 1.19, a restriction coefficient is defined that incorporates all components contributing to the loss of pressure in the air circuit, making it possible to compare flow systems with each other. Effectively this allows engineers to compare the relative restriction between two configurations. Implementing this to the data recorded by El-Bourini [37] for a vehicle without a fan, it is found that the total restriction coefficient with all components included is ζ_t = 78 at a vehicle speed of 128km/h. Omitting all the components from the undercover to the licence plate results in a total restriction coefficient of 7.78 at the same vehicle speed. This show that a much higher flow rate will result due to a less restricted system.

$$\zeta_t = \left(\frac{V_D}{v_{akmh}} \right)^2 - 1 \tag{1.19}$$

Non-uniform air temperatures also play a large role in heat exchanger performance. This phenomenon is frequently created by including oil-coolers and condensers in the inlet air-stream, causing localised temperature differences. Chiou [40] investigated the effect of non-uniform inlet air temperature distributions on the performance of heat exchangers and found that the positioning of the components that cause non-uniformities, play an immense role in the heat exchange efficiency. It was found that the performance of a heat exchanger will decrease when the highest temperature in the non-uniform temperature distribution is near the water inlet region of the heat exchanger. Moving the high temperature zones closer to the water outlet regions of the heat exchanger would generally increase the relative performance [40]. Ultimately one would however want to exclude any temperature uniformities from the system to increase the heat transfer performance.

Once the effect of water- and airflow is defined, it is required to investigate the heat source. The input to a cooling system is the *heat generated by the engine*, which is dependent on a vast number of engine variables that are determined during the design of the engine, such as the water channel design around the cylinder; the valve design and camshaft design to name a few. Changes cannot be easily made to the engine to reduce the heat generated and for the purpose of this study, the heat generated is regarded as a specific engine characteristic.

Methods to quantify the heat load produced by the engine is widely discussed in literature, with the most common method to characterise this phenomena being physical testing through measurement of the cylinder wall temperature of a specific engine [41-42]. Various mathematical models have been derived for heat transfer prediction, but are only applicable to specific engine designs due to the number of variables that influence

heat generation. To illustrate the differences between engines, figure 1.10 was compiled to show the heat load generated per brake horse power for a number of different engines [39].

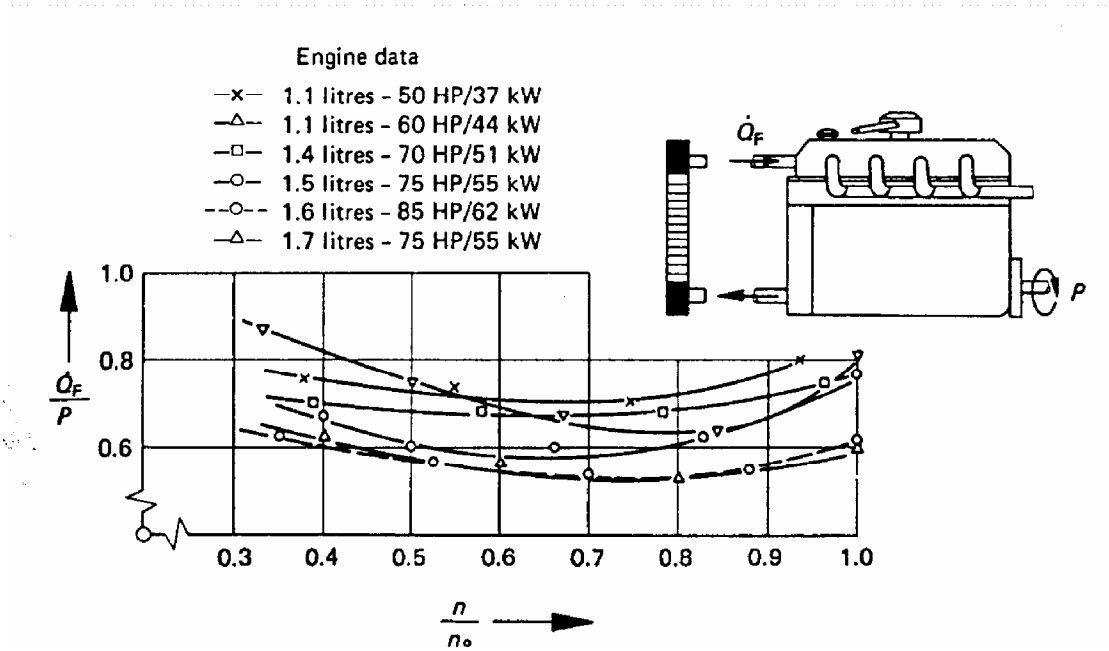

Figure 1.10 - Engine heat rejected to output power vs. engine speed factor [39]

As a general empirical equation is not available in the literature to describe the heat generated by an engine, only the trends will be discussed. An indication of the orders of magnitude for the heat load placed on the cooling system can be found through the portion of fuel heating values documented by Heywood [45]. The heat load can be expressed as a percentage of the energy produced through the combustion of fuel in an engine. This is done by dividing the fuel energy into brake power, heat transfer to the cooling system, exhaust gas enthalpy flux, exhaust enthalpy flux due to incomplete combustion and miscellaneous factors, described in equation 1.20.

$$P_b + \dot{Q}_{cool} + \dot{Q}_{misc} + \dot{H}_{e,ic} + \dot{m}_e h_{e,s} = \dot{m}_f Q_{\mathrm{LHV}} \qquad (1.20)$$

Heywood [45] documented typical values for these variables:

Table 1.2 - Portion of fuel heating values at maximum load

	P_b	$\dot{Q}_{cool}$	$\dot{Q}_{misc}$	$\dot{H}_{e,ic}$	$\dot{m}_e h_{e,s}$
Spark ignition engines	25%-28%	17%-26%	3%-10%	2%-5%	34%-45%

It is evident that only 17%-26% of the energy is transferred to the cooling system. If one considers the ratio of heat transferred to the cooling system relative to the brake power generated, the worst and best case scenarios are 1.04 and 0.607 respectively. According to Emmenthal [39], these values are relatively conservative as he found the ratio of heat transferred to the cooling system relative to the brake power generated is between 0.9 and 0.5. It is therefore safe to assume that the ratio will be between 1.04 and 0.5, depending on the engines capability to expel heat through the exhaust system. It is extremely important to note that the ratios quoted should only be used to verify the order of magnitude of the heat generated by an engine which is physically tested.

When the heat generated by an engine has been determined, this can be used as *design criterium* for the heat exchanger to be used in the cooling system. By doing so, the resulting cooling system will always be able to meet the cooling requirement. An over designed system will however result as the vehicle will not always operate at maximum load conditions.

Literature shows that the maximum coolant temperature for a vehicle is usually developed in first gear. The low airflow rate through the heat exchanger core associated with low vehicle speeds cause reduced heat transfer through the exchanger as can be seen in figure 1.11 [39]. To increase heat transfer at low vehicle speeds, electric fans or engine driven fans are commonly used with great effect. Power is however required to drive the fan, which is obtained from the engine through the alternator or directly from the

crankshaft. In the field of rally vehicles the reduction in power due to the use of such a power consumer is undesirable.

Although maximum coolant temperatures will be recorded in first gear, the application of the vehicle also needs to be taken into account. Passenger vehicles offered to the commercial market will develop maximum thermal load in steady state when the vehicle is driving up the maximum permissible slope. These conditions will only be encountered for short distances in the normal operating life of a vehicle and is not realistic as design criteria. Through observing traffic conditions in Europe, the most common design criteria for a passenger vehicle cooling system was documented to be [39]:

- Continuous 10% gradient at 25 km/h at the vehicle's rated gross combination mass,
- Continuous maximum speed.

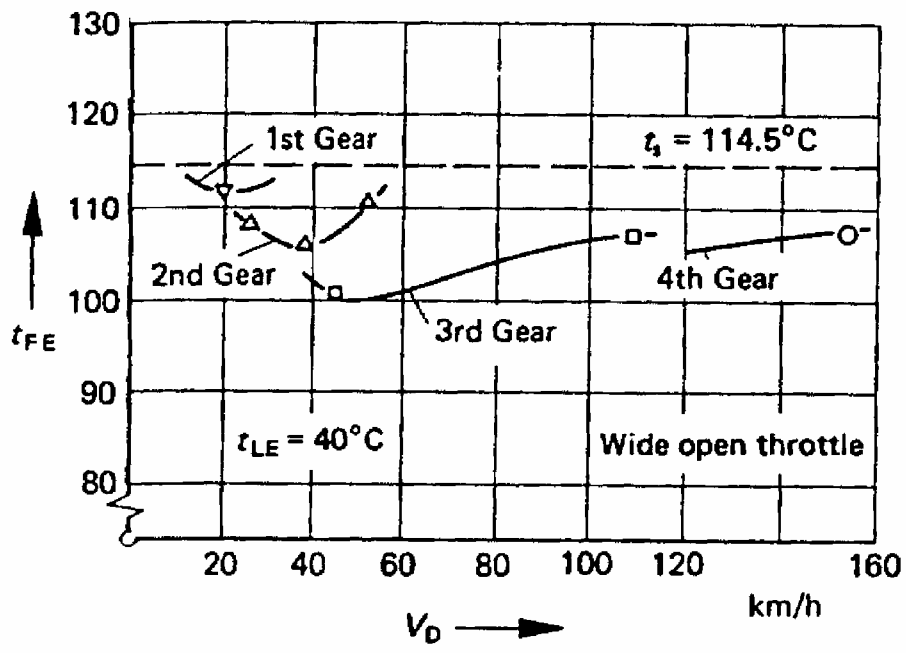

Figure 1.11 - Engine temperature vs. vehicle speed at full open throttle conditions [39]

High performance vehicles, such as rally cars are subjected to harsh accelerating and decelerating conditions, with heat load design requirements different to normal

production passenger vehicles. Literature to be used as design criteria for the cooling system in this application could not be found.

Assumptions on the heat load criteria can however be made. Information on previous experience at a specific event can prove to be extremely valuable. By analysing recorded data on the gears most frequently used, assumptions can be made for expected operating conditions. Should it be found that the first gear was only used at the start of the stage, and that the driver mostly used second gear, the heat exchanger can be sized for second gear. It should however be noted that such a decision is associated with a certain risk, as the drivers failure to avoid a lower gear, may lead to overheating of the engine. In order to minimise the risk, and possibly have an over designed system for the sake of reliability, it is recommended that first gear conditions be used to base heat exchanger selection on. The final decision however remains with the team manager.

1.3 Need for the study.

Cooling systems of normal production passenger cars are usually designed to cater for almost any road or ambient condition. This leads to an over designed system due to conservative assumptions made with regard to the operating conditions. Applying the same cooling system design methodology to rally cars is not feasible as a possibility exists to minimise cooling system losses.

It will be advantageous for a team to predict the cooling system performance and identify opportunities to minimise losses at specific ambient conditions as it will increase the competitiveness of the vehicle. The literature evaluated could not provide a model through which a systems performance under specific ambient conditions can be evaluated. It is, however, theoretically possible to predict the performance of a cooling system by using an energy balance for heat generated and dissipated in the vehicle.

Once a cooling system has been identified as being unsuited for the conditions under which it operates through an energy balance model, a modification to the system should be made. Since the heat generated by the engine cannot easily be changed without altering the performance of the engine, a reduction in heat generated is not feasible. Changes can however be brought about by selecting an appropriate heat exchanger that can be used in the cooling system. The heat dissipation characteristics of specific heat exchanger cores thus need to be known. Experimental evaluation of these heat exchangers can result in a single characterisation equation per cooling system configuration.

Ultimately, a rally team needs to specify the heat exchanger to be used in a cooling system, based on the specific characteristics expected of the time trial stage, as well as the ambient conditions. A need thus exists to express the cooling system performance as a function of ambient conditions, engine speed and gear selected or vehicle speed. Furthermore, it is required to present the performance of different cooling system configurations in such a manner as to make the selection of a suitable heat exchanger under the prevailing ambient and assumed operating conditions relatively easy.

1.4 Scope of the project and the selected method for investigation outlined

In order to design a cooling system for a vehicle, knowledge of the heat transfer characteristics of a heat exchanger is required. The most common method used to characterise the total cooling system of a normal production car, is through experimental investigation of the actual vehicle in a wind tunnel. A wheel dynamometer is used in such a wind tunnel to obtain the maximum heat load at a certain engine speed, while the air speed which is dependent on the driveline characteristics, is simulated through the use of the wind tunnel fans [46-47]. Using an air-to-boil value as parameter, the cooling system is assessed based on the outlet water temperature of the engine, for the specific vehicle configuration tested.

Due to the competitive nature of rally cars, most of the components in the vehicle are constantly being researched to maximise the performance of the vehicle, resulting in frequent component changes. Configuration changes such as engine components, transmission and driveline ratios, grill and body spoilers as well as cooling system components may also be made shortly prior to an event, within the limitations set out by the race officials. Component selection as well as configuration changes thus provide the team with numerous vehicle configuration possibilities. This limits the use of the information obtained from a single wind tunnel test as outlined above, since changes in the aerodynamic properties inside the engine bay or restrictions in the coolant circuit, may have an enormous influence on the cooling system performance as identified in the literature. It would therefore be necessary to test each vehicle configuration separately to determine its effect on the total cooling system. The financial implications associated usually deem this method unsuitable if the rally team does not have access to the above mentioned facilities.

A need therefore exists to use the performance characteristics of individual components in a heat transfer model to predict a cooling system's suitability for specific conditions. This requires characterisation of different heat exchanger cores independently from the factors that will have an impact on the total cooling system performance. Once the core performance is known, incorporation of the various external factors through a mathematical model will result in a characterised vehicle cooling system.

The scope of this study is therefore to experimentally evaluate the characteristics of different heat exchanger cores, and investigate the influence of ambient conditions on the heat transfer problem for the total vehicle. The vehicle configuration, with regard to the effect it will have on the heat transfer process, will not be experimentally characterised in this study. Data supplied by the manufacturer will be used to incorporate its effect on the total cooling system. Similarly, heat produced by the engine and the characterisation method used to determine this will also not be discussed in depth. Once again, data from the manufacturer will be presented and included in the model.

Process diagram 1.1 shows the broad outline of the model which will be used to characterise the cooling system and determine its suitability under specific ambient conditions in this study. Evaluating the process, we find that two key areas form the basis of the mathematical model, i.e. the heat dissipated through the heat exchanger core and the heat generated by the engine as previously mentioned. Both these characteristics are determined through experiments which are performed in controlled environments, resulting in the exclusion of vehicle and ambient influences in the models. In order to modify the energy balance model in such a manner that it describes the actual cooling system on the vehicle, it needs to be expressed in terms of vehicle and ambient variables.

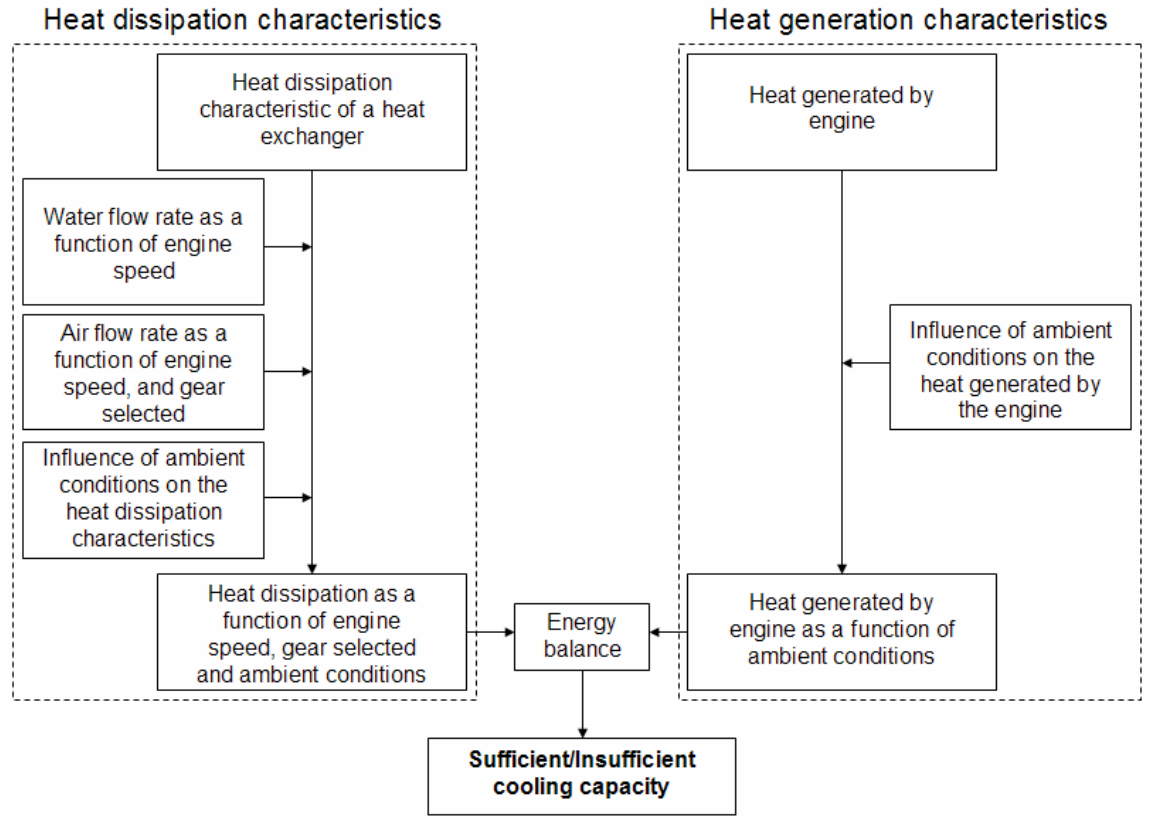

Process diagram 1.1 - Cooling system characterisation model

The heat dissipation characteristic of a core is mainly dependent on the *mass flow rates of the fluids* used. In the automotive application, these fluids are driven by vehicle components. In the case of water, a pump is used to establish flow, which is dependent on

the engine speed of the vehicle. Airflow on the other hand is maintained by the speed of the vehicle, and in some cases, an electric or crankshaft driven fan. The vehicle speed is dependent on the engine speed through the transmission ratio selected. Knowledge of the dependence of the fluid flow on the engine speed is essential as it partially bridges the gap between the tests performed on a heat exchanger in a wind tunnel and the actual cooling system on the vehicle.

A large number of factors influence the *heat generated by an engine*. Many of these factors can be related to the engine and exhaust system design as well as the combustion process. The heat generated is directly related to the engine power generated which is a function of the engine speed of the vehicle. A relationship between heat generated and engine speed will thus describe the input energy to the cooling system and define the heat dissipation requirement for the model to be derived.

Finally, *ambient conditions* have an effect on both the heat generated as well as the heat dissipated. Low ambient temperatures are favourable when high heat loads are to be dissipated from the system. In combination with high air pressures, low temperatures increase the density of air. This results in an increase in the mass airflow through the heat exchanger, but also allows for higher power generated by the engine.

Evaluating the outline of this model, three critical elements are thus identified which will have a direct impact on the accuracy with which the cooling system configuration in a rally car can be predicted. These elements are:

a) The heat transfer performance of a heat exchanger,
b) Knowledge of the heat produced by the engine as well as the effect of the vehicle configuration on the cooling system,
c) The influence of ambient conditions on the system.

The study that follows uses these factors to evaluate the cooling system of a rally car for specific road and environmental conditions.

1.5 Outline of the study.

In Chapter Two the cooling capability of two different heat exchanger cores are determined. It describes the experimental method and equipment used in evaluating the heat exchanger cores independently of the influence of the vehicle. The modified Wilson plot method is deployed in this section to determine the thermal resistance of each heat exchanger under varying fluid flow rates. Using a published ε-*NTU* equation as basis, the heat transfer characteristics of each heat exchanger core are expressed as a function of the fluid flow rates. The chapter concludes with two contour maps showing each heat exchanger's performance as a function of the Reynolds number of fluid flow for air and water.

Chapter Three presents a case study of typical vehicle and ambient conditions, incorporating its influence on the characteristic equations derived in chapter two. Data supplied by the manufacturer on the air and waterflow rates through the system of a vehicle is presented and included in the characteristic equation through further data manipulation. The effect of ambient conditions on the heat transfer rate of each exchanger is also included by using the ideal gas law. From the data obtained, the flow restriction through the heat exchanger is benchmarked. This serves as a guide to the team concerning the airflow through the system when changes are made to component configurations in the engine compartment.

The heat generated by the engine is evaluated in Chapter Four. Data from the manufacturer is used to describe the heat load as a function of engine speed. The effect of ambient conditions on the heat generated is included through the use of the SABS standards on engine performance testing, resulting in a final characteristic equation describing the heat load generated as a function of engine speed and ambient conditions . Evaluating the energy balance, the spare capacity is defined as the excess or lack of cooling capacity. Based on this variable, a cooling system is defined as either over or under designed at specific ambient conditions. The chapter concludes with contour maps

summarising the cooling system performance for both exchangers as functions of ambient temperature and pressure, for first and second gear.

Chapter Five consists of a summary of the work done in the study as well as the applicable conclusions. Applications in which the mathematical model can be used are discussed, as well as the recommendations for future work relevant to the present study.

CHAPTER 2
HEAT EXCHANGER CHARACTERISATION

2.1 Preamble

In this chapter the experimental setup used to characterise the heat exchangers are discussed. This includes the heat exchangers selected as well as the domain in which the experiments were conducted. Mathematical equations that predict the heat transfer characteristics are populated using the modified Wilson plot method, concluding in a gradient graph for each heat exchanger. The final characteristic equations and gradient graphs for each heat exchanger core reveal the heat transfer through the particular exchanger as a function of the Reynolds numbers for both the air and water.

A competitive rally car was made available by a team to serve as a case study in the investigation of the cooling system in this application. The team provided assistance in the manufacturing and modification of heat exchangers to ensure that the tested heat exchangers would indeed interface with the rest of the vehicle for which the cooling system was under investigation. As the car was used as a case study in developing the mathematical model, some of the heat exchanger dimensions, parts as well as the position of the water inlet and outlet ports were governed by the teams' requirements in the engine compartment. Development and investigation into the heat exchanger size, positioning in the engine compartment as well as the top and bottom tank geometry therefore does not form part of this study, and are considered to be fixed variables.

2.2 Heat exchangers selected for evaluation

The triangular air duct heat exchanger core geometry was selected for characterisation due to its availability and the documented advantages compared to other designs. Various

heat exchanger designations are found in the literature, and it is therefore necessary to firstly explain the designation that will be used in this study by means of an example.

2 Tube core, 4mm fin pitch

2 Tube core, → Also referred to as a 2 core heat exchanger with two rows of water channels situated directly behind each other. This designation indicates the depth of the heat exchanger.

4mm fin pitch → The fin pitch refers to the dimension A as shown in figure 2.1.

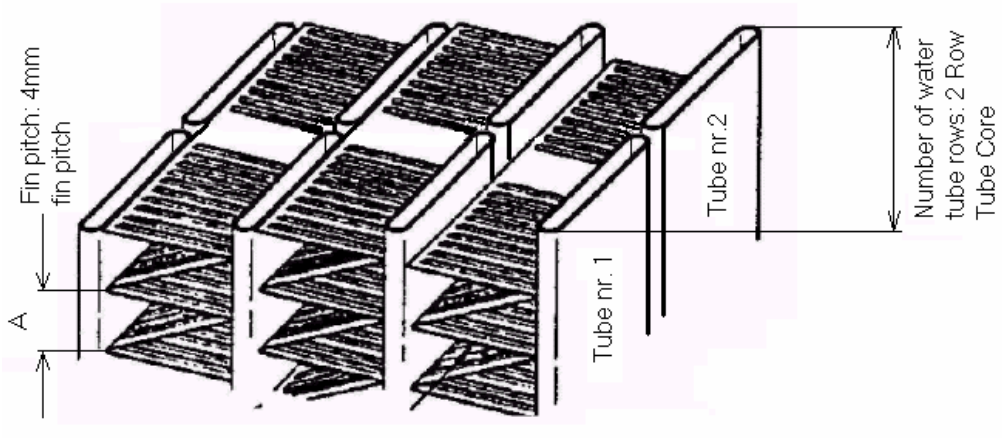

Figure 2.1 - Heat exchanger designation by an example of a 2 core, 4mm fin pitch heat exchanger

Two heat exchanger cores were selected for characterisation, with differences in the fin pitch. Having carefully evaluated the heat exchangers available in the triangular air duct louvered fin geometry, the following well constructed heat exchangers were selected:

- 3 Tube core, 3mm fin pitch
- 3 Tube core, 4mm fin pitch

The heat exchangers all have the following common characteristics, assisting in easy comparison of heat transfer characteristics:

- Heat exchanger material: Aluminium,
- Thickness of fins: 0.2 mm,
- Distance between 2 adjacent waterflow tubes (parallel to the frontal plane of the heat exchanger): 8 mm,
- Pitch between water flow tubes: 10 mm,
- Thickness of waterflow channel walls: 0.4 mm,

Not only does the aluminium aid in saving weight on the vehicle, but is also advantageous in testing the heat exchangers, as the high thermal conductivity associated with the material, will reduce uncertainties as mentioned in chapter 1.

The volumetric dimension of the heat exchanger to be used in the test vehicle is governed by the space available for the component in the engine compartment. In this case, the maximum volumetric dimension available for the heat exchanger core is 730mm in length, 320mm in height and a maximum depth of 70mm. The aluminium top and bottom tanks for the exchangers are excluded from the quoted volumetric constraint, but remain an important parameter that needs to be considered when designing a heat exchanger. The tanks used for the two heat exchangers were manufactured and mounted by the vehicle manufacturer, ensuring that the heat exchangers could be used in the vehicle at a later stage. It is important to note that the designs of the tanks are identical for the two heat exchangers tested resulting in the same water flow distribution to the water tubes for both exchangers. Please refer to appendix A for the overall dimensions of the heat exchanger cores and tanks.

2.3 Experimental facility used for characterisation

The Mechanical and Aeronautical department at the University of Pretoria has a heat exchanger test facility used for the characterisation of exchangers under steady state

conditions. The facility is equipped with a warm water boiler that supplies water at a preset temperature and flow rate to the heat exchanger and a combining wind tunnel that provides air at a preset air speed to the air-side of the heat exchanger. A computerised control system is used to control selected variables for both the air and water side of the heat exchanger. A detailed description of the system can be found in Appendix B.

Figure 2.2 shows a schematic representation of the air side of the facility. In this facility, part of the air can be circulated in a controlled closed loop system that bleeds to the atmosphere in order to accurately control the temperature of the air supplied to the heat exchanger at temperatures well above the ambient temperatures. Warm air exiting the system was however dumped outside of the building during the experiments to prevent a gradual increase in atmospheric temperature during testing.

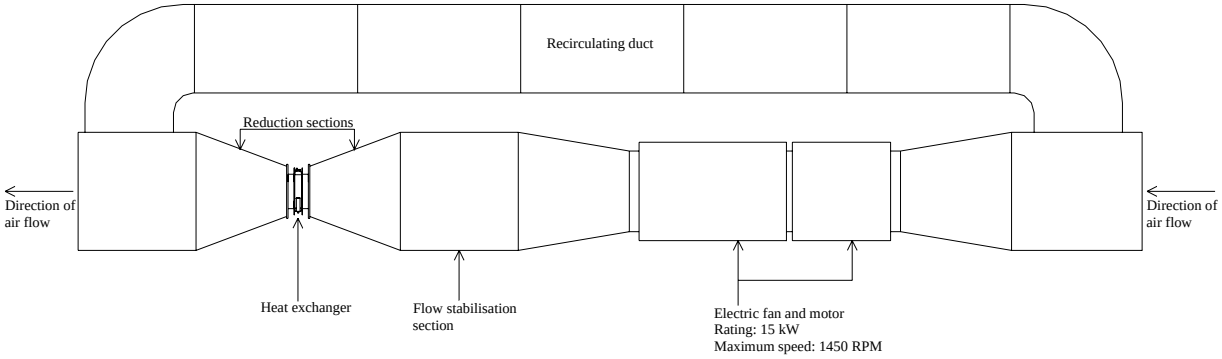

Figure 2.2 - Schematic representation of wind tunnel used

Various test sections are available to match the size of the heat exchanger being tested. To prevent the build-up of a boundary layer on the walls close to the heat exchanger, interface ducting was built and installed between the reduction section and the heat exchanger core, as shown in figure 2.3.

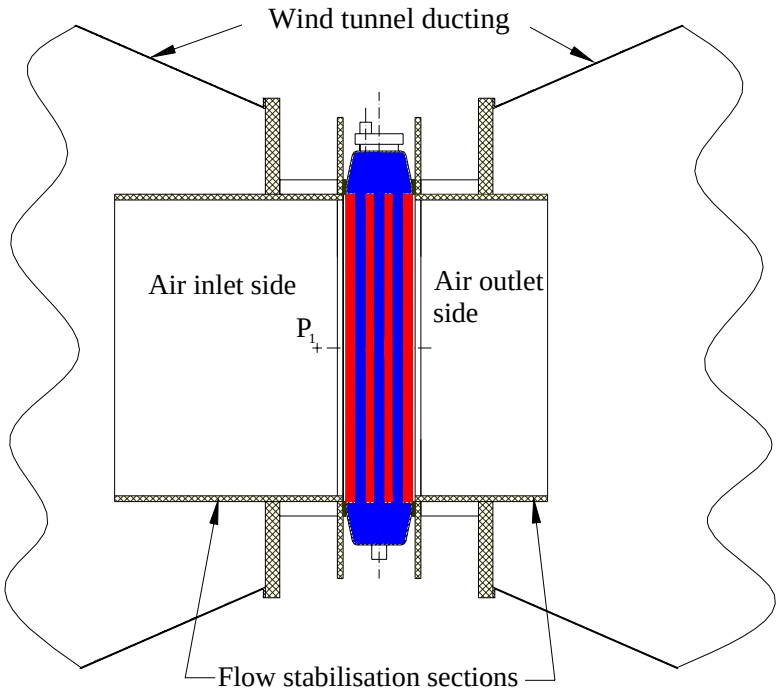

Figure 2.3 – Heat exchanger test section

The test facility is equipped with calibrated temperature and airflow measuring equipment that measures the temperature just before the heat exchanger. The flow measuring system does, however, not measure the velocity of the air accurately at the heat exchanger inlet side as is required for the calculations to follow. The velocity through the heat exchanger was measured by inserting a pitot tube at position P_1 as shown in figure 2.3. In that way the difference between the stagnation and static pressure was recorded. In order to verify the use of a single pitot tube to measure the air speed, measurements were taken at various positions in front of the heat exchanger as explained in appendix C. A maximum deviation of 5.24% relative to the average air speed was recorded for the experimental set-up, which is an acceptable distribution for this type of experiment.

The water flow circuit found in the laboratory is more complex than the airflow circuit in the experimental setup. Figure 2.4 provides a schematic flow diagram of the water circuit. Water without any additives such as anti-freeze, is heated in the un-pressurised

water boiler which is equipped with a two stage diesel burner. The water temperature in the boiler is controlled at a fixed preset temperature by the computerised control system.

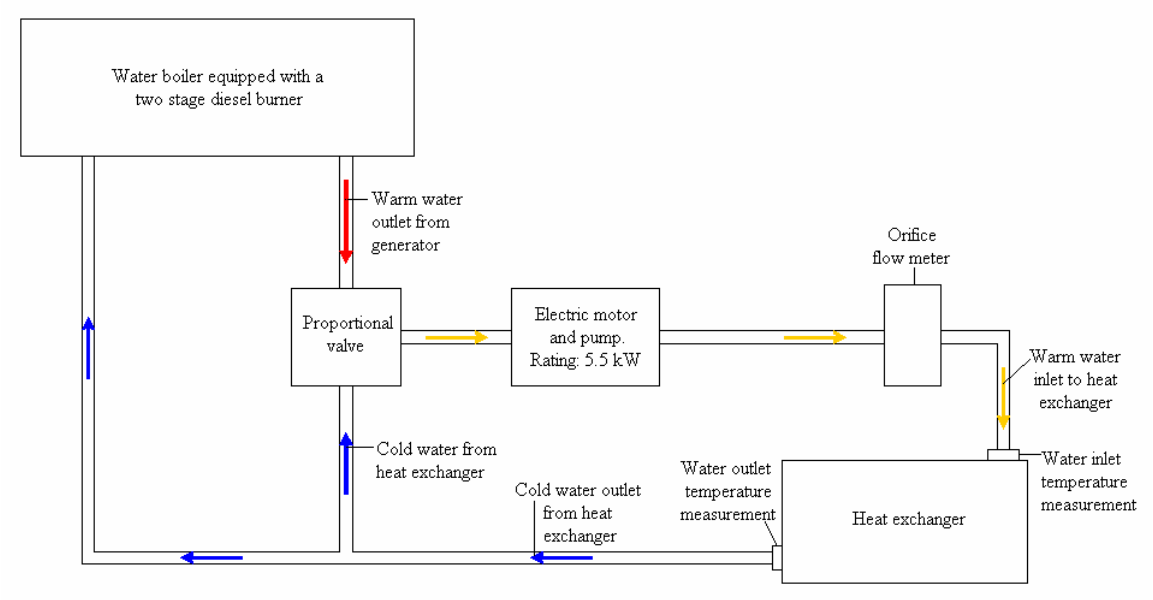

Figure 2.4 - Schematic representation of water circuit of the test facility

A proportional valve is used to mix the return water from the heat exchanger with water from the boiler to ensure a fast responding control system that will accurately control the temperature of the inlet water. From the proportional valve, water is pumped at the preset flow rate to the heat exchanger.

2.4 Control system used during the experimental characterisation

The success with which meaningful data can be collected under steady state conditions is directly dependent on the ability with which the variables that drive the heat transfer process can be kept constant. In the case of heat exchanger evaluation using the modified Wilson plot method, it is imperative to keep the following variables constant:

a) Inlet temperature difference between the fluids,
b) Mass flow rate of the water,
c) Mass flow rate of the air.

Apart from the airflow transducer, all sensors measuring the variables during the experimental testing of the heat exchanger in the facility used were connected to a computer with a closed loop control system program (BAS 2000®) to adjust the values through controlling the following powered devices:

a) Water pump controlled through the input frequency to the electric motor,
b) Activation of both stages of the diesel burner,
c) The proportional valve.

The inlet temperature difference between the fluids is kept at a constant value though entering the desired value in the computerised control system. The inlet temperature of air ($T_{a,in}$) is deducted from the inlet water temperature ($T_{w,in}$). Should this temperature deviate from the required value entered into the system, the control system adjusts the proportional valve in the water circuit until the required temperature value is met. With a continuous loss in thermal energy of the water, one expects the system not to be able to meet the desired values once the proportional valve is in the closed position, i.e. when only water from the heated tank is channelled to the heat exchanger. To overcome this problem, the system also controls the diesel burner and activates it once the inlet temperature difference cannot be maintained by only using the proportional valve.

The system also has the capability to collect all the relevant data, resulting in relatively easy manipulation using a computer. The following data is made available which can be captured electronically once the operator has identified that the system has reached steady state conditions:

- Waterflow rate (l/s),
- Heat exchanger water inlet temperature (ºC),
- Heat exchanger water outlet temperature (ºC),
- Heat exchanger air inlet temperature (ºC).
- Heat exchanger air outlet temperature (ºC).

2.5 Domain of variables in which cores were evaluated

As found in the literature discussed in chapter 1, the two experiments associated with the modified Wilson plot method had to be conducted at maximum flow rates possible, while measuring thermal energy change at predetermined variations of flow rate at steady state conditions. The equipment used together with the characteristics of the heat exchanger cores determined this domain within which characterisation tests could be performed.

As the two heat exchangers identified for evaluation, had the exact same tube and tank configuration, the same pressure drop and water flow characteristics were expected over the exchanger. For this evaluation either heat exchanger could be used to determine the minimum and maximum water flow rates through the system. Testing of the 3 core 3mm fin pitch heat exchanger, showed that the minimum water flow rate obtainable was limited by the orifice flow meter's capability to produce a sufficient pressure fall over the exchanger to be noticeable on the differential pressure transducer. On the other side of the scale, the maximum flow rate was governed by the water pump's capacity. The range of operation for the water flow was established to be between 1.4l/s to 4.45l/s.

The maximum airflow rate obtainable through the heat exchanger cores, limited by the equipment available, was established by testing the heat exchanger with the largest air pressure drop over the core. Testing the 3 core 3mm fin pitch heat exchanger at maximum airflow, the maximum test speed for comparable characterisation was found not to exceed 9m/s. To determine the effect of airflow on the heat exchangers' heat transfer characteristics, it was decided to evaluate each heat exchanger at 3m/s, 6m/s and 9m/s in the wind tunnel. It should be noted that the experimental testing was conducted at high altitude atmospheric conditions. Data on the absolute atmospheric conditions were obtained from a weather buro after the completion of the experiments. Atmospheric pressures were found to vary only between 86 kPa and 88 kPa

The third variable for which the domain was tested is the inlet temperature difference between the fluids. In order to quantify the maximum inlet temperature difference

between the fluids, the maximum water temperature at the inlet of the heat exchanger as well as the ambient air inlet temperatures needed to be evaluated. By testing the worst-case scenario, it was found that the maximum consistent inlet temperature to the heat exchanger was 75°C measured at the inlet to the heat exchanger. During the experimental evaluation of the heat exchangers, it was however noted that the ambient air temperature was in the region of 25°C during the period of testing, but due to the heat of the fan motor dissipated into the air stream, the temperature of the air at the heat exchanger inlet was increased by approximately 5°C. This left a maximum obtainable temperature difference between the inlet temperatures of the fluids of 45°C. As small variances in the ambient conditions were to be expected, as well as the instability of the system to maintain the temperature difference at this temperature difference, the maximum consistent testable temperature difference between the fluids was found to be 40°C. During the experiments, the temperature difference between the fluids was varied in steps of 5°C, between 25ºC and 40ºC.

The domain in which the heat exchangers were evaluated can thus be summarised as follows:

- Waterflow rate variations between 1.4 l/s to 4.5 l/s,
- Fluid inlet temperature differences varying between 25°C and 40°C,
- Air speed rates at 3m/s, 6m/s and 9m/s,
- Ambient pressure between 86 kPa and 88 kPa.

2.6 Experimental procedure

Having explained the capability of the experimental equipment and the range within which the characterisation could be performed, the experimental procedure required to employ the modified Wilson plot method follows.

The literature in chapter 1 shows that two distinct experimental procedures should be followed in order to obtain suitable results for use in the modified Wilson plot method.

The first procedure includes the evaluation of the heat exchanger at a constant water flow rate under varying airflow rates. To minimise the thermal resistance on the water side of the heat exchanger, the water flow rate was set to the maximum consistent flow rate possible, i.e. 4.5 l/s. The first set of data under varying airflow rates of 3m/s, 6m/s and 9m/s was logged at an inlet temperature difference of 40 ºC. To validate the experiments and data obtained in later calculations, the experiments were repeated for inlet temperature differences between the fluids of 35 ºC, 30 ºC and 25 ºC, for data sets 2 through 4.

The second test is similar to the first with the difference being that the waterflow rate is varied whilst the airflow rate is kept constant. The airflow rate was set to the maximum value of 9m/s in this experiment, minimising the thermal resistance associated with the air stream. Using an inlet temperature difference of 40ºC, the waterflow rate was varied from 1.4l/s to 4.5l/s. After completion of the first data set, the inlet temperature difference between the fluids was set to 35 ºC, 30 ºC and 25 ºC whilst repeating the above mentioned procedure. In order to ensure repeatability and identify false data collected, 8 measurements were logged per set of variables for both the first and second test procedure.

During the experimental evaluation, the following data was recorded at each test point:

- Air inlet temperature to the heat exchanger,
- Water inlet temperature to the heat exchanger,
- Water outlet temperature from the heat exchanger,
- Airflow rate,
- Waterflow rate.

Using the data obtained through the experiments, the heat transfer rate could be calculated at each variable set. Having 8 measurements for each variable set, the repeatability of the experiment could be evaluated, providing the opportunity to critically evaluate the data collected. Although every effort was made to ensure that the tests were as accurate as possible, small deviations within the 0.1°C tolerance between the inlet and

outlet temperature sensors caused uncertainties with regard to the average value for the set of variable. Furthermore, small fluctuations in waterflow rate and inlet temperature differences of 5% and ± 1°C were respectively noticed during the testing phase. For this reason, a method was derived to select the most appropriate data points, in order to disregard inaccurate measurements. Please refer to appendix D for an example of the calculations as well as the method used to identify the most appropriate data for use in calculating the average heat dissipation per variable set.

2.7 Modified Wilson Plot method used to determine a characterisation equation

A two stage modified Wilson plot method was used to determine the constants for the heat transfer characterisation. Having performed the experimental evaluation in such a manner as to promote constant waterflow rate at varying airflow rates and vice versa, the results obtained after the data elimination process is used in a two stage method to characterise each heat exchanger core. The literature discussed in chapter 1 show that the characterisation relies on accurately determining the values for the four constants of equation 1.18. While variables a and C_4 are associated with the heat transfer resistance between the water and the tube wall, d and C_5 governs the accuracy with which the thermal resistance between the external heat transfer surface and the air can be predicted.

The following assumptions with regard to the thermal resistance equation are made based on the work of other authors:

- The thermal resistance due to conduction is negligible,
- The thermal resistance due to fouling on the water and air side surfaces are negligible as new heat exchangers are tested.

The process to determine the constants are discussed in the following two sections.

2.7.1 Determining the constants associated with the water side

To determine constants a and C_4 it was essential to ensure that the second term in equation 1.15 remained constant. This was done by using measured and calculated data at a constant air speed of 9m/s, while the waterflow rate was varied. The process of determining the values of the two constants consisted of two distinct calculations. Firstly the value of C_4 was determined under an assumed value of a. The second part consists of the calculation of a using the value of C_4 calculated in the first step. Only after the values of the assumed a and the calculated a was found to be within a reasonable tolerance did the iteration process cease.

The first step, i.e. determining C_4 under an assumed value of a, was performed by plotting the data collected as a straight line using equation 1.16. Noticeably the relationship expressed in equation 1.16 was done so in terms of UA, and the Reynolds numbers of both the water and air as governing variables in determining the heat transfer.

To this point, the heat transfer characteristics ($\dot{Q}_{dissp}$) had been recorded with associated waterflow and airflow rates as well as the inlet temperature difference between the fluids. In order to use the data collected, the experimental results had to be further manipulated to express the thermal resistance using the required variables.

For each data point recorded in the experimental test, the effectiveness (ε) was calculated using equation 1.1., as well as R_c using equation 1.3. With these variables known, the NTU was calculated through manipulation of equation 1.8 as recommended by the Engineering Science Data Unit [24] for a 3 core heat exchanger. The value for UA could now be determined using the variables determined by rewriting equation 1.4 as follows:

$$UA = NTU \times C_{\min} \tag{2.1}$$

The wall and bulk/mean dynamic viscosities for both fluids were calculated using the wall and bulk/mean temperatures respectively for each fluid, and obtaining the values from the documented values for dynamic viscosities [6]. Assuming that the thermal resistance due to conductance was negligible allows that the wall temperature in the air calculation could be assumed to be the bulk/mean temperature of the water. Similarly, the wall temperature for the water side calculation was assumed to be the bulk/mean temperature of the air. As only the air inlet temperature was recorded during the experimental test, the outlet temperature required to calculate the bulk/mean temperature was calculated using the following equation:

$$T_{a,out} = \frac{\dot{Q}_{diss}}{\dot{m}_a c_{pa}} + T_{a,in} \tag{2.2}$$

A number of constants were also identified in equation 1.16 that was either a dimensional property of the heat exchanger core, or was a fluid property dependent on the temperature of the fluid or core. Table 2.1 gives the values for both heat exchangers evaluated since their water channels are identical. The method of calculating is explained in appendix E.

Table 2.1 - Constant values associated with the water side

Constant	**Value (Both heat exchangers)**	**Reference to view calculation/data sheets**
A_w	1.3665m^2	Please refer to appendix E, paragraph E.1
k_w	0.665W/m K	Value obtained from data sheet in Mills [6]
D_{hw}	0.002171173m	Please refer to appendix E, paragraph E.2
Pr_w	2.55	Value obtained from data sheet in Mills [6]

With the need to calculate two variables, a guessed value for a was used in the second term of equation 1.16, making it possible to plot the manipulated experimental data as shown in figure 2.5. The value of C_4 was determined by fitting a line through the data using the method of least squares using a first order polynomial function. Calculating the

inverse of the slope found for the function, the value of C_4 was obtained which is associated with the guessed value of a.

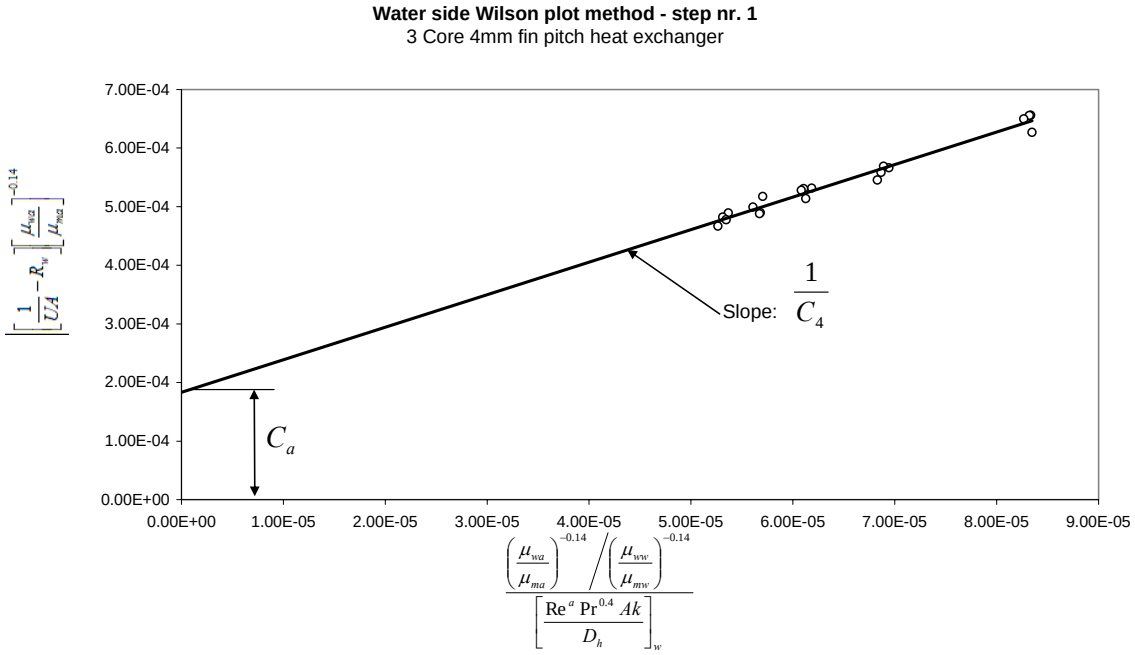

Figure 2.5 - Wilson plot method to determine the value of C_4

As part of the second step in determining the constants, the guessed value of a was validated. Employing equation 1.17 in the form of equation 1.18, yet another straight line could be plotted using the modified Wilson plot method.

In this plot, the value for C_4 obtained in the first step of this process was used. Figure 2.6 shows the resulting graph, with a straight line fitted through the data points to reveal the value of a as it is the slope of the fitted curve. As previously explained, the value for a determined through figure 2.6 must be equal to the value guessed for a in the first step of the process.

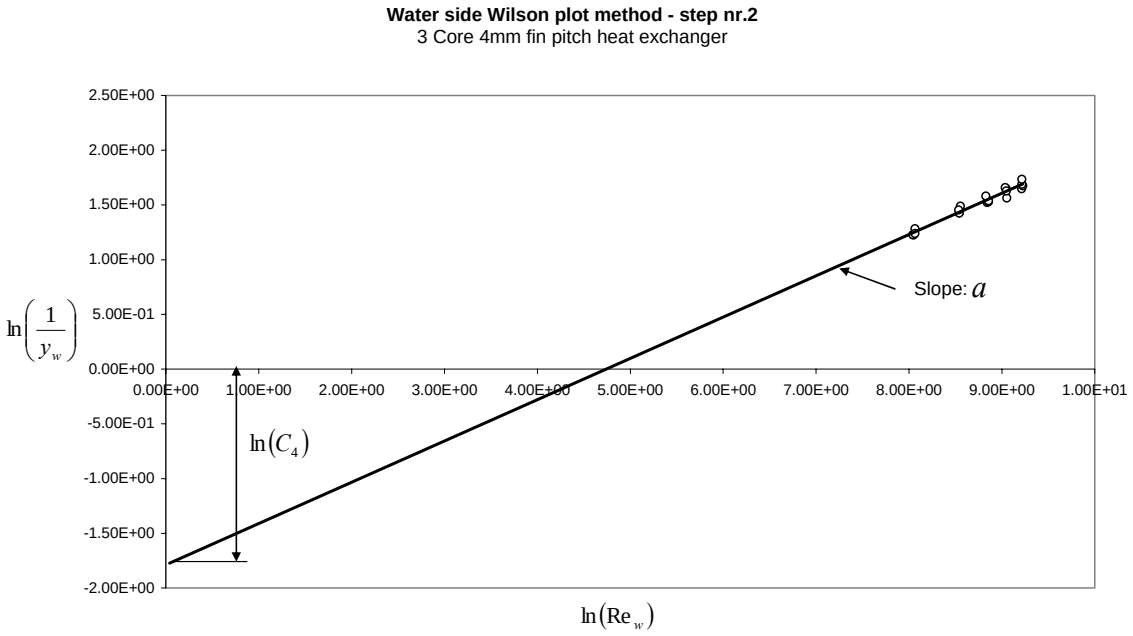

Figure 2.6 - Wilson plot method to determine the value of a

An iterative process now followed, where values of *a* were guessed again, with the knowledge of the previous results for *a* and C_4, until the values for *a* and C_4 from both figure 2.5 and figure 2.6 corresponded within reasonable limits. A minimum deviation of 7.75% was found for the variables using this iteration process. Please refer to table 2.2 for a summary of the results obtained through this process.

Table 2.2 - Results associated with the water side obtained through the modified Wilson plot method

Core	Variable	Value from 2nd last iteration	Value from last iteration	Variance	Average
3 Core, 3mm fin pitch	*a*	0.6495087	0.6487838	0.11%	0.6491463
	C_4	0.0233576	0.0216586	7.27%	0.0225082
3 Core, 4mm fin pitch	*a*	0.3774755	0.3773013	0.05%	0.3773883
	C_4	0.1800915	0.1671350	7.75%	0.1736133

2.7.2 Determining the constants associated with the air side

Using the same method but different equations, it was also possible to determine the values for d and C_5. Equation 2.3 shows equation 1.15 in a rewritten form which was used for this modified Wilson plot. It should be noted that in this calculation, the heat transfer rate of the Reynolds number of the water needed to remain constant within reasonable limits to ensure that C_w remained constant. Table 2.3 gives a summary of the constants required to perform the calculation.

$$\left[\frac{1}{UA} - R_w\right]\left[\frac{\mu_{ww}}{\mu_{mw}}\right]^{-0.14} = \frac{1}{C_5}\left[\frac{\left(\frac{\mu_{ww}}{\mu_{mw}}\right)^{-0.14} \Big/ \left(\frac{\mu_{ma}}{\mu_{ma}}\right)^{-0.14}}{\left[\frac{\mathrm{Re}_a^{d}\,\mathrm{Pr}_a^{0.4}\,A_a k_a}{D_{ha}}\right]}\right] + C_w \tag{2.3}$$

where

$$C_w = \frac{1}{C_4\left[\frac{\mathrm{Re}_w^{a}\,\mathrm{Pr}_w^{0.4}\,A_w k_w}{D_{hw}}\right]}$$

Table 2.3 - Constant values associated with the air side

Constant	Value (3 Core 3mm fin pitch)	Value (3 Core 4mm fin pitch)	Reference to view calculation/data sheets
A_a	13.5423m^2	10.6599m^2	Please refer to appendix E, paragraph E.3
k_a	0.02705W/m K	0.02705 W/mK	Value obtained from data sheet in Mills [6]
D_{ha}	0.0024898m	0.0031231m	Please refer to appendix E, paragraph E.4
Pr_a	0.693	0.693	Value obtained from data sheet in Mills [6]

As the values of a and C_4 were known by this time, the values were used in equation 2.4. A value for d is however guessed, to start the iteration process. Figure 2.7 shows the

results obtained from the first plot, showing how the value for C_5 was obtained in the first iteration of this section of the Wilson plot.

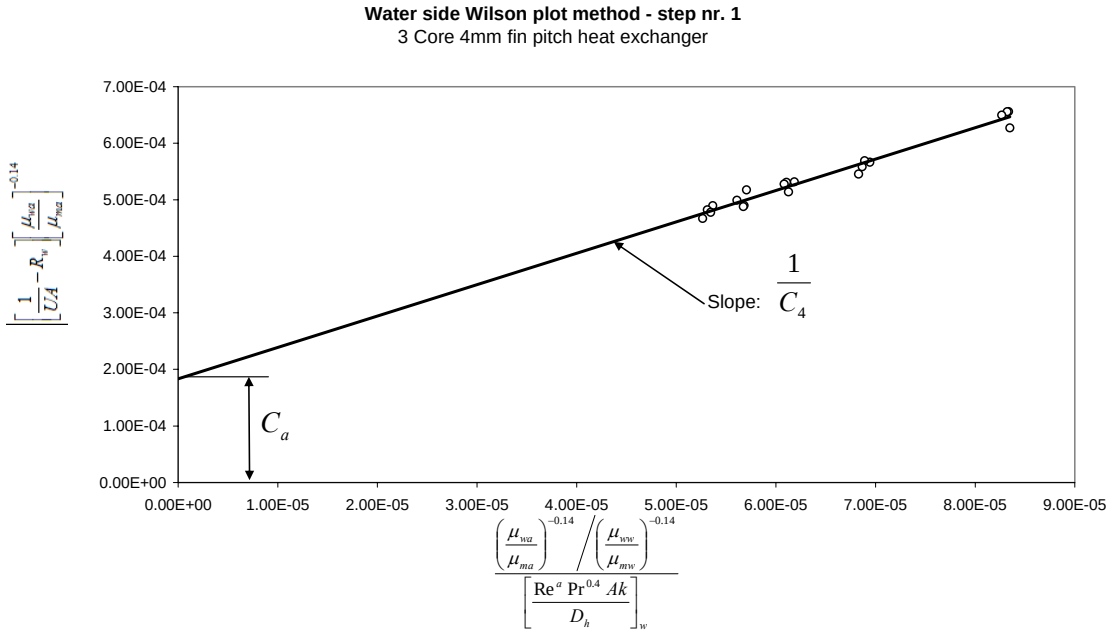

Figure 2.7 - Wilson plot method to determine the value of C_5

Similar to the previous process of determining a and C_4, equation 2.3 can be rewritten as follows:

$$\left[\frac{1}{UA} - R_w - \frac{C_a}{\left(\frac{\mu_{ww}}{\mu_{mw}}\right)^{-0.14}}\right]\left[\frac{\mathrm{Pr}^{0.4}\,Ak}{D_h}\right]_a\left(\frac{\mu_{wa}}{\mu_{ma}}\right)^{-0.14} = \frac{1}{C_5\,\mathrm{Re}_a^{\,d}} \tag{2.4}$$

By substituting y_a with the left-hand term in equation 2.5, the following equation results:

$$\ln\left(\frac{1}{y_a}\right) = d\ln(\mathrm{Re}_a) + \ln(C_5) \tag{2.5}$$

where

$$y_a = \left[\frac{1}{UA} - R_w - \frac{C_a}{\left(\frac{\mu_{ww}}{\mu_{mw}} \right)^{-0.14}} \right] \left[\frac{\mathrm{Pr}^{0.4}\, Ak}{D_h} \right]_a \left(\frac{\mu_{wa}}{\mu_{ma}} \right)^{-0.14}$$

Once again the data was plotted and a straight line fitted through the various points. From figure 2.8, the value for *d* was determined, using the value of C_5 obtained in figure 2.7.

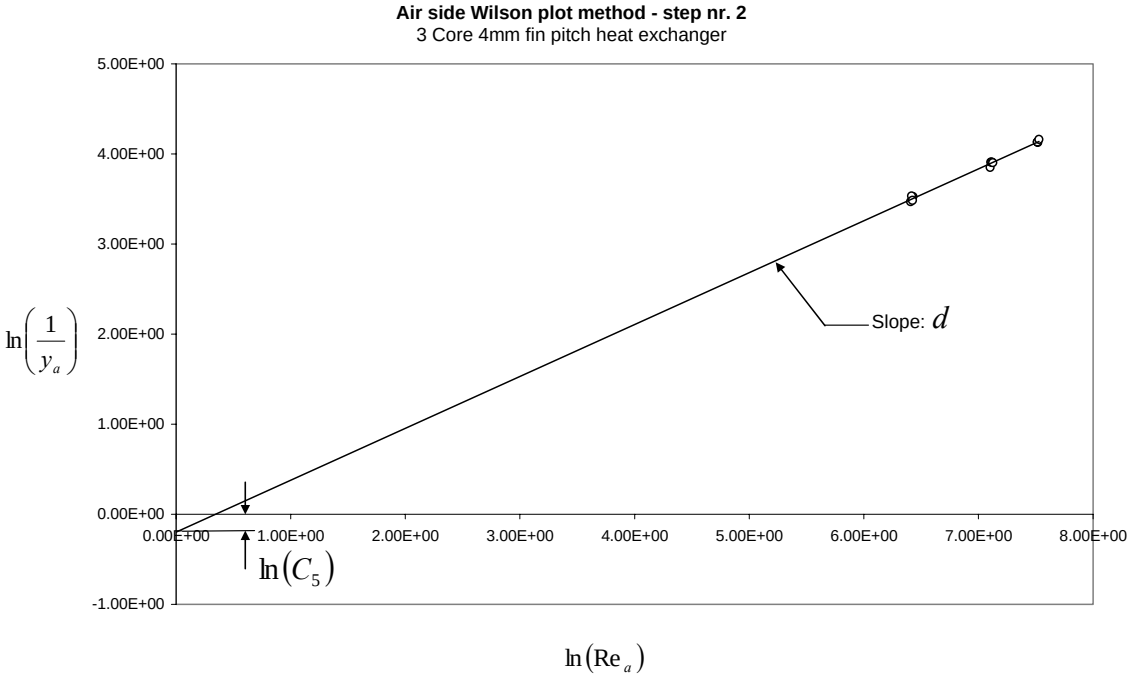

Figure 2.8 - Wilson plot method to determine the value of d

An iteration process followed once again, substituting or guessing new values for *d*, and comparing the results for *d* between figures 2.7 and 2.8. A minimum variance of 4.18% resulted between the iterations. The constant values for *d* and C_5 for both heat exchangers are presented in table 2.4.

Table 2.4 - Results associated with the air side obtained through the modified Wilson plot method

Core	Variable	Value from step 1	Value from step 2	Variance	Average
3 Core, 3mm fin pitch	d	0.4890928	0.4830638	1.23%	0.4860783
	C_5	1.0153558	1.0578384	4.18%	1.0365971
3 Core, 4mm fin pitch	d	0.5736116	0.5762401	0.45%	0.5749259
	C_5	0.8353207	0.8203995	1.79%	0.8278601

2.7.3 Combining the results to have a single characterisation equation

The heat exchanger characterisation was completed by substituting the average value determined for the 4 constants (a, d ,C_4 and C_5) into equation 1.15. By doing so, the populated equation describes UA as a single function of both the Reynolds number of the water as well as air for the specific heat exchanger. To obtain a characteristic equation for each heat exchanger, equation 1.1 is rewritten as follows:

$$\dot{Q}_{dissp} = \dot{m}_a c_{pa}(T_{win} - T_{ain})\varepsilon \tag{2.6}$$

Substituting equation 1.4 into 1.8 and 1.8 into 2.6 results in an equation which describes the heat transfer as a function of inlet temperature difference of the fluids ($T_{w,in}$ and $T_{a,in}$), mass flow rate of the air ($\dot{m}_a$) and the Reynolds numbers of both fluids (Re_a and Re_w). The final form of the characteristic equation can be viewed in terms of constants in equation 2.7.

$$\dot{Q}_{dissp} = \dot{m}_a c_p (T_{w,in} - T_{a,in}) \frac{1}{R_c}\left[1 - (\exp(-3KR_c))\left(1 + R_c K^2 (3 - K) + \frac{3R_c^2 K^4}{2}\right)\right] \tag{2.7}$$

where

$$K = 1 - \exp\left\{ \frac{-\left(\frac{1}{C_4\left(\left(\frac{\mathrm{Re}_w^{a}\,\mathrm{Pr}_w^{0.4}\,A_w k_w}{D_{hw}} \right)\left(\frac{\mu_{ww}}{\mu_{mw}} \right)^{-0.14} \right)} + \frac{1}{\left(C_5\left(\frac{\mathrm{Re}_a^{d}\,\mathrm{Pr}_a^{0.4}\,A_a k_a}{D_{ha}} \right)\left(\frac{\mu_{wa}}{\mu_{ma}} \right)^{-0.14} \right)} \right)^{-1}}{3 \times C_{\min}} \right\}$$

To test the accuracy of the characterisation, the experimental data was used to determine the largest deviation from the recorded data in the experiments. A total number of 28 heat transfer measurements were used in the characterisation of each heat exchanger core, with a maximum deviation from the actual heat transfer rate measured of 4.52%. Appendix F shows the deviation from measured values to the approximated values found through equation 2.7 for both heat exchanger cores. Please note that a maximum NTU of 3 was not exceeded as to the requirements listed in the literature.

2.8 Findings with regard to the heat transfer of heat exchangers tested

In order to visualise the heat transfer rate of the heat exchangers and comparisons between the exchangers, the functions of both the 3 core 3mm fin pitch and 3 core 4mm fin pitch heat exchangers are given in a map in figure 2.9 and 2.10 for an inlet temperature difference of 40°C.

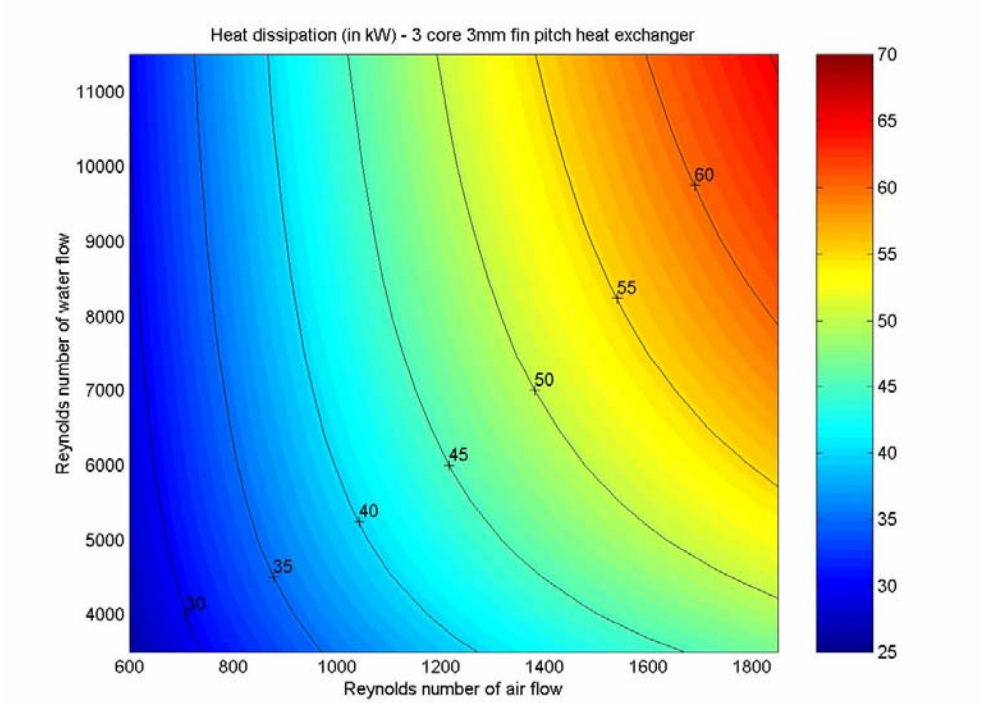

Figure 2.9 - Heat map for 3 core 3mm fin pitch heat exchanger as a function of the Reynolds numbers of the fluids

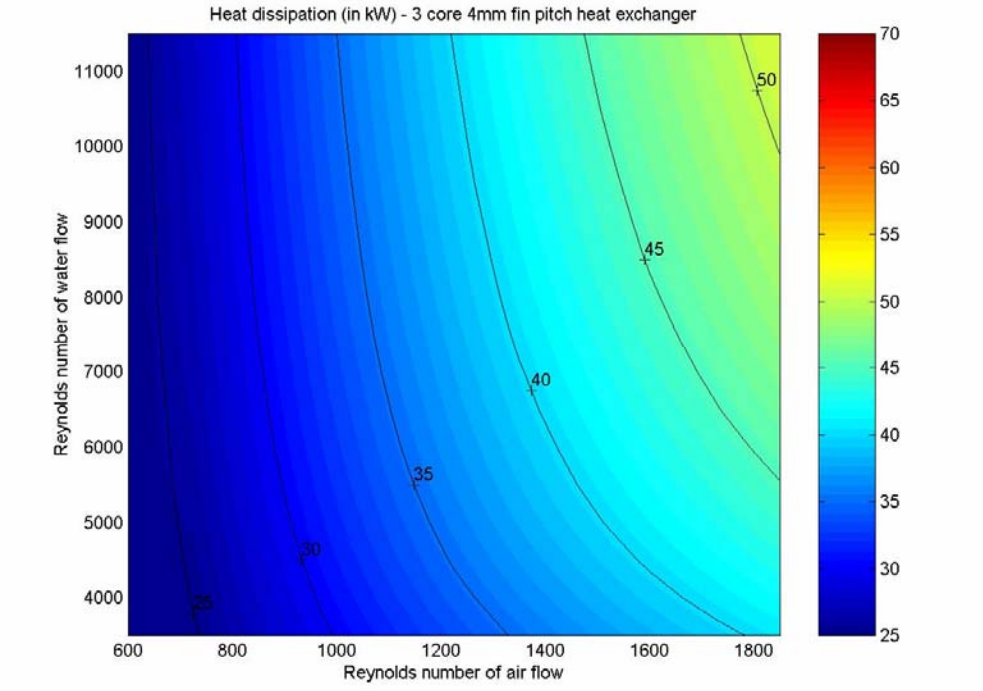

Figure 2.10 - Heat map for 3 core 4mm fin pitch heat exchanger as a function of the Reynolds numbers of the fluids

The heat maps are plotted against the same colour key, making comparison between the two maps easily digestible. The maps clearly show that the 3 core 3mm fin pitch heat exchanger has a superior heat transfer rate at every point on the map in the range that is presented, i.e. higher heat transfer at lower Reynolds numbers. It is also noticeable that this heat exchanger has a larger gradient in the direction of the waterflow Reynolds number compared to the 3 core 4 mm fin pitch heat exchanger. Similarly, the gradient is also higher in the direction of increasing airflow Reynolds number.

Although the heat transfer maps clearly identify the 3 core 3mm fin pitch heat exchanger as the exchanger with more favourable heat transfer characteristics, a conclusion as to the superiority of the heat exchanger cannot be made as the effect of the vehicle has not been included. Whilst both heat exchangers have the same waterflow geometry through the exchanger, differences in the airflow rate through the heat exchangers are expected once installed in the vehicle. In essence, the heat maps presented in this chapter cannot be used in isolation to identify the most appropriate heat exchanger for an application, but give a good understanding of the potential capability of the exchanger when the same Reynolds numbers of flow are maintained in the system.

2.9 Summary

This chapter has presented the characterisation of two heat exchanger cores in a controlled environment as part of the input required for a total cooling system model. The cores selected for characterisation and their properties are discussed. Furthermore, the experimental equipment and facility used during the tests are outlined as well as the procedure followed to obtain the required data. Using the modified Wilson plot method, the heat transfer resistances on the water side of the heat exchanger as well as the air side are determined through an iteration process revealing 4 constants. Through manipulation of the standard equation governing heat transfer through a compact heat exchanger it is possible to summarise the heat transfer characteristics as a single equation for each heat exchanger. To highlight the difference between the two cores evaluated, heat transfer

contour maps are presented as functions of the Reynolds numbers of the fluids, making comparison between the cores in ideal conditions possible at a specific inlet temperature difference between the fluids.

CHAPTER 3
INCLUDING THE INFLUENCE OF THE VEHICLE ON THE HEAT TRANSFER PROCESS

3.1 Preamble

The characteristic equations predicting the heat transfer through a heat exchanger core was obtained for two heat exchangers operating in a controlled environment in chapter 2. By changing the input frequency to the motors driving the fluid flow, the flow rates of the fluids were adjusted to suit the requirements for the tests. When the application of such a heat exchanger is evaluated in a vehicle, it is found that the fluid flow rates are dependent on the engine and vehicle speed. As it has been shown in chapter 1, the specific vehicle configuration as well as the speed of the vehicle will have an effect on the airflow through the heat exchanger. The water flow rate on the other hand will be dependent on the engine speed. Using these relationships, it is possible to develop a version of equation 2.7 that is more user friendly for a rally team, relating the appropriate variables to vehicle operating variables. In short, the first objective of this chapter is to include the effect of the vehicle on the cooling system through rewriting the fluid flow rates in terms of the vehicle or engine speed.

It is known that the ambient conditions in which a vehicle is operated will also have an effect on the cooling performance of the cooling system. To include this effect, the primary variables that will be dependent on atmospheric temperature and pressure variations will be identified. Rewriting the characterisation equation to include this will result in an equation that can be used to determine the cooling capability of a specific cooling configuration under certain ambient conditions.

It should be noted that the vehicle dependent information used to rewrite the characteristic equations was obtained from the vehicle manufacturer for the specific

vehicle under evaluation. The experimental procedure to determine the dependence of airflow rate and water flow rate on vehicle speed and engine speed respectively will not be discussed, as the focus will be placed on deriving the cooling capability shown on the left of process diagram 1.1. The *influence* of the relationships will however be evaluated by comparing the performance of both cooling systems at standard ambient conditions.

3.2 Case study vehicle cooling system configuration

The vehicle made available to serve as a case study, is a modified production vehicle equipped with a high performance engine and driveline, as well as all the equipment required to comply with the national South African rally championship of 2000. Due to the competitive nature of rally cars, the exact components used as well as their specifications cannot be published. Reviewing the cooling system of the specific vehicle on a high level, we find that it consists of:

- a fan belt driven water pump,
- thermostat,
- a heat exchanger core,
- an oil-to-water heat exchanger fitted at the inlet of the waterflow channel to the heat exchanger,
- ram air duct at the inlet of the heat exchanger,
- and the necessary piping to complete the system.

The omission of a cooling fan on the vehicle should be noted. This is due to volumetric constraints in the engine compartment. On the standard vehicle set-up, airflow through the heat exchanger depends only on the ram effect on the inlet of the exchanger. Without a fan the mass flow of air through the standard system is totally dependent on the speed of the vehicle, with the driver enjoying the benefit of the additional power available due to the omission of this power consumer. It should also be noted that the case study vehicle with the standard configuration is a good representation of most vehicles found in this application including the cooling system configuration.

3.3 Vehicle dependent variables

The water pump on the case study vehicle is driven by means of a pulley and belt, obtaining the power required from the crankshaft. Only increases and decreases in the engine speed affect the volume flow rate of water through the heat exchanger. On the other hand, the volume flow rate of air through the heat exchanger core is driven by the vehicle speed. Further factors do however influence the mass flow rate of air through the exchanger. The aerodynamic properties of the vehicle's outer skin as well as the placement of components in the engine compartment play a large role and have a huge impact on the thermal flow rate.

The influence of the relationships between the engine speed and waterflow rate through the cooling system, as well as the vehicle speed and air speed will now be discussed. It is important to note that the information received from the vehicle manufacturer in this section is only applicable to the specific vehicle and furthermore the configuration of the vehicle during testing, which from here on will be referred to as the standard configuration.

3.3.1 Airflow rate characteristics of the vehicle

The airflow rate through the heat exchanger is not only a function of the pressure drop over the heat exchanger, but also of the geometry of the vehicle, as it will dictate the high and low pressures surrounding the vehicle. There are two methods of confronting this problem. The first option is to determine the airflow rate through the exchanger core through the use of computational fluid dynamics (CFD). The second method is to physically test the airflow through the exchanger by using a number of pressure transducers at the inlet and outlet of the heat exchanger whilst measuring the vehicle speed.

Even though a three dimensional CFD analysis would reveal more pressure points, and thus more detail of the velocity flow pattern over the heat exchanger inlet, the rally team decided to use the latter option as a CFD analysis would in any case require experimental verification. An experimental test was performed by the team through which the correlation between the vehicle speed and the airflow rate through the heat exchanger core was determined. The test included measuring the static and stagnation pressures at various positions in front of the heat exchanger inlet, whilst simultaneously measuring the vehicle speed. Using this information the air speed at the heat exchanger inlet was determined for each vehicle speed at which the test was performed.

Figure 3.1 shows the data points collected by the team during their investigation into the relationship. Similar to the results published by El-Bourini [37], refer to figure 1.9a, it is found that the relationship between vehicle speed and air speed is not linear. In order to use this data in the characteristic equations, it is required to express the air speed as a function of the vehicle speed. Having obtained the data between vehicle speeds of 0 and 120 km/h, extrapolation of the fitted curve beyond 120 km/h is not required as the range is representative of vehicle speeds on demanding stages. A second order polynomial, of the form shown in equation 3.1, is thus utilised to describe the dependence of the air speed through the heat exchanger on the vehicle speed.

$$V_a = fV_D^2 + gV_D \tag{3.1}$$

Using the method of least squares to fit the curves, the constants in table 3.1 resulted. To justify the use of a second order polynomial function, the maximum percentage deviations were calculated. A deviation of only 5.73% was found between the actual data and the mathematical approximation which is suitably accurate for the purpose of the model.

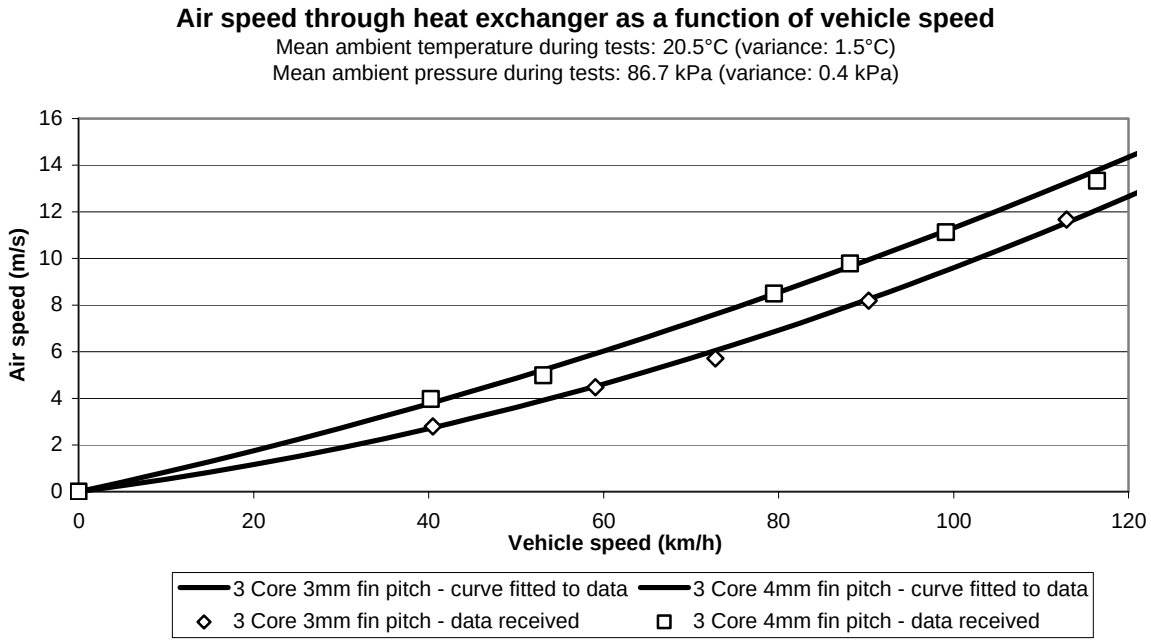

Figure 3.1 - Air speed through heat exchanger core as a function of vehicle speed

Table 3.1: Curve fit results for data fitted to equation 3.1 using the method of least squares

Heat exchanger	***f***	***g***	**Maximum percentage deviation**
3 Core 3mm fin pitch	4.7486×10^{-4}	4.8523×10^{-2}	5.73%
3 Core 4mm fin pitch	3.1614×10^{-4}	8.1545×10^{-2}	4.58%

Equation 2.7 requires that the flow rate of the air be expressed as the *mass* flow rate. This is achieved by taking the frontal area of the heat exchanger as well as the air density into consideration. Please refer to equation 3.2.

$$\dot{m}_a = \rho_a A_{front} V_a \tag{3.2}$$

Substituting equation 3.1 in 3.2 the mass flow rate of the air can be expressed as a function of vehicle speed in kilometres per hour as shown in equation 3.3.

$$\dot{m}_a = \rho_a A_{front}\left(fV_D^2 + gV_D\right) \tag{3.3}$$

Similarly, the Reynolds number of the air stream can be described as a function of vehicle speed:

$$\mathrm{Re}_a = \frac{\rho_a D_{ha}\left(fV_D^2 + gV_D\right)}{\mu_a} \tag{3.4}$$

Knowing the relationship of the vehicle speed as a function of the engine speed for a specific vehicle driveline configuration it is also possible to describe the mass flow rate of air as a function of the engine speed per selected gear. Equation 3.5 describes this relationship for the first gear, with the constant n_1 giving the relationship between the engine speed and the vehicle speed, thus taking into account the transmission ratio, final drive ratio as well as the size of the tyres. As these ratios are known for all the gears in the six speed transmission, n_1 can be substituted with n_2 and n_3 for second and third gear relationships respectively up to n_6 for sixth gear. Please refer to appendix G for the actual values of n_1 to n_6 as well as the method of calculation.

$$V_D = n_1 v_{engine} \tag{3.5}$$

Substituting equation 3.5 into 3.3 and 3.4 yields the dependence of the mass flow rate and Reynolds number on the engine speed through equations 3.6 and 3.7 respectively for first gear. These equations summarise the effect of the vehicle on the mass flow rate and Reynolds number of air through the heat exchanger.

$$\dot{m}_a = \rho_a A_{front}\left(f\left(n_1 v_{engine}\right)^2 + g\left(n_1 v_{engine}\right)\right) \tag{3.6}$$

$$\mathrm{Re}_a = \frac{\rho_a D_{ha}\left(f\left(n_1 v_{engine}\right)^2 + g\left(n_1 v_{engine}\right)\right)}{\mu_a} \tag{3.7}$$

3.3.2 Waterflow rate characteristics of the vehicle

The waterflow rate as a function of engine speed was obtained for the two heat exchangers under evaluation. The vehicle manufacturer supplied the information recorded in a simple experiment with a waterflow meter inserted in the waterflow line, and a tachometer on the engine. By running the engine at a constant engine speed with the thermostat blocked in the open position, the waterflow rate through the water system was measured for different engine speeds. It should be noted that the data recorded was in terms of volume flow per second as a function of engine speed. Figure 3.2 was plotted by including the effect of water density, giving the mass flow rate of water as a function of engine speed.

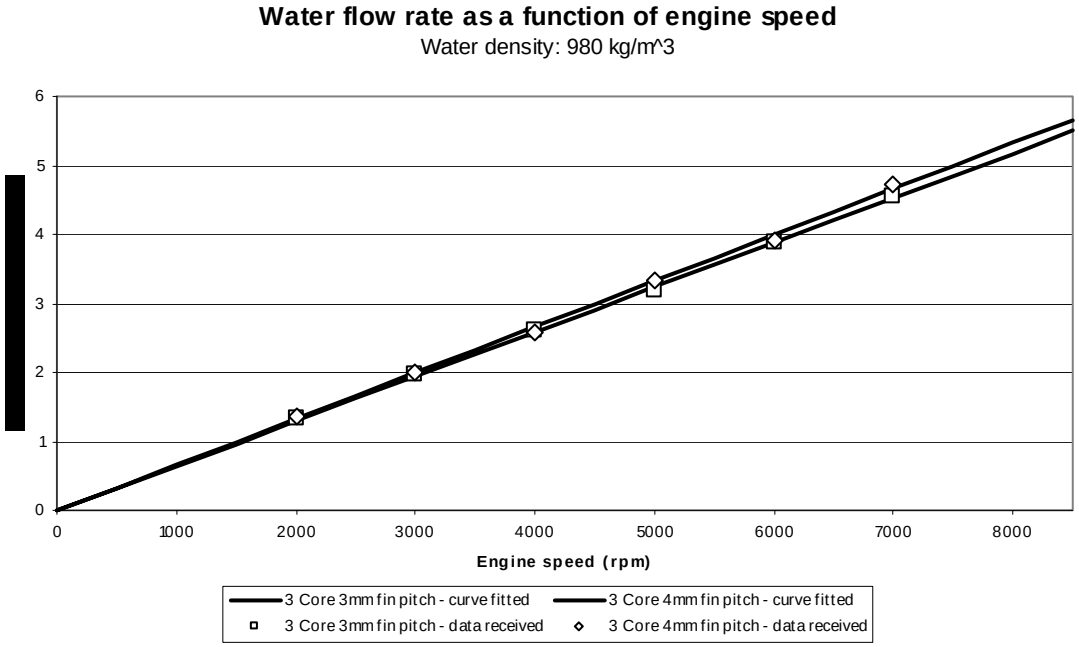

Figure 3.2: Water mass flow rate through the cooling system as a function of engine speed

Knowing that the two heat exchangers under evaluation have the same waterflow channel as well as top and bottom tank arrangement, it was expected that the data recorded would have been the same. A maximum difference of 4.6% is however recorded, which

although relatively small, may have an effect on the cooling characteristics. The difference in functions can be ascribed to:

- Experimental errors during the recording of the data by the rally team,
- Manufacturing differences such as the friction on the inside of the waterflow channels differing between the heat exchanger cores.

Through fitting a curve using a first order polynomial, shown in equation 3.8, the mass flow rate of the water is described as a function of engine speed. Please refer to figure 3.2 to view the curve fit to the actual data. In this case a maximum deviation of the data from the fit is 3.23% showing that the error associated with the mathematical approximation is small.

$$\dot{m}_w = j\, v_{engine} \tag{3.8}$$

Table 3.2: Curve fit results for data fitted to equation 3.8 using the method of least squares

Heat exchanger	***j***	**Maximum percentage deviation**
3 Core 3mm fin pitch	6.4640×10^{-4}	2.28%
3 Core 4mm fin pitch	6.6602×10^{-4}	3,23%

To integrate equation 3.8 in the characterisation equations 2.7, it is required to obtain the water velocity through the individual tubes. The bulk volume flow as measured by the team can be found by dividing the approximation equation for the mass flow rate as per equation 3.8 on the left and right hand side by the density of the water.

$$\dot{Vol}_w = \frac{\dot{m}_w}{\rho_w} = \frac{j\, v_{engine}}{\rho_w} \tag{3.9}$$

From equation 3.9, the velocity in the heat exchanger tube is calculated by dividing the volume flow rate passing through the heat exchanger by the nett tube inlet area. The nett

tube inlet area is defined as the sum of all the inlet areas of the tubes for a specific heat exchanger (please refer to appendix E to view calculations). As the water sides of the heat exchangers tested are identical, the nett inlet area will also be identical for both heat exchangers evaluated. Equation 3.9 is thus included in the Reynolds number calculation as follows:

$$\mathrm{Re}_w = \frac{D_{hw}\, j\, v_{engine}}{\mu_w A_{caw}} \tag{3.10}$$

3.4 Ambient conditions

The prevailing ambient conditions, i.e. ambient temperature and pressure, affect three variables in equation 2.7 to a greater or lesser extent. Only one direct dependency is however found on the ambient temperature, being the *air inlet temperature* to the heat exchanger. The air inlet temperature partially dictates the maximum amount of heat transferable at a constant water inlet temperature and subsequently has a great effect on the total characteristic equation. The other variables dependent on the ambient conditions are the *mass flow rate of the air* passing through the heat exchanger, and the *Reynolds number for the airflow*. Both these variables are indirectly influenced as the driving factor is the changing density of air with changing ambient conditions.

As the inlet air temperature is automatically included in the characteristic equation, manipulation of the equation in this regard is not required. However, to include the dependence of the air density on the ambient conditions, the ideal gas law is employed as given in equation 3.11.

$$\rho_a = \frac{P_{amb}}{RT_{amb}} \tag{3.11}$$

Substituting equation 3.11 into 3.6, the ambient conditions are included as per equation 3.12. Although the density of the fluid will change as the fluid is heated passing through the heat exchanger, the mass flow of air measured at the entrance of the heat exchanger will remain constant for a given vehicle speed.

$$\dot{m}_a = A_{front}\left(\frac{P_{amb}}{RT_{amb}}\right)\left(f\left(n_1 v_{engine}\right)^2 + g\left(n_1 v_{engine}\right)\right) \tag{3.12}$$

Substituting equation 3.11 in 3.7 yields the Reynolds number for airflow as a function of the ambient conditions, as shown in equation 3.13.

$$\mathrm{Re}_a = \frac{D_{ha}\left(f\left(n_1 v_{engine}\right)^2 + g\left(n_1 v_{engine}\right)\right)}{\mu_a} \times \left(\frac{P_{amb}}{RT_{amb}}\right) \tag{3.13}$$

Equations 3.12 and 3.13 conclude the ambient effect on the cooling capability of the heat exchanger. It should be noted that the ambient conditions do have an effect on the heat generated which will be included and discussed in Chapter 4.

3.5 Overall cooling capacity of the cooling systems

Three variables have been rewritten in the previous sections to take the effect of the vehicle into account as well as the ambient conditions. The altered variables are:

- Reynolds number for waterflow (equation 3.10),
- Mass flow rate of air (equation 3.12),
- Reynolds number for air (equation 3.13).

Through substitution of these relationships into equation 2.7, the heat transfer for a specific vehicle can be expressed as a function of:

- Engine speed (rpm),

- Vehicle speed – engine speed relationship (ratio),
- Ambient pressure (Pa),
- Ambient temperature (K).

Evaluating the modified versions of equation 2.7, it now becomes possible to predict the cooling capability of the cooling system in the standard vehicle per gear for the prevailing conditions. Using standard conditions the cooling performance is shown for both the 3 core 3mm fin pitch as well as the 3 core 4mm fin pitch heat exchanger in figures 3.3 and 3.4 for standard ambient conditions. Noticeably, the heat dissipation characteristics for each heat exchanger correlates with Emmenthal's [39] finding in that the minimum cooling capacity is present in the lowest gear, due to the low mass airflow through the heat exchanger. The cutt-off line coincides with the 120 km/h maximum vehicle speed for which airflow data was obtained. Further extrapolation beyond 120 km/h is not recommended as the extrapolated value cannot be validated experimentally.

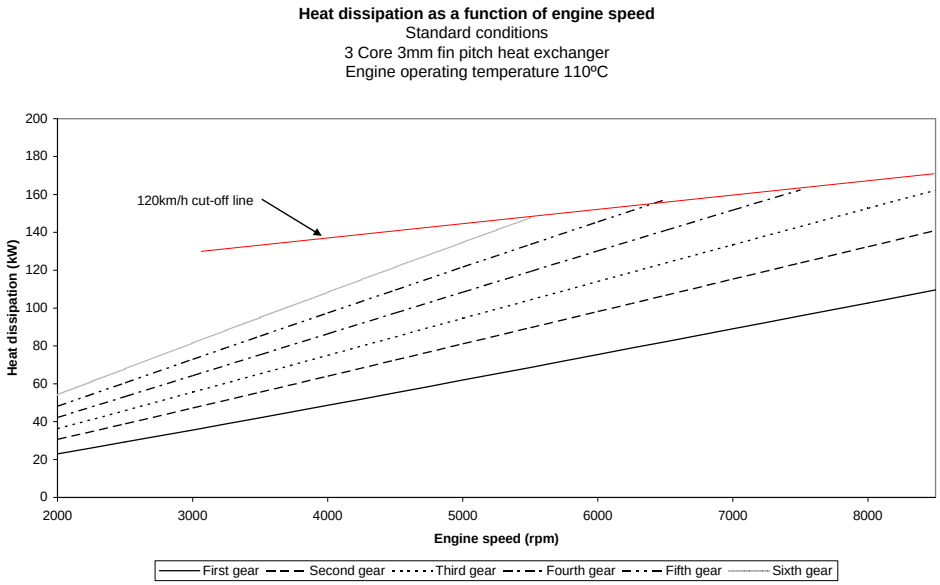

Figure 3.3 - Heat transfer rate as a function of vehicle speed and engine speed (3 core 3mm fin pitch exchanger)

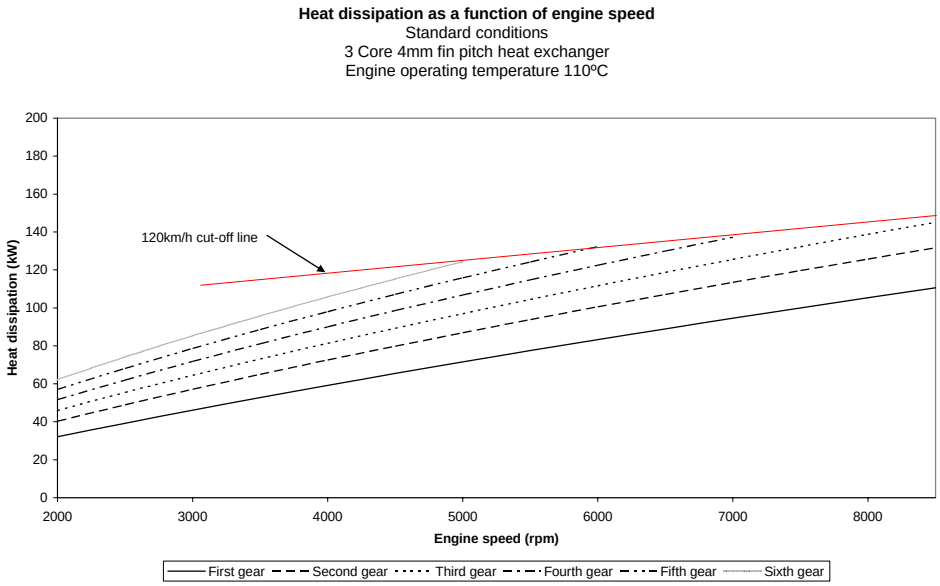

Figure 3.4 - Heat transfer rate as a function of vehicle speed and engine speed (3 core 4mm exchanger)

Comparing the performance of the 3 core 3mm and 3 core 4mm fin pitch heat exchangers in first gear, it is found that the 3 core 4mm fin pitch heat exchanger has the superior heat transfer capability over the full range of engine speed. Although the 3 core 3mm fin pitch heat exchanger has a larger heat transfer surface available, it cannot be effectively utilised at low speeds as the pressure differential over the heat exchanger is not large enough to accommodate the required airflow through the heat exchanger. This highlights the fact that heat transfer characteristics obtained from a wind tunnel experiment cannot be used in isolation, as the vehicle will dictate the flow of fluids through the exchanger for a specific vehicle and engine compartment configuration. Increasing the fin pitch further, could on the other hand lead to higher airflow rates but insufficient surface to dissipate the required heat. An optimum fin pitch will thus exist for every engine/vehicle speed.

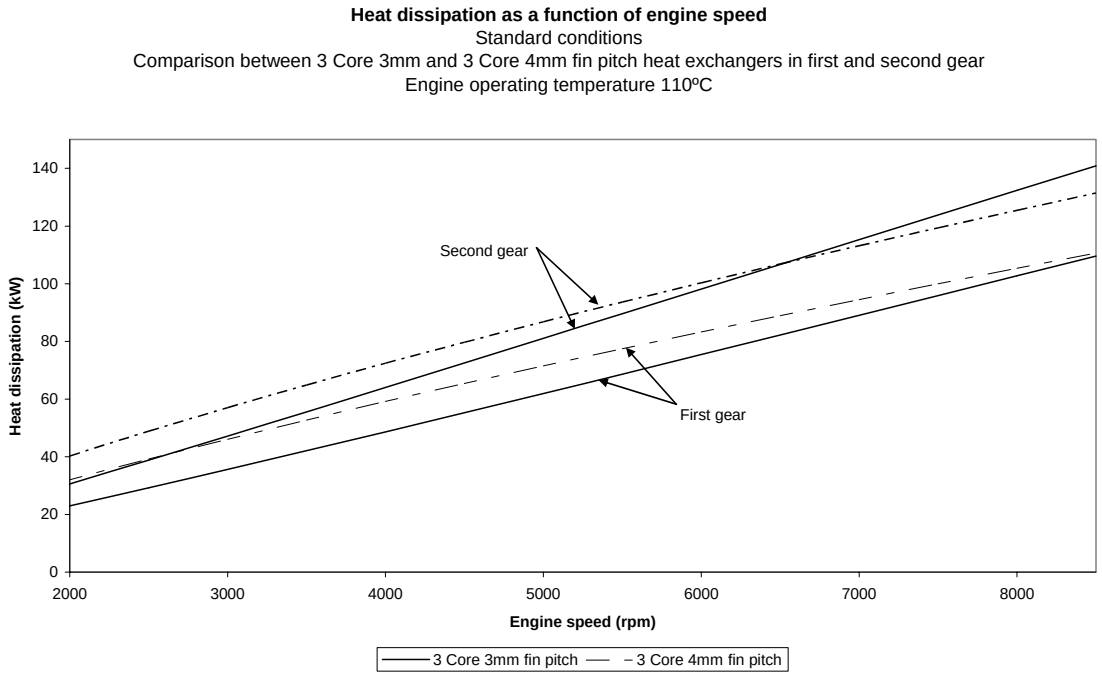

Figure 3.5 - First gear comparison between 3 core 3mm and 3 core 4mm fin pitch heat exchangers

3.6 Benchmarking the configuration for which the data was obtained

The information supplied by the rally team is for the standard configuration vehicle. As previously mentioned, the configuration in the engine compartment can be changed prior to a race, leaving the team little time to recalculate the model to include the changes in either waterflow or airflow rate. It is however possible to determine whether changes to the engine compartment configuration will have either a positive or negative effect on the airflow by performing a quick experiment.

Using equation 1.19, a heat exchanger can be classified as being porous or constricted. By using the standard configuration as a benchmark, the team will have an indication if better or worse cooling performance can be expected from the system after changing the lay-out in the engine compartment. Furthermore, this information can also help a team to

identify opportunities for improved airflow by changing the component lay-out in the engine compartment in an attempt to reduce the airflow restriction.

As seen in equation 1.19, the relationship between the air speed through the heat exchanger and the vehicle speed is required to calculate the pressure loss coefficient which identifies the porosity of the total system. Figure 3.6 shows the coefficient for the standard configuration tested in this study as a function of the vehicle speed. As expected, the lowest pressure loss coefficient is experienced by the 3 core 4mm fin pitch heat exchanger installed in the system. The outcome of the calculation shows that the pressure loss coefficient for all heat exchangers tend to decrease with an increase in vehicle speed. Comforting to the team would however be that the restriction is not as high as the restriction for the vehicle with all components installed in El-Bourini's [37] experiment, but improvements might be possible and worth investigating.

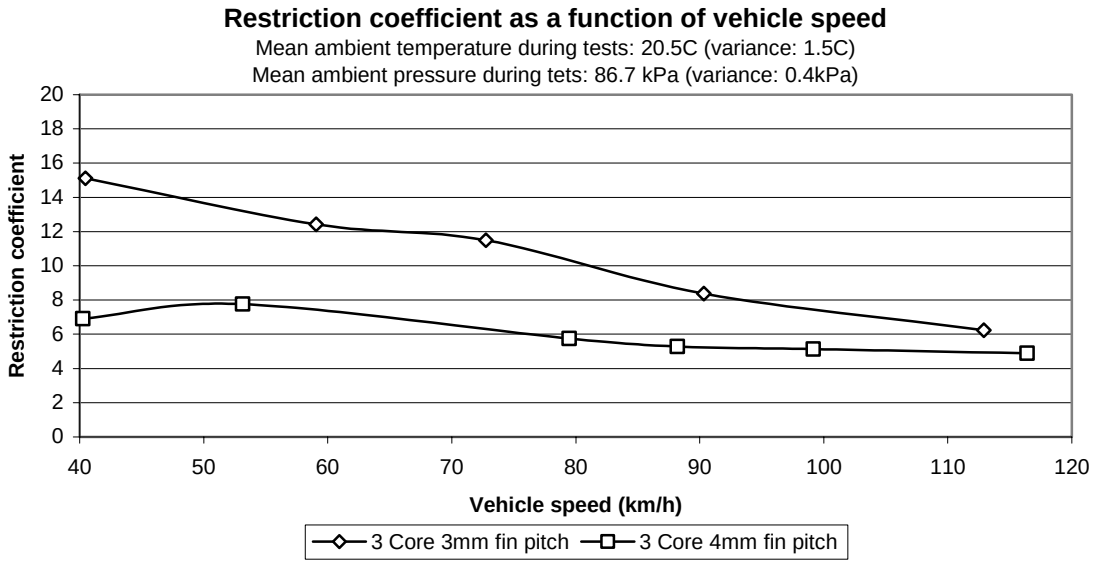

Figure 3.6: Restriction as a function of vehicle speed

3.7 Summary

This chapter has given a brief description of the cooling system and components found on the case study vehicle, stressing the omission of a cooling fan on the heat exchanger. Information with regard to the dependence of the airflow rate on the vehicle speed and the waterflow rate on the engine speed was obtained from the manufacturer. Fitting curves through the data obtained and using driveline information it was possible to express both the flow rates as functions of engine speed and gear selection. Furthermore, the influence of the ambient conditions were identified and included in the characterisation equations, making it possible to express the heat transfer capability as a function of engine speed, gear selection and ambient conditions. Using the modified characteristic equation, the cooling system performance was predicted for both heat exchangers in the cooling system, clearly showing that the lowest cooling performance is in first gear in both cases. A comparison between the performances in first gear also shows that the influence of the airflow rate is significant. Finally the standard configuration for both heat exchangers in the cooling system was benchmarked in terms of a pressure loss coefficient, making it possible for a team to optimise the placement of components in the engine compartment, as well as assess whether changes will have a negative or positive effect on the cooling system performance.

CHAPTER 4
EVALUATING ENGINE CHARACTERISTICS AND SOLVING THE ENERGY BALANCE

4.1 Preamble

Only the heat dissipation characteristics have been discussed in the previous two chapters. The final input required in the heat transfer problem is the heat generated by the engine at specific ambient conditions as shown in process diagram 1.1. The ability to predict the heat produced by the engine has enjoyed much attention in previous research but remains highly dependent on the engine design. A *general equation* to accurately predict the portion of heat transferred to the cooling system for all engine configurations does not exist [40][41][42]. The only method that remains for heat load prediction is experimental testing of the engine, which will provide the cooling requirement as a function of engine speed at maximum load. A further variable in this function is the effect of prevailing ambient conditions on the power produced by the engine, which directly affects the heat load produced.

Once the heat load on the cooling system of a vehicle is known, the manner in which the vehicle is typically operated will define the heat load requirements on the cooling system. Emmenthal's [37] design criteria for passenger type vehicles operating in typical European traffic conditions can be a valuable first order estimation to review a specific cooling system. However, as massive weight savings can be made on rally cars without the requirement to operate at maximum gross vehicle mass, the applicability of this design parameter can be questioned.

Information on the engine characteristics and the heat load generated by the engine was obtained from the manufacturer at specific ambient conditions. Once again, the focus in this chapter is to use the information in such a manner as to include it in the model, and not an in-depth investigation into the experimental procedure followed to

obtain the heat load results. A general overview of experiments performed, will however be given.

Finally, the results obtained through the previous chapters are combined with the characteristic equation of the heat load generated through the use of an energy balance equation. With the energy balance being sensitive to the prevailing ambient conditions, it becomes possible to predict whether or not a heat exchanger will be able to dissipate the required heat. If the exchanger is indeed suitable, the possibility of pumping power savings can be identified.

4.2 Case study engine and heat load characteristics

The engine, being the largest contributor to the competitiveness of the rally car, has been the main focus of development in previous years for the specific team. Figure 4.1 shows the tremendous performance of the 4-cylinder, naturally aspirated 1998 cm^3 displacement engine at various engine revolutions. Having tested the performance characteristics of the engine on a dynamometer at ambient conditions, the results are normalised to standard conditions through the use of the SABS 013 Part 1 – 1998 standard [44]. Please refer to appendix H to view the basis for these calculations, as well as the calculations performed to obtain figure 4.1.

In order to obtain the heat load transferred to the cooling system, the rally team performed an experiment on the engine dynamometer at maximum load. Thermocouples were used in the water system to obtain the thermal energy change of the water due to the heat transferred from the engine as well as the oil cooler, whilst recording the waterflow rate through the system. With the thermostat blocked in the open position and the tests performed at steady state conditions, the heat load was recorded. Using this data, the heat transferred to the cooling system was calculated using equation 4.1 for the specific engine speed at which the test was performed.

$$\dot{Q}_{gen} = \dot{m}_w \, c_{pw} \left(T_{wout\_engine} - T_{win\_engine} \right) \qquad (4.1)$$

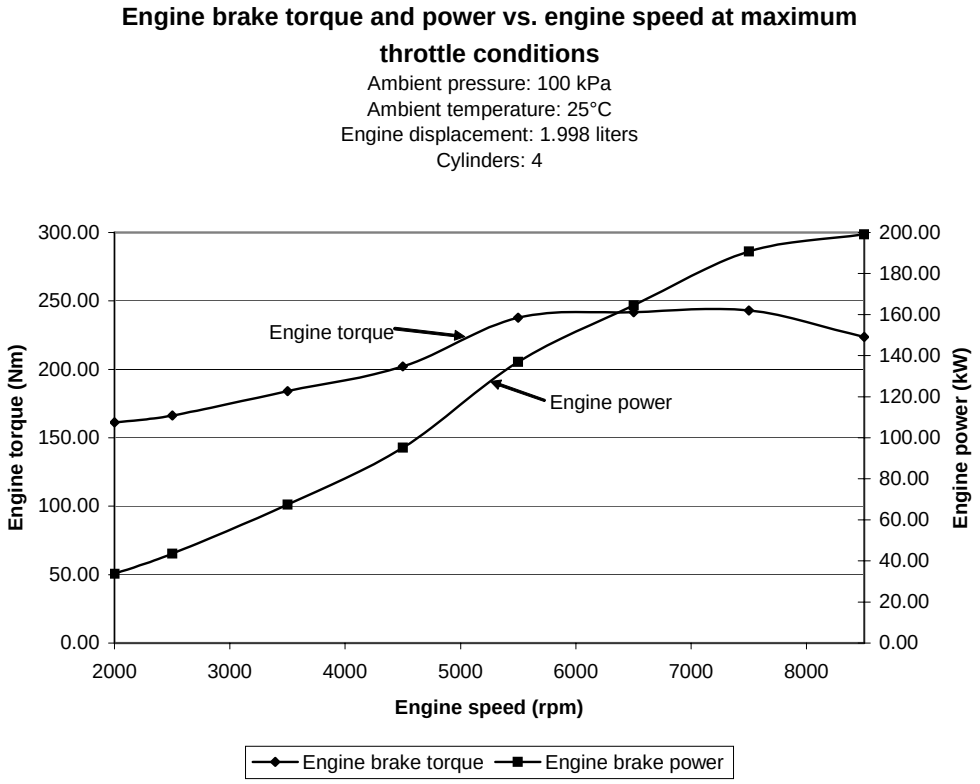

Figure 4.1 - Engine power and torque as a function of engine speed

Knowing that the mass flow rate of the water is dependent on the engine speed, the experiments were repeated at intervals of 1000 revolutions per minute in order to determine the dependence on the engine speed. Please refer to figure 4.2 for the results obtained by the team for the specific test. All tests were performed at maximum load on the engine, i.e. full throttle position at the recorded ambient conditions. Calculating the ratio of heat load to brake power generated, makes it possible to obtain a relationship between the two variables which can be used to calculate the heat load at various ambient conditions.

Evaluating the findings of the heat load to brake power ratio as shown in figure 4.2, it is found to be at the lower end of Emmenthals' [39] documented values in table 1.2. The reason for this is due to the high energy load transported through the exhaust gasses to the ambient air for this high performance engine. The explanation for this finding tendered by the manufacturer is based on the lower exhaust back pressure of the vehicle compared to standard production vehicles. Hot exhaust gasses are

dispersed into the atmosphere faster and with less effort than a normal production vehicle, hence limiting the heat transfer from the gasses to the cylinder walls, piston, valves and manifolds. As the vehicle is equipped with a high performance engine, these findings correlate with the statement that in order to obtain higher performance, the heat flux into the engine must remain as low as possible, else the combustion gas temperature and pressure will be lowered during the combustion cycle, reducing the work that is transferred to the piston [45].

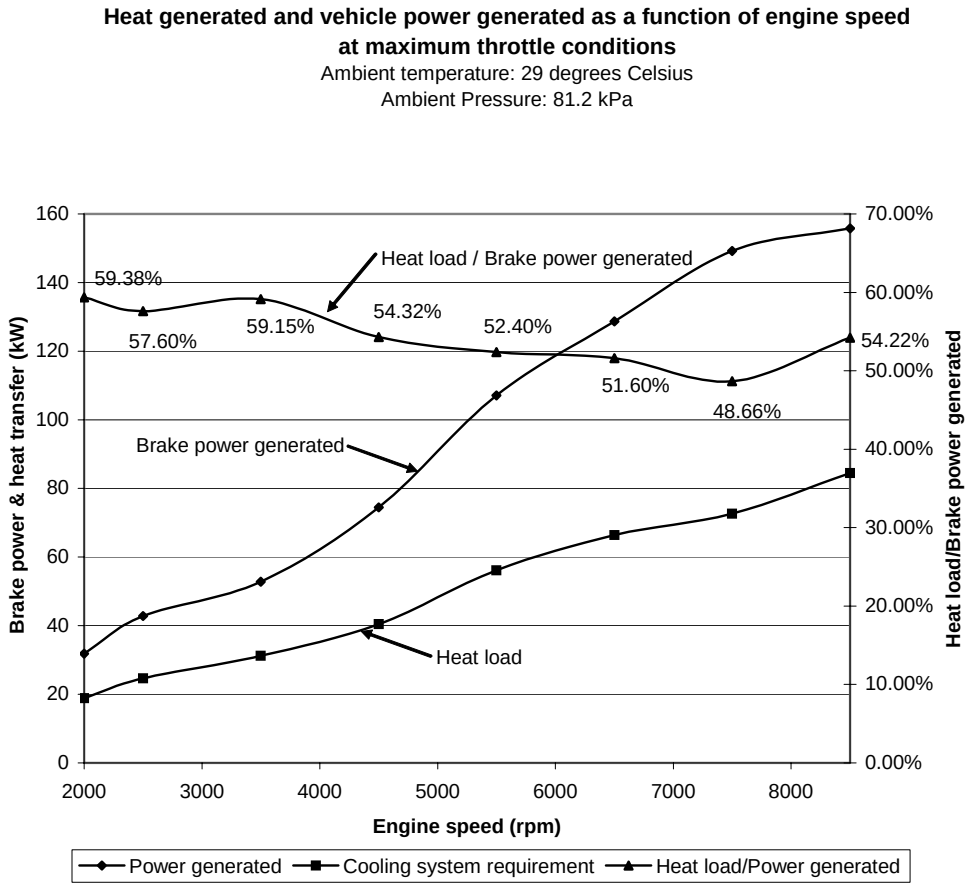

Figure 4.2 - Engine heat and power generated – tested ambient conditions

The SABS 013 standard [48] is now used to predict the power and heat load generated at standard conditions. Noticeably the ratio of heat load to brake power remains constant as the correction factor (α_a) is applied to both variables. Please refer to figure 4.3 for the normalised results.

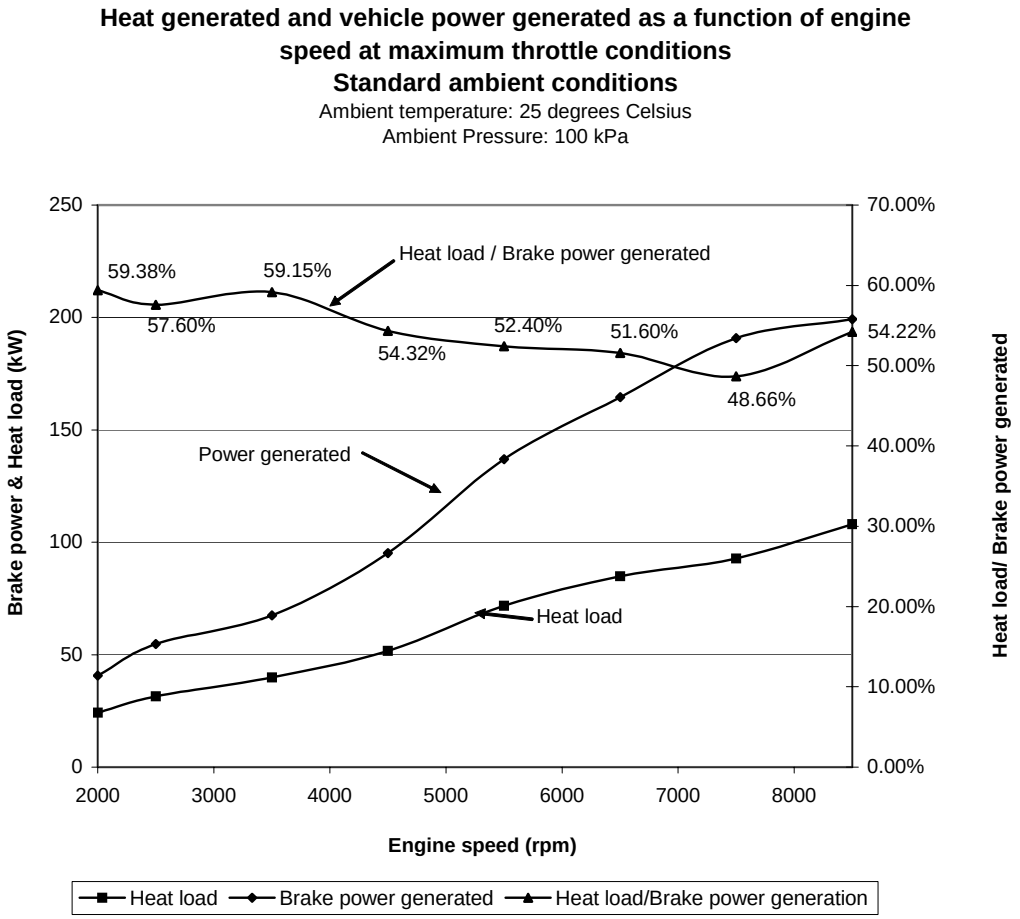

Figure 4.3 - Engine heat and power generated – standard conditions

To include the heat load data in the mathematical model, it is required to express the heat load as a function of both the engine speed, as well as the prevailing conditions. The first of these two requirements are obtained by fitting a polynomial function to the data points recorded by the team. As a recommended base function for such a curve fit is not available in published literature, a polynomial function was chosen to describe the relationship. Starting at a first order polynomial function, and evaluating the square root difference for each order fitted, it was found that a fifth order polynomial function was most accurate in describing the relationship with a square root difference of only 0.9997. Please refer to equation 4.2 and table 4.1 for the base function and constants obtained through the curve fit process.

$$\dot{Q}_{gen\_std} = pv_{engine}^{5} + rv_{engine}^{4} + sv_{engine}^{3} + tv_{engine}^{2} + wv_{engine}^{1} + x \qquad (4.2)$$

where the constants in this curve fit are found to be:

Table 4.1 – Constants associated with curve fit for heat generated at standard conditions

Constants	Values
p	1.16760×10^{-16}
r	-2.99142×10^{-12}
s	2.88565×10^{-8}
t	-1.29537×10^{-4}
w	2.80728×10^{-1}
x	-2.05927×10^{2}

As the energy balance will *only be evaluated at the tested engine speeds* for which the heat load is known, the results obtained from the curve fit can be used for the calculations to follow.

The second requirement on a characteristic equation is the inclusion of the effect of ambient conditions on the heat load generated. Using the SABS 013 standard to manipulate the heat load generated by the engine, it becomes possible to adjust the heat load at standard conditions to ambient conditions within the range for which the SABS 013 standard is applicable as stated in appendix H. Applying the adjustment factor to equation 4.2, a general relationship between heat generation, engine speed and ambient conditions results:

$$\dot{Q}_{gen} = \frac{\left(pv_{engine}^{5} + rv_{engine}^{4} + sv_{engine}^{3} + tv_{engine}^{2} + wv_{engine}^{1} + x\right)}{\alpha_a} \tag{4.3}$$

4.3 Heat load criteria for complete vehicle

Apart from the cooling system, vehicle configuration and ambient conditions, the operating conditions under which the vehicle will be driven is unknown. Not being confined to a set and known route, the engine and vehicle speed as a function of time cannot be used as an input condition in order to define a heat dissipation requirement with the help of equation 4.3. Rally routes and obstacles to be negotiated by drivers differ from one stage to the following, making it impossible to scientifically predict the heat load on the engine as a function of time.

A conservative approach to define an operating condition is to assume a worst case operating scenario, i.e. the cooling system having to dissipate the maximum heat at the low vehicle speeds associated with first gear. This guarantees that the cooling system will be able to dissipate the associated heat generated under maximum throttle conditions. The frequency and duration of the vehicle being subjected to these operating conditions are however questionable but as the exact route and route conditions are not known prior to the race, this criterion represents the highest cooling requirement for the vehicle.

Having knowledge from previous experiences at a specific venue, rally teams usually adjust transmission ratios and vehicle set-ups to suit the expected conditions. Included in this is the teams' expectation of a race with either a high or low average speed per stage. Similarly, cooling system configurations can also be pre-empted, being dependent on the engine speed and vehicle speed expected. If it is expected that the utilisation of first gear is extremely low and will only be engaged for short periods of time, the team can for instance decide to base the operating condition on second gear conditions. It should be noted that this introduces risks as overheating may occur should the system demand be greater due to harsher operating conditions, i.e. higher and longer first gear utilisation. The decisions to take the risk will ultimately remain with the team manager who will best be able to decide on historical event information. For this reason, the cooling system performance in second gear will also be presented and discussed.

4.4. Solving the heat transfer problem at a set of ambient conditions

For the two heat exchangers evaluated in this study, energy balance equations will be used to solve the heat transfer problem. Through subtracting the heat generated at a specific gear and engine speed from the heat dissipated at the associated vehicle speed, the spare heat transfer capacity is defined at specific ambient conditions through the energy balance equation shown in equation 4.4.

$$\dot{Q}_{scap} = \dot{Q}_{dissp} - \dot{Q}_{gen} \tag{4.4}$$

A negative value for the spare capacity indicates that the heat load will not be dissipated without exceeding the maximum allowable water temperature at the specific engine speed. A value of zero indicates that the heat will be sufficiently dissipated, while a value greater than zero will show that the heat will be sufficiently dissipated and that an opportunity exists to minimise the water pumping power.

Substituting equations 2.7 and 4.3 into equation 4.4, it is possible to compare the heat transfer spare capacity between the two cooling systems evaluated at a set of ambient conditions. Figure 4.4 and 4.5 shows the results obtained from each system at standard ambient conditions. It should be noted that the minimum spare capacity is regarded as the limiting factor per gear function, and serves as the criteria of either being over or under designed

It can be seen in figure 4.4 that the 3 core 3mm fin pitch heat exchanger does not fulfil the requirement of sufficiently cooling the engine in first gear with a minimum spare capacity of -3.75kW noted at 6000 rpm. The heat exchanger core is thus not suitable in the cooling system at standard ambient conditions when first gear is used as criteria. However, evaluating the cooling performance in second gear, a huge increase in minimum spare capacity is noted (10.27kW). Under second gear operating

conditions, the cooling system configuration would thus be sufficient with 6.52kW spare capacity, indicating that an opportunity also exists for pumping power minimisation.

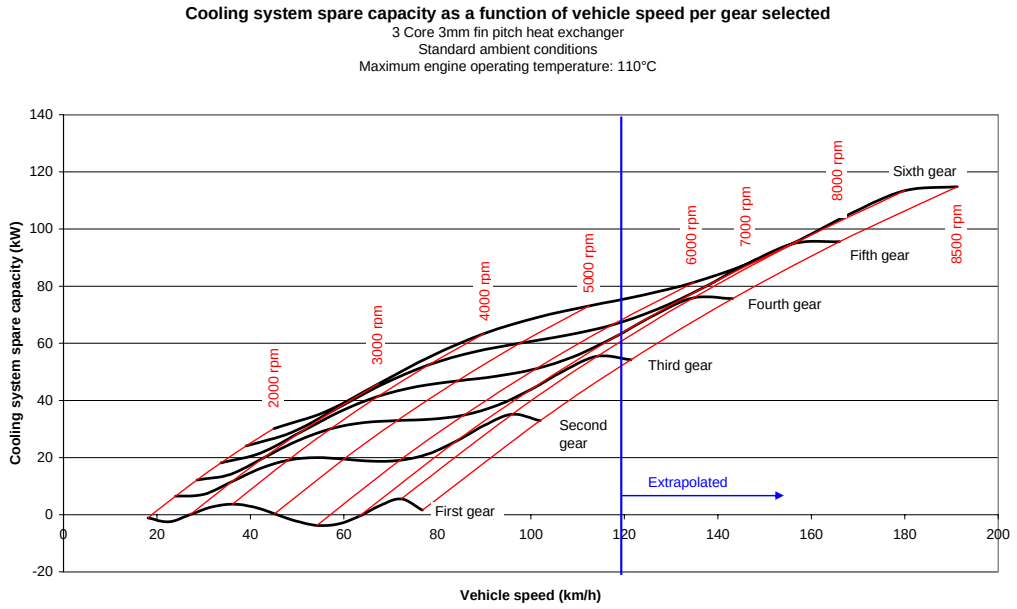

Figure 4.4 - 3 Core 3mm fin pitch heat exchanger spare capacity

Evaluating the 3 core 4mm heat exchanger in the cooling system, as shown in figure 4.5, it is found that this heat exchanger is suitable for use in first and second gear. With a spare capacity of 2.36kW in first gear, a reduction in water pumping power will be possible. As the use of this heat exchanger will also have a reduced drag on the vehicle, due to lower air stream friction experienced through the exchanger, it will be to the team's advantage to use this heat exchanger at standard ambient conditions.

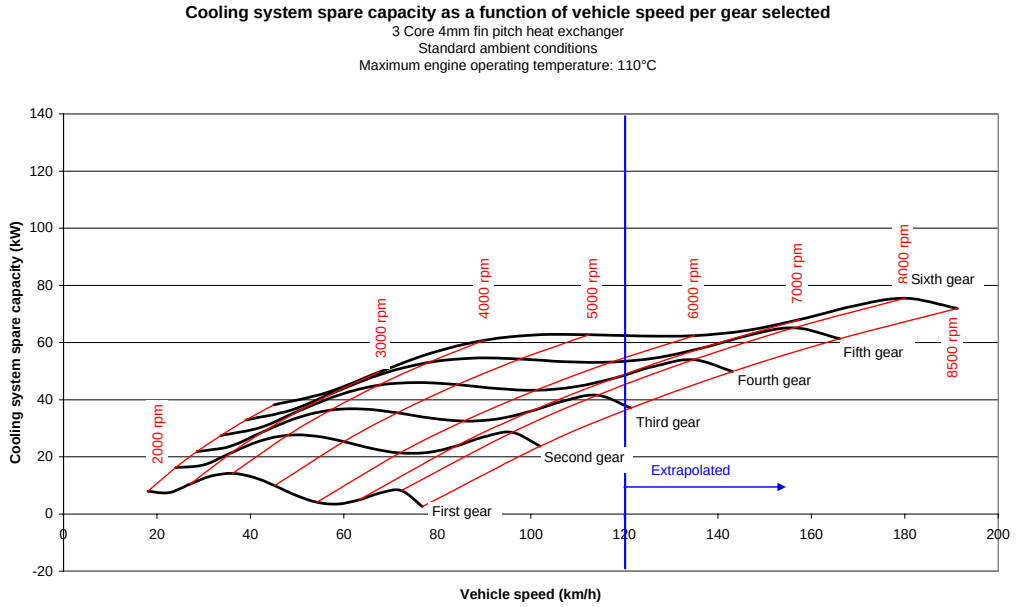

Figure 4.5 - 3 Core 4mm fin pitch heat exchanger spare capacity

4.5 System capacity as a function of ambient conditions

Having determined the spare capacity and the requirements that need to be met for a system to be suitable in first or second gear, it now becomes possible to summarise the cooling system configurations. Contour plots are now generated for each heat exchanger and selected gear ratio by repeating the calculations that resulted in figure 4.4 and 4.5 at different ambient conditions using the lowest spare capacity in each instance as the associated value at the corresponding coordinate. Please refer to figures 4.6 and 4.7 to view the results for an operating criterion in first gear.

From these contour plots a team is now able to clearly identify which heat exchanger is more suitable considering the ambient conditions. Using the ambient temperature as the x-coordinate and the pressure as the y-coordinate, the spare capacity for each heat exchanger is found. Once this is obtained it becomes apparent whether a heat exchanger is suitable or not for operation in such conditions, and if an opportunity exists to reduce the water pumping power utilised.

The process of evaluation can best be explained through an example using the first gear plots (figures 4.6 and 4.7). An ambient temperature of 30°C and a pressure of 90kPa are selected as example ambient conditions in this exercise. From figure 4.6 it can be seen that the spare heat capacity for the 3 core 3mm fin pitch heat exchanger is less than zero indicating that the heat exchanger is unsuitable in this set of ambient conditions. The 3 core 4mm fin pitch heat exchanger plot however shows that a spare capacity in excess of zero is available predicting that the heat exchanger is indeed suitable. With an excess in spare capacity identified the opportunity to reduce the water pumping power is possible in an attempt to further optimise the power available at the wheels. It should however be noted that the contour plots presented are only applicable to the standard vehicle configuration as used in the airflow and waterflow tests. Equally important is the transmission ratios for which these plots are valid. Should the tyre size, final drive or transmission ratios be changed, new plots are to be generated to reveal the true cooling system performance and define the spare capacity.

Further evaluation of the plotted graphs renders more interesting results. In contrast with what might have been expected, it is found that the spare capacity generally reduces with an increase in ambient pressure when the contour plots of the two heat exchangers are evaluated in first gear at high ambient temperatures. Although the mass flow rate of air increases and subsequently also the cooling performance of the heat exchanger with an increase in ambient pressure, the heat produced by the engine also increases and proves to surpass the benefit gained through a higher mass air flow.

At low ambient temperatures this effect reduces, and in the case of the 3 core 4mm fin pitch heat exchanger inverts, showing that the spare capacity increases with an increase in ambient pressure. Ultimately the effect is governed by the SABS 013 correction factor (α_a), the change in ambient air density derived from the ideal gas law and the effect mass flow rate has on the heat dissipation characteristics.

Overall comparison between the two systems in first gear reveals that the 3 core 4mm fin pitch heat exchanger is more suitable at higher ambient temperatures and pressures in the domain plotted. This results once again from the higher airflow through the heat exchanger at lower vehicle speeds, even though the heat exchanger has a lower heat transfer surface exposed to the air stream. Noticeably the gradients in the direction of

both pressure and temperature suggest that with a further increase in these variables to outside the domain shown in the associated figures will result in the opposite trend.

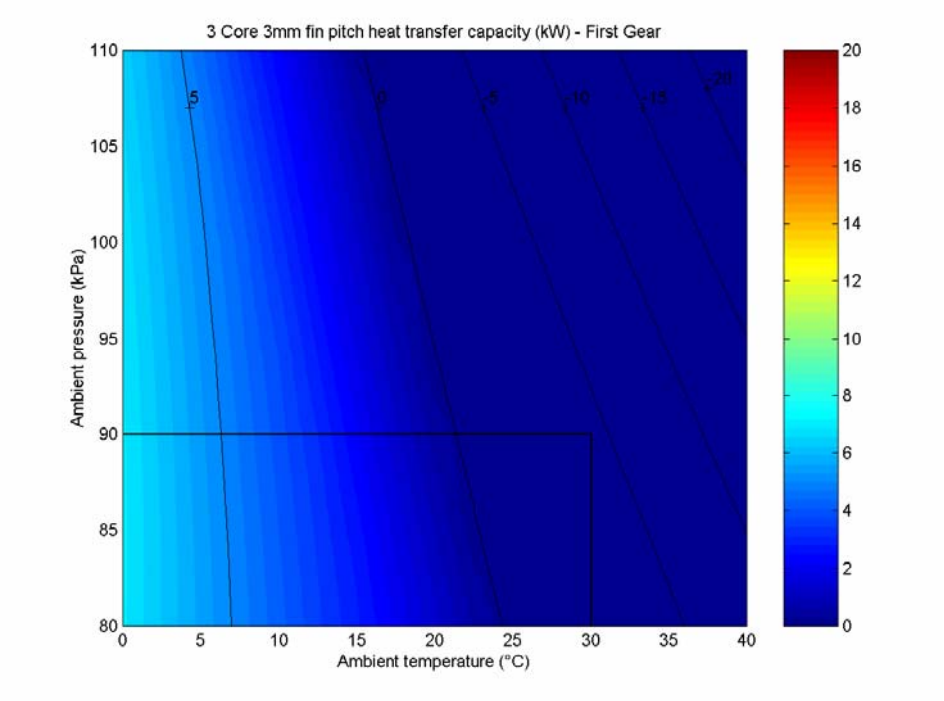

Figure 4.6 – First gear spare capacity as a function of ambient conditions – 3 core 3mm fin pitch heat exchanger

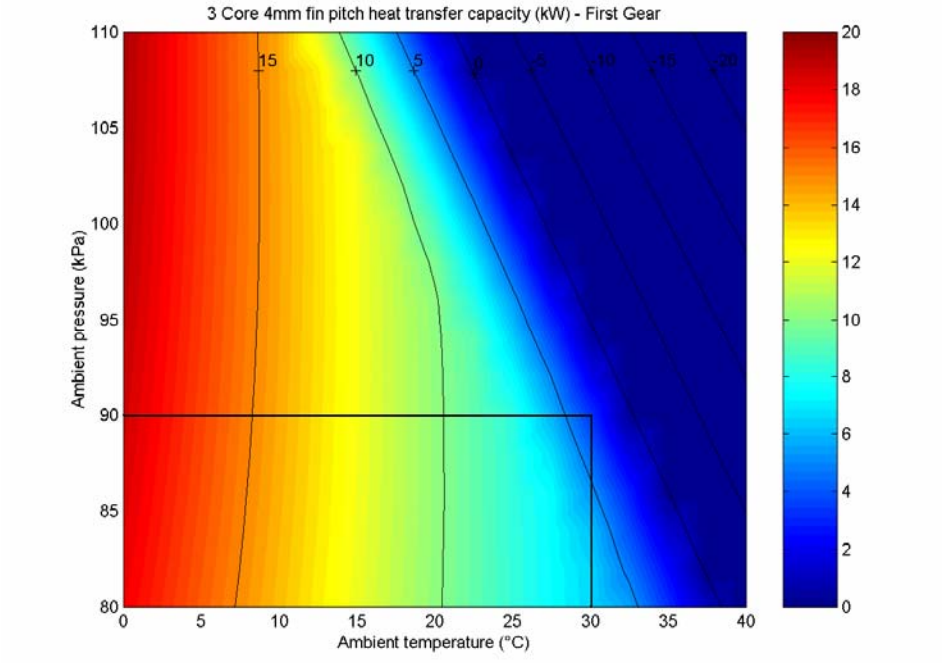

Figure 4.7 – First gear spare capacity as a function of ambient conditions – 3 core 4mm fin pitch heat exchanger

Second gear plots show a more complex result as seen in figure 4.8 and 4.9. At first glance it appears as if the 3 core 4mm fin pitch heat exchanger has superior heat transfer capabilities over the entire domain considered. An interesting result is however found at high ambient pressures where the 3 core 3mm fin pitch heat exchanger is performing better than the 3 core 4mm fin pitch heat exchanger. The zero contour shows that at an ambient pressure of 110kPa the maximum permissible ambient temperature for a suitable system is 37°C in the case of a 3 core 3mm fin pitch exchanger while it is only 35°C for the 3 core 4mm fin pitch exchanger.

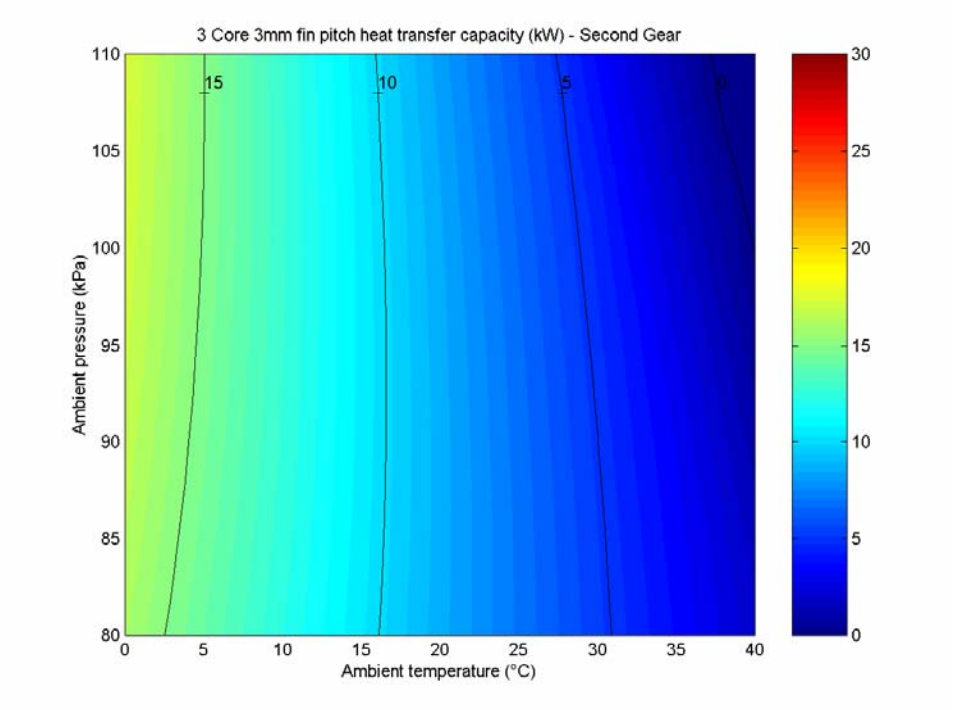

Figure 4.8 – Second gear spare capacity as a function of ambient conditions – 3 core 3mm fin pitch heat exchanger

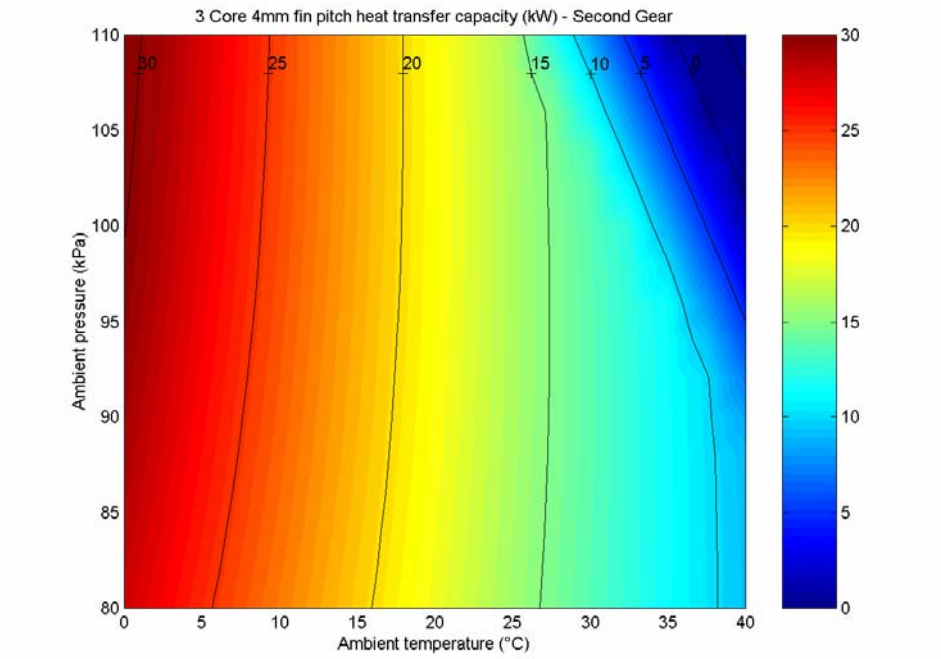

Figure 4.9 – Second gear spare capacity as a function of ambient conditions – 3 core 4mm fin pitch heat exchanger

4.6 Summary

Using the information on the heat load produced under maximum throttle conditions, a relationship between the brake power generated was established at standard ambient conditions. With the help of a polynomial function, the heat load is predicted as a function of engine speed. The influence of ambient conditions is included in this function using the SABS 013 standard resulting in a versatile function over the associated range of ambient temperatures and pressures. Combining the heat generated with the cooling capability as defined in chapter 3 through an energy balance equation, the spare heat load capacity is defined, making assessment of the complete cooling system possible. To do this, the team must however decide on the operating condition of the vehicle. Using the first gear heat cooling conditions as criteria is conservative, but is however recommended due to the nature of the racing conditions being unknown in most cases. Second gear cooling information is however included and should only be used if the team is confident that a quick pace will be maintained through the rally stage, with almost no use of first gear.

This chapter concludes with 4 contour maps for the 2 cooling systems. The contour maps show the spare capacity of the heat exchangers in first and second gear, satisfying the need for a tool to assess the heat exchanger suitability. Through an example the performance of each cooling system can be predicted for ambient conditions in which the vehicle will operate resulting in a classification of being suitable or unsuitable. Identification of the opportunity to further optimise the water pump in an effort to increase power at the wheels is done when a spare capacity greater than zero is obtained for the specific ambient conditions.

The contour maps also revealed that the 3 core 4mm fin pitch has superior cooling characteristics in first gear over the entire range of ambient conditions shown and should thus be used should this be the criteria. As the heat exchanger is not sufficient over the entire range of ambient conditions, the installation of a fan should be considered at high ambient pressures and temperatures. On the other hand, second gear cooling shows that the 3 core 3mm fin pitch exchanger has superiority in a small band of operating conditions at high ambient pressures. Due to the lower airflow through the 3 core 3mm fin pitch heat exchanger, it would thus be recommended that this heat exchanger only be used in combination with an additional air supply to the exchanger.

CHAPTER 5
SUMMARY, CONCLUSIONS AND RECOMMENDATIONS

5.1 Summary

Modern day production vehicles are fitted with cooling systems that can cater for a large range of ambient conditions. This is done to ensure that sufficient cooling will always be available to the system, keeping the engine within the designed operating temperature range. In a small number of automotive applications, minimisation of losses associated with over designed systems is possible by sizing the heat exchanger based on specific operating and ambient conditions. Rally cars fall in this category where changes can be made to the cooling system before a race, to ensure that a system close to optimal is used for performance reasons. This is done by selecting a heat exchanger core from a range of heat exchangers to obtain the desired cooling capacity.

With a rally team having a large number of vehicle configurations available for a single car, evaluation of the cooling system for each configuration is not feasible. Instead, a mathematical model consisting out of a number of “modular” characteristics which can describe the cooling performance of a vehicle will be of greater value. In this study such a model is derived using information from different experiments to result in a tool which can assess a cooling system under certain conditions.

A description of the heat exchanger cores selected for evaluation was given with the dimensions required for installation in the case study vehicle. Both heat exchangers were tested in a wind tunnel to asses their cooling performance in a controlled environment. With the aid of the modified Wilson plot method, characteristic equations were derived for each exchanger, expressing performance in terms of flow Reynolds numbers and the inlet temperature difference between the fluids. On this basis, the heat exchangers were compared with each other, identifying the exchanger

with the highest surface area exposed to the air stream as having the superior transfer characteristics.

Data on the vehicle, and the relationship between the fluid flow rates and the variables that drive them in the vehicle was obtained from the team. Using this information, relationships were derived predicting the flow rate using functions dependent on vehicle operating variables. Through manipulation of the functions using information on the driveline characteristics of the vehicle, both fluid functions could be expressed in terms of engine speed and the gear selected. Furthermore, the effect of the ambient conditions on fluid flow was included. Integrating the modified fluid functions in the heat exchanger characteristic equations, resulted in an equation capable of predicting the cooling performance of the case study vehicle for each heat exchanger.

As the cooling system characteristic equation only predicted the system capability, it was necessary to include the heat load produced by the engine. From the data received from the rally team, a relationship between the heat load and engine speed was established at standard ambient conditions. As the aim is to have a model that can predict the suitability of a cooling system at various ambient conditions, the effect of the ambient on heat generation was included using the SABS 013 standard.

Finally, an energy balance was used to integrate the cooling performance available with the heat generated at a specific engine speed and gear selected. This resulted in a mathematical equation being able to predict whether or not a specific cooling system configuration is able to cope with the heat load at a certain ambient conditions. Using the mathematical model generated, 4 contour maps summarising the suitability of a cooling system configuration at various ambient conditions were generated which serves as a tool for a rally team to select the most appropriate heat exchanger for the prevailing ambient conditions of the day. A discussion on the trends found through the contour maps followed regarding the dependence of heat generated and heat dissipated in the domain of ambient conditions considered.

5.2 Conclusions

The main conclusions and contributions reached during the course of this study can be summarised as follows:

- The model derived in this study is capable of identifying the difference in performance between heat exchanger cores which form an integrated part of a cooling system in a range of ambient conditions. Using the model, a team is capable of predicting the suitability of a specific heat exchanger for use in a specific environment. For an environment where a high spare capacity is present for a certain heat exchanger, the model effectively identifies the opportunity to minimise pumping power.

- The cooling system performance at high ambient pressures shows a surprising result. Although higher ambient pressures are associated with higher mass flow rates through the heat exchanger core, the heat transfer spare capacity reduces. The additional power generated at high ambient pressures is also associated with higher heat generated by the engine. In this case the additional heat generated outweighs the benefit of higher mass airflow rates through the exchanger, causing a reduction in cooling system performance.

- The results obtained from experiments on a heat exchanger core in a wind tunnel cannot be used in isolation from the vehicle characteristics in which it is to be used. In this study it was found that the heat exchanger that appeared to have superior heat transfer performance characteristics in the wind tunnel experiments actually performed worst when integrated in the cooling system of the vehicle in first gear operating conditions. As the vehicle defines the fluid flow rates through the heat exchanger, the performance of the heat exchanger is largely dependent on the vehicle characteristics.

- For every engine and associated vehicle speed, an optimum heat exchanger fin pitch and total surface area should exist. Although the 3 core 4mm fin pitch has a smaller total heat transfer area compared to the 3 core 3 mm fin pitch

exchanger, it outperformed the heat exchanger in terms of heat transfer capability. This is due to the larger airflow which the heat exchanger could accommodate at low vehicle speeds. With a further increase in fin pitch, a reduction in total heat transfer area can also be expected, until a point will be reached where insufficient area limits the heat transfer.

5.3 Recommendations

Recommendations for further work applicable to the present study can be summarised as follows:

- The model derived in this study can be applied to track racing vehicles. With knowledge of the throttle position, engine speed and vehicle speed as a function of the position on the track, the cooling system performance can also be predicted as a function of the position on the track. Knowing these variables and the mass of water in the cooling system, the cooling water temperature can be calculated as a function of position around the track, which could reduce the heat load criteria. The model would however need to be expanded as heat load criteria at partial throttle positions will be required.

- Further improvement of the accuracy with which the system performance can be predicted through the model may be achieved by further investigating the air inlet to the heat exchanger. The information received which describes the relationship between the vehicle speed and the air speed through the heat exchanger in this study is given for the bulk airflow through the exchanger. Even though a ram air duct is a component on the exchanger, the flow pattern on the heat exchanger might not be uniform. As non-uniform flow patterns may affect the heat transfer through the heat exchanger, this effect can be investigated.

- The model can be further verified through fitment of a data logger on the vehicle, and recording engine speed, gear selected, inlet and outlet water temperatures, ambient conditions and throttle positions. Through building a data bank of this information, the risk can be reduced when selecting a gear other than first as the cooling system operating condition.

- The model can further be used in a closed loop control system connected to an electric water pump. With data on the ambient conditions, the control system will be able to predict spare heat capacity for the heat exchanger. This will make it possible for the system to reduce the water flow rate at higher vehicle speeds, whilst increasing flow at low speeds to optimally minimise the power loss to the water pump.

APPENDIX A
HEAT EXCHANGER DRAWING – OVERALL DIMENSIONS

Figure A.1 gives the heat exchanger overall dimensions. Both heat exchangers evaluated have the same dimensions, with the only difference being the fin pitch. All components are manufactured from aluminium and welded to the heat exchanger core. The top and bottom tanks are manufactured from 1.4mm sheet aluminium which is bent and welded to the geometry shown. Round locating pins are found on both the top and bottom tanks for easy installation of the heat exchanger in the vehicle.

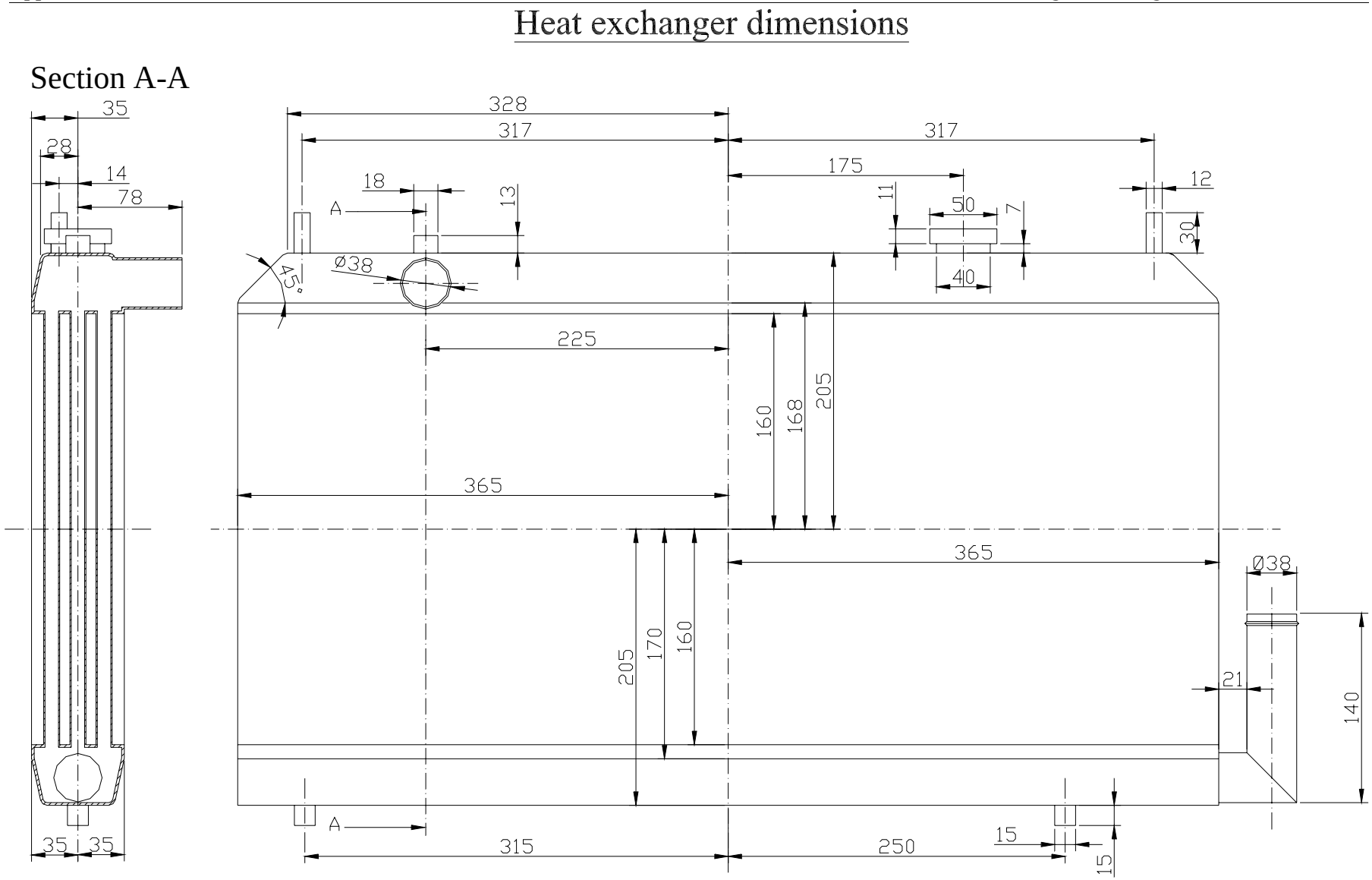

Figure A.1 – Overall dimensions of the heat exchangers evaluated

APPENDIX B
WINDTUNNEL OVERALL DIMENSIONS, COMPONENTS AND TEST SECTION DRAWINGS

B.1 Airflow equipment and the use thereof

In order to establish the required airflow through the heat exchanger, a variable speed windtunnel was used in the experiments. Please refer to figure B.1. to view the dimensions of the windtunnel used.

Re-circulation of the air can be advantageous should the need exist to increase the temperatures of the air to obtain a specific inlet temperature difference between the fluids for a limited time. As heat is dissipated into such a circuit, the temperature of the air will steadily increase, approaching the inlet water temperature of the heat exchanger at which point heat transfer between the fluids will cease to exist. Partial re-circulation through controlling the louver opening to the re-circulation section on the other hand, can also be of assistance should it be required to control the inlet temperature difference between the fluids through the inlet temperature of the air stream. Using this function will however be associated with changes in the density of the air. As hotter air will rise to the top of the duct, the possibility exists that an uneven temperature distribution will be present on the heat exchanger should sufficient mixing of the air in such an air circuit not be present. In order to completely eliminate this effect, the re-circulating section was eliminated from the system by closing the horizontal louvers, and fully opening the vertical louvers during the tests (please refer to figure B.2). Air at ambient conditions was thus used for the test, whilst the inlet temperature difference between the fluids was manipulated through changes to the inlet water temperature, as will be explained in the latter part of the section. With the exclusion of the re-circulating section, the flow channel drawing air from the ambient will be evaluated.

Overall windtunnel dimensions

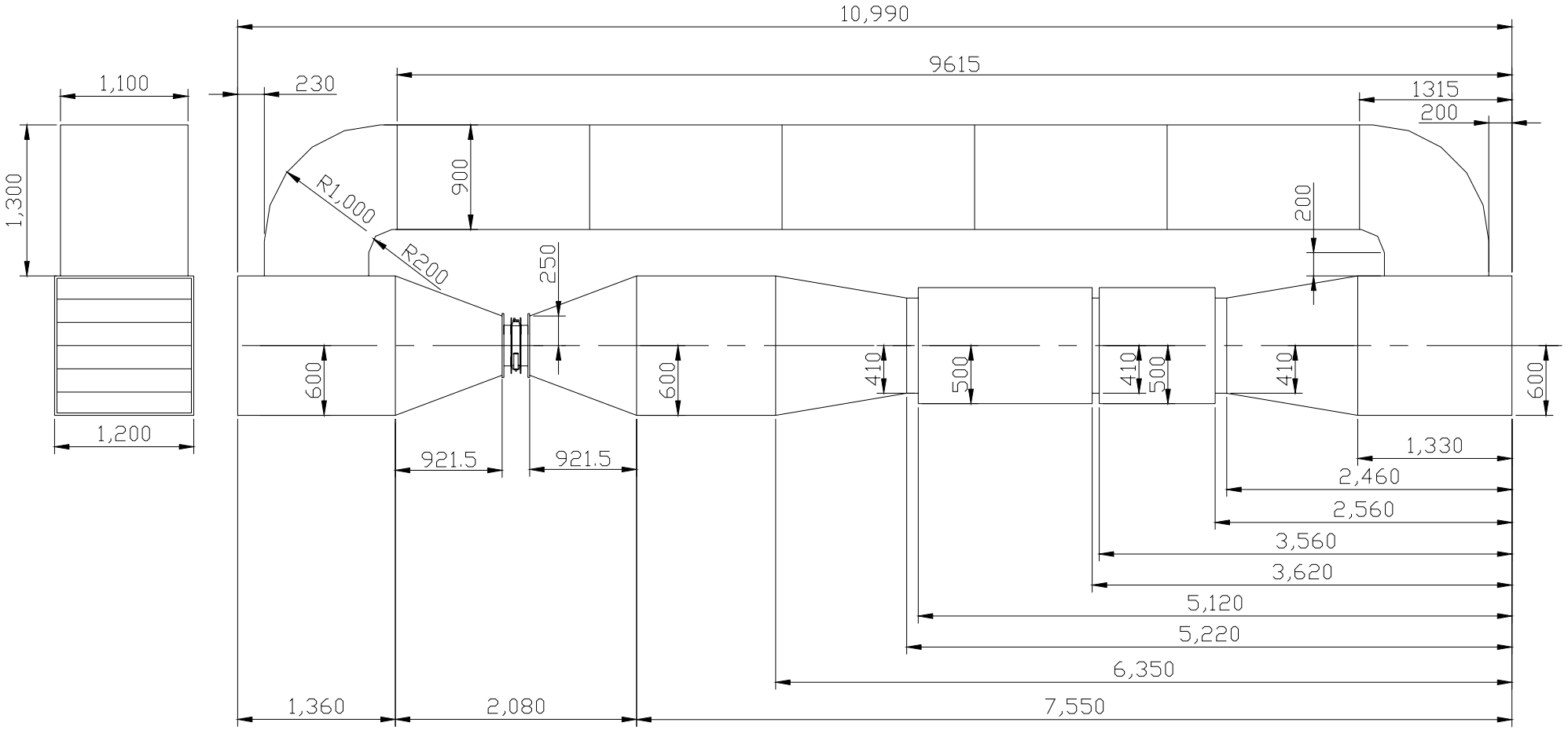

Figure B.1 – Overall windtunnel dimensions

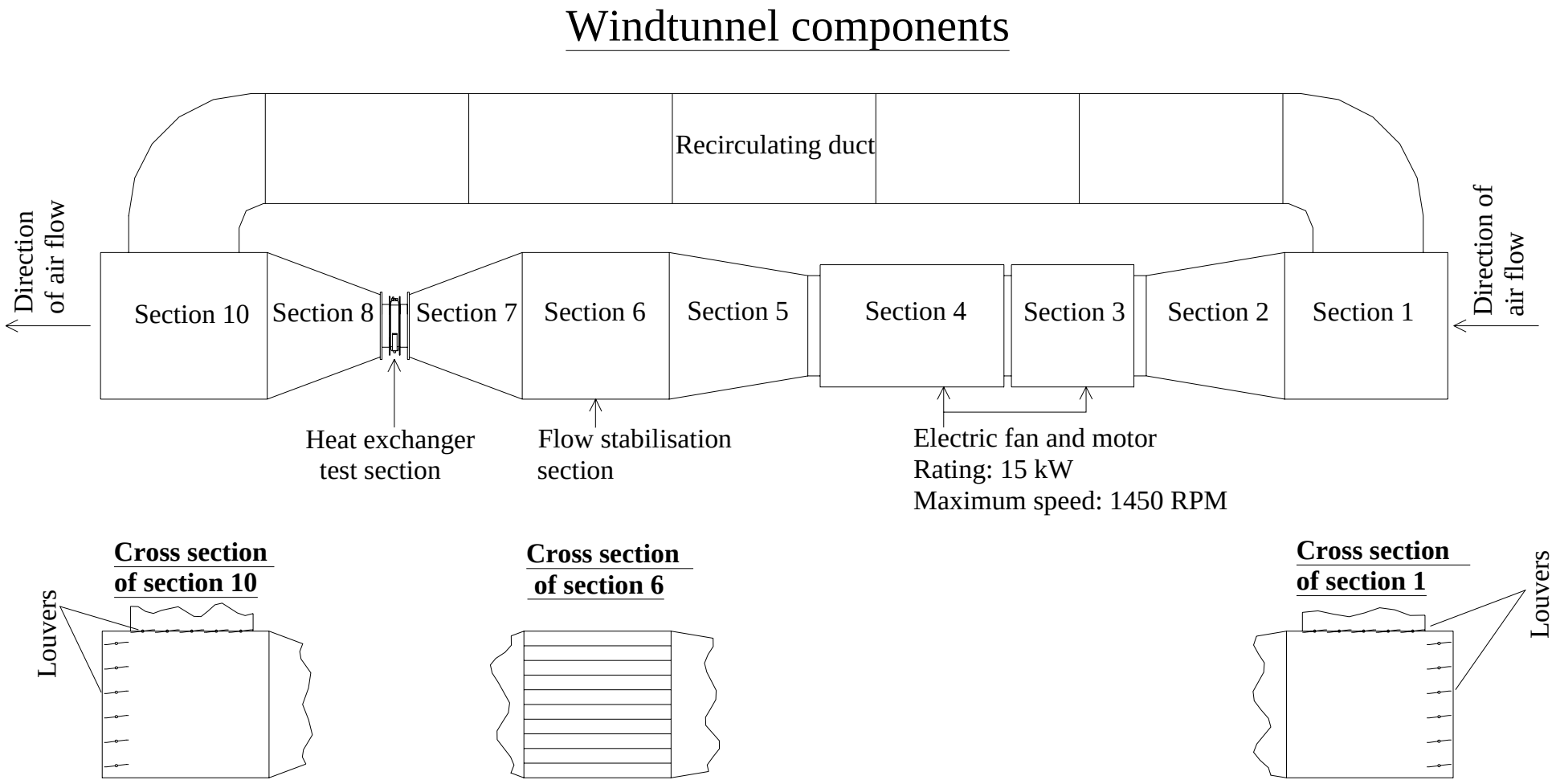

Figure B.2 – Windtunnel components

Airflow through the wind tunnel and heat exchanger is established through a fan driven by a 15 kW electric motor equipped with a frequency inverter. By adjusting the input frequency to the electric motor, the air speed can be controlled to obtain a specific flow rate. The designer of the wind tunnel included a flow stabilisation section in the wind tunnel to reduce the circulating effect associated with a rotating fan. This section consists of plates positioned vertically at a distance of 120mm from each other in the flow stabilisation section of figure B.2 (cross section of section 6). Also present in this section is a calibrated air temperature sensor that measures the temperature of the air downstream from the fan, which is used as a partial input for the control of the inlet temperature difference between the fluids.

The flow stabilisation section in the wind tunnel (section 6) has a cross sectional dimension of 1200mm x 1200mm. Since the heat exchangers under evaluation have specific dimensions dictated by the rally team, reduction sections available were used to reduce the cross section of the wind tunnel to 800mm in length and 500mm in height (sections 7 and 8). In order to further reduce the cross section to the required 730mm x 320mm, interface ducting was built and installed between the reduction section and the heat exchanger core, as shown in figure 2.3. Please note that the blue sections indicate the waterflow through the exchanger, while the red sections indicate the heat exchanger fin areas.

The reduction in cross section of the wind tunnel causes the air to accelerate through the section, increasing the air speed on the heat exchanger. For this reason, the air pressure and air speed needs to be measured as close as possible to the heat exchanger frontal surface. Pressure position P_1 was defined for measurement of the stagnation and static pressures using a pitot tube and a handheld manometer. Converting the pressures to air speed, the frequency inverter on the fan motor can be adjusted to obtain the desired flow rate through the heat exchanger. Note that pressure position P_1 is situated in the middle of the heat exchanger and 30mm in front of the face of the heat exchanger.

Due to the reduction in cross section, a further obstacle can be identified with regard to the airflow to the heat exchanger. The air near the walls of the reduction section in the wind tunnel is expected to approach the heat exchanger core in the interface plate

at an angle. This necessitates the incorporation of flow stabilising sections on the interface ducting between the heat exchanger core and the reduction section in order to reduce the angle of attack between the heat exchanger core fins and the approaching air – please refer to figure 2.3. Theoretically, the flow stabilising sections should allow the air to re-attach to the flat surface of the stabilisers, reducing the turbulent flow areas that will form on the edges of the intake to the heat exchanger.

As identified in the literature, proper sealing of the wind tunnel to eliminate false airflow readings is essential to increase the accuracy with which a heat exchanger can be characterised. The flow channels were sealed by bonding compressible sponges to all surfaces used as interfaces during the assembly of the test section. This includes sealing of the interface ducting against the reduction channel, as well as the reduction channel against its interface with the wind tunnel. Prior to initiating the experimental testing, the airflow rate was maximised by setting the fan frequency inverter to the maximum 50 Hz, whilst the wind tunnel was inspected for any leaks. Only after the set-up was found to be satisfactorily sealed, did the tests commence.

A second factor increasing the accuracy of the tests was ensuring sufficient insulation of the heat exchanger surfaces from the ambient. As can be seen in the cross section of the test section in figure 2.3, the top and bottom tanks were effectively exposed to the ambient conditions of the room, which would result in heat loss, and inaccurate heat transfer characterisation of the core. Not illustrated are the sides of the heat exchanger which were also exposed to the ambient room temperature. Covering the exposed areas with an insulation material effectively eliminated the heat loss to the ambient through these surfaces, reducing the experimental errors associated with a test of this nature.

Finally, the air exits the wind tunnel to the ambient through the open horizontal louvers. While the air inlet to the wind tunnel is found inside the laboratory, the air exits the facility outside the room. By supplying the wind tunnel with air from the furthest point of exit, by opening windows at this position, re-circulation of warm air to the inlet of the wind tunnel is effectively eliminated.

B.2 Waterflow equipment and the use thereof

The requirement on the water circuit is not only to establish waterflow through the heat exchanger, but also to supply heated water to the exchanger. Furthermore, it is important to be able to control the inlet temperature difference between the fluids as previously mentioned.

The water temperature in the boiler is monitored by the internally mounted thermocouple in the tank which relays the water temperature in the boiler to a computerised control system. Being able to monitor the temperature, it is possible to prevent the water from boiling in the tank.

Galvanised piping, with an outer diameter of 2.5", connects the outlet of the heated water tank to a proportional valve. The proportional valve has two inlets, one from the heated water tank and the other from the return line from the heat exchanger. By changing the proportion of heated water from the tank, and cooler water from the heat exchanger outlet, the proportional valve is used to supply the heat exchanger inlet with a predetermined inlet water temperature. This proves to be extremely useful in maintaining a constant inlet temperature difference between the fluids as sudden fluctuations of the ambient air temperature is unlikely.

From the proportional valve, water is channelled to the water pump which is driven by a 5.5 kW electric motor, equipped with a frequency inverter. The orifice flow meter situated further down the flow line, measures the waterflow rate which can be adjusted through the input frequency to the motor driving the pump.

Next in the waterflow system, the inlet temperature sensor, heat exchanger and outlet temperature sensor are found. The accuracy in temperature measurements between the inlet and outlet of the heat exchanger is essential in order to accurately characterise a specific heat exchanger. As galvanised piping is used in the experimental set-up, temperature losses can be expected through all the pipes leading to the heat exchanger. To exclude these heat transfer losses from the characterisation process, the thermocouples used to determine the thermal energy loss were installed directly at the

inlet and outlet of the heat exchanger respectively. To further increase the accuracy with which the experiments were done, the thermocouples were calibrated in a separate experiment at 0°C and 95°C within 0.1°C from each other.

Following the water channel from the heat exchanger, as shown in figure 2.4, the water returns to the water boiler. In this line a T-section is found with one end connected to the proportional valve, supplying colder water to the inlet depending on the valve setting.

Prior to experimental testing, all joints to the water system were visually inspected for water leaks which can cause inaccurate waterflow measurements. Only after satisfactory sealing of all the leaks did the testing begin.

APPENDIX C
EVEN DISTRIBUTION OF AIRFLOW IN WINDTUNNEL

C.1 Positions measured in front of heat exchanger

To qualify the even distribution of airflow at the inlet of the heat exchanger, air speeds were measured at different positions. Figure C.1 shows the points where measurements were taken, 30mm from the frontal plane of the heat exchanger.

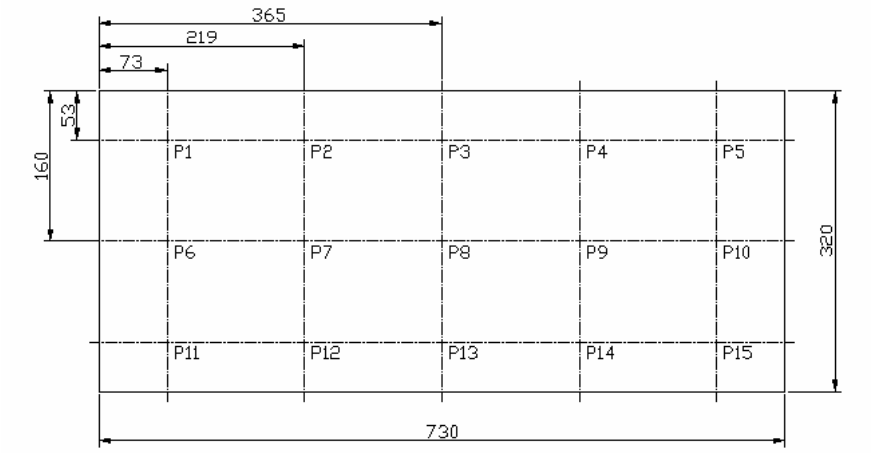

Figure C.1 - Positions where air speeds were measured

C.2 Findings with regard to the even distribution of air flow on the heat exchanger

The experiment was performed at two different air speeds for the 3 core 4mm fin pitch heat exchanger. Through measurement of the air speeds at the different positions indicated in Figure C.1, the average airflow could be calculated as well as the percentage deviation of each point relative to the mean air speed. A maximum deviation of 5.24% from the average was found which is a sufficiently even airflow distribution on the heat exchanger for the characterisation experiments that are to follow. Please find the data recorded for both air speeds evaluated in Table C.1.

Table C.1 – Airflow distribution measurements for 3 core 4 mm fin pitch heat exchanger

Measuring position	**Measurement nr.1**		**Measurement nr.2**	
	Air speed (m/s)	**Deviation from average (%)**	**Air speed (m/s)**	**Deviation from average (%)**
1	10.90	-5.24	4.56	-2.51
2	11.48	-0.21	4.71	0.75
3	11.80	2.65	4.74	1.42
4	11.63	1.12	4.63	-0.86
5	11.01	-4.31	4.58	-2.09
6	11.48	-0.21	4.65	-0.46
7	11.88	3.30	4.77	1.95
8	11.85	3.04	4.86	3.91
9	11.93	3.73	4.75	1.68
10	11.48	-0.21	4.72	1.02
11	11.35	-1.33	4.56	-2.51
12	11.53	0.24	4.59	-1.82
13	11.80	2.65	4.75	1.68
14	11.48	-0.21	4.70	0.48
15	10.92	-5.01	4.55	-2.65
Average	**11.50**		**4.68**	

APPENDIX D
CALCULATING THE HEAT TRANSFER RATE AND SELECTING THE MOST APPROPRIATE DATA

D.1 Heat transfer calculated

The heat transfer rate at each experimental test position can be calculated from the data collected through the evaluation of the heat exchanger in the windtunnel. Each test was conducted at an intended variable set, and through the computerised control system, every effort was made to achieve steady state conditions at the specific set as explained in chapter 2. Table D.1 shows a sample of the actual data recorded during the experimental evaluation which will now be used as an example in calculating the heat transfer for each data set.

Table D.1 – Example of experimental data recorded per measurement point

Data recorded during the experiments - Heat exchanger: 3 Core 4mm fin pitch

Intended variable set for test:

Air speed: 9m/s

Water flow rate: 1.4 l/s

Inlet temperature difference: 35°C

Reference	Description	Data points measured							
		A	B	C	D	E	F	G	H
1	Air temperature at inlet of heat exchanger ($T_{a,in}$) in °C	27.37	27.47	27.52	27.52	27.13	27.28	27.28	27.37
2	Water temperature at inlet of heat exchanger ($T_{w,in}$) in °C	67.13	67.06	66.75	66.88	67.37	67.19	67.19	67.00
3	Water temperature at outlet of heat exchanger ($T_{w,out}$) °C	64.55	64.02	64.18	64.10	64.56	64.50	64.48	64.30
4	Water flow rate (F_w) in liters per second	4.512	4.343	4.527	4.483	4.412	4.412	4.329	4.315

In order to calculate the heat transferred at each data set, it is required to first calculate a number of variables. Table D.2 reveals the calculations as well as a brief explanation of the method used to finally obtain the heat transferred.

Table D.2 – Calculating the heat transfer

Description	Equation	Explanation
Inlet temperature difference between fluids	$\Delta T_f = T_{w,in} - T_{a,in}$ (D.1)	The inlet temperature of the air is subtracted from the inlet temperature of the water
Water temperature difference between inlet and outlet	$\Delta T_w = T_{w,in} - T_{w,out}$ (D.2)	The outlet temperature of the water is subtracted from the inlet temperature of the water
Average water density (ρ_w)	$\rho_w = (\rho_{wg} - \rho_{ws})\left(\frac{T_{wav} - T_{ws}}{T_{wg} - T_{ws}}\right) + \rho_{ws}$ (D.3) where $T_{wav} = \left(\frac{T_{w,out} + T_{w,in}}{2}\right)$	The water density is interpolated based on the average water temperature of the fluid through using the values documented by Mills [8].
Average specific heat of water (c_p)	$c_{pw} = (c_{pwg} - c_{pws})\left(\frac{T_{wav} - T_{ws}}{T_{wg} - T_{ws}}\right) + c_{pws}$ (D.4) where $T_{wav} = \left(\frac{T_{w,out} + T_{w,in}}{2}\right)$	Similar to the water density, the specific heat of the water is interpolated based on the average water temperature of the fluid through using the values documented by Mills [8].

Heat transfer rate of heat exchanger	$\dot{Q}_{dissp} = \rho_w F_w c_{pw}\left(T_{w,out} - T_{w,in}\right)$ (D.5)	Using the variables obtained in this table, the heat transfer is calculated.

Applying the method listed in table D.2 to the data recorded and listed in table D.1, the heat transfer and all the variables required to calculate the heat transfer are listed in table D.3.

Table D.3 – Example of heat transfer calculation

Heat transfer results calculated from experimental data									
Intended variable set for test: Air flow rate: 9m/s Water flow rate: 4.45 l/s Inlet temperature difference: 40°C									
Reference	**Description**	**Data points measured**							
		A	**B**	**C**	**D**	**E**	**F**	**G**	**H**
1	Inlet temperature difference between fluids	39.76	39.59	39.23	39.36	40.24	39.91	39.91	39.63
2	Water temperature difference between inlet and outlet	4.09	3.97	4.10	4.07	4.02	4.02	3.96	3.95
3	Average water density (ρ_w)	980.7	980.9	981.0	981.0	980.6	980.7	980.7	980.8
4	Average specific heat of water (c_{pw})	4183	4183	4183	4183	4183	4183	4183	4183
5	Heat transfer rate of heat exchanger in kW	47.76	54.17	47.74	51.14	50.86	48.69	48.13	47.81

It should be noted that a minimum heat transfer of 47.74kW and a maximum of 54.17kW results from the data set used as an example with a total deviation of 13.47% relative to the lowest heat transfer value. Small variations in the water flow rates and water

temperature differences cause these discrepancies. As the accuracy with which the experiments were performed cannot be increased, the need for a meaningful data selection method becomes important.

D.2 Process of selection of meaningful data and calculating an average

The method used to eliminate improper data, is one in which a ±5% tolerance is used in order to group the results relative to a specific data point. In essence, each data point is used as a basis to evaluate the other data points. The process can best be explained by means of an example shown in table D.4.

Table D.4 – Elimination process of unfit data

Data review	% Deviation from data points measured								**Compliance**	**Average heat dissipated (kW)**	**Water flow rate (l/s)**
	1	**2**	**3**	**4**	**5**	**6**	**7**	**8**			
Comparison 1	X	13.4	-0.04	7.08	6.49	1.95	0.78	0.10	5	48.03	4.42
Comparison 2	-11.8	X	-11.9	-5.6	-6.11	-10.1	-11.2	-11.7	1	54.17	4.34
Comparison 3	0.04	13.5	X	7.13	6.54	2.00	0.82	0.15	5	48.03	4.42
Comparison 4	-6.61	5.93	-6.65	X	-0.55	-4.79	-5.88	-6.52	3	50.23	4.44
Comparison 5	-6.10	6.51	-6.14	0.55	X	-4.26	-5.36	-6.00	3	50.23	4.44
Comparison 6	-1.91	11.3	-1.96	5.03	4.45	X	-1.15	-1.81	6	48.50	4.42
Comparison 7	-0.77	12.6	-0.82	6.25	5.67	1.16	X	-0.67	5	48.03	4.42
Comparison 8	-0.10	13.3	-0.15	6.97	6.38	1.85	0.68	X	5	48.03	4.42

Comparison 1 shows the percentage deviation of each value of the heat transfer relative to the first value of heat transfer (data point A), in the “Deviation from data points measured” column. The compliance column shows that 5 data points, including the first data point, is within a 5% tolerance relative to data point A, with an average heat

dissipation over the 5 data points of 48.03kW. The corresponding water flow rate for which the measurements were taken is given as 4.42 l/s. Repeating the calculations relative to all the other data points in comparison 2 to 8, makes it possible to identify the most appropriate set of data points in the compliance table. From this it is evident that Comparison 6 reveals the best results as 6 data points (including itself) fall within 5% of each other. It is thus obvious that data point 2 and 3 exceeds the 5% tolerance of the average of the largest number of data points used. These data points are thus excluded from the group of data used to determine the average value for the specific variables. Using this method, the inaccurate data was eliminated from the results obtained from the experimental tests.

APPENDIX E
CALCULATING CONSTANTS FOR USE IN THE MODIFIED WILSON PLOT METHOD

E.1 Calculating the total wetted tube area

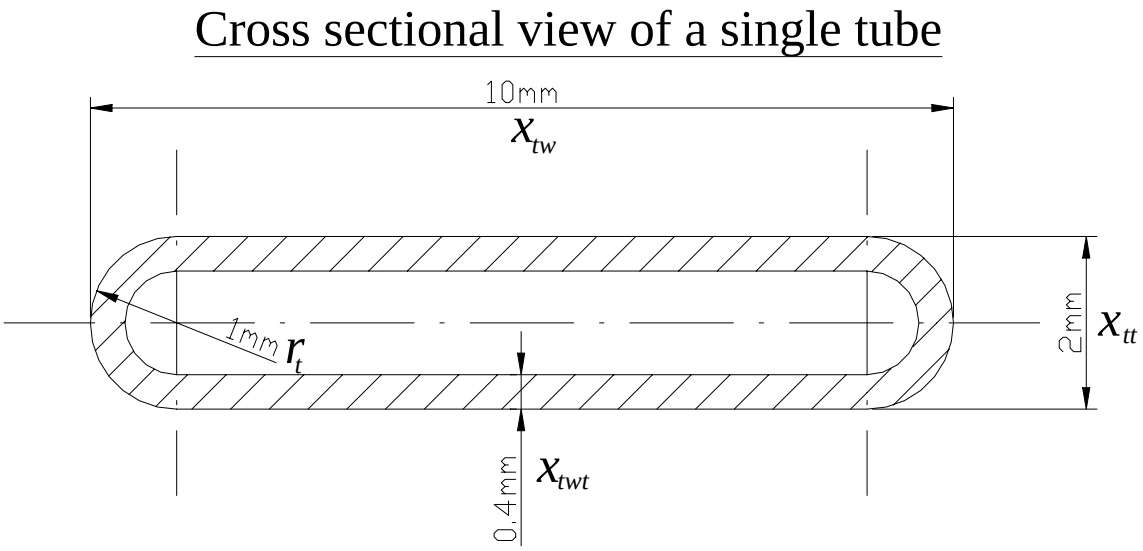

Figure E.1 – Cross section of a single tube

Wetted circumference of a single tube can be calculated using equation E.1. Please refer to figure E.1 for a visual definition of the variables involved.

$$P_{tw} = 2\pi\left(r_t - x_{twt}\right) + 2\left(x_{tw} - x_{tt}\right) \tag{E.1}$$

Once the wetted circumference is known for a single tube, the wetted area in a single tube can be calculated through multiplying equation E.1 by the length of the tube, which in this case is 0.32m (refer to figure A.1). Furthermore, the number of tubes counted for the total

heat exchanger is 216. The total wetted tube area through which heat is transferred in the core is thus:

$$A_w = P_{tw} \times 0.32 \times 216$$
$$= 0.01977 \times 0.32 \times 216 = 1.3665 m^2 \quad \text{(E.2)}$$

E.2 Calculating the water stream hydraulic diameter of a tube

White [49] defines the hydraulic radius of a non circular duct as:

$$R_h = \frac{A_{tcs}}{P_{tw}} \quad \text{(E.3)}$$

Using the definition of a hydraulic diameter also documented by White [49], the hydraulic diameter can be calculated as follows:

$$D_{hw} = 4 \times R_h \quad \text{(E.4)}$$

Substituting equation E.3 in E.4, and using the variables defined in figure E.1, the hydraulic diameter is found to be:

$$D_{hw} = 4 \times \frac{A_{tcs}}{P_{tw}} = 4 \times \left[\frac{\pi (r_t - x_{twt})^2 + (x_{tw} - x_{tt})(x_{tt} - 2x_{twt})}{P_{tw}} \right] \quad \text{(E.5)}$$
$$= 4 \times \left[\frac{\pi (0.001 - 0.0004)^2 + (0.01 - 0.002)(0.002 - 2(0.0004))}{0.01977} \right] = 2.17117 \times 10^{-3} m$$

E.3 Calculating the total wetted area exposed to the air stream

In order to calculate the total area exposed to the air stream, a unit cell fin assembly is defined as is done for the 3 core 3mm fin pitch heat exchanger in figure E.2. In reality a radius is found on the fin where it is attached to the water tube, but due to the inconsistency of the actual radius, an angled attachment is assumed for the purpose of this calculation.

The total area exposed to the air stream in this unit cell consists of two elements:

- External tube surface
- Fin surface

Reviewing the external tube surface, the area can be calculated using equation E.6:

$$A_{teu} = \left[2\pi r_t + 2\left(x_{tw} - x_{tt}\right)\right]x_{fp} \tag{E.6}$$

The unit fin surface is obtained by calculating the area of the four surfaces:

$$A_{feu} = 4\left(x_{ful}\right)\left(\sqrt{\left(\frac{x_{fp}}{2}\right)^2 + \left(x_{fw}\right)^2}\right) \tag{E.7}$$

The total area exposed to the air stream is thus:

$$A_{au} = A_{teu} + A_{feu} \tag{E.8}$$

Unit cell for the 3 Core 3mm fin pitch exchanger

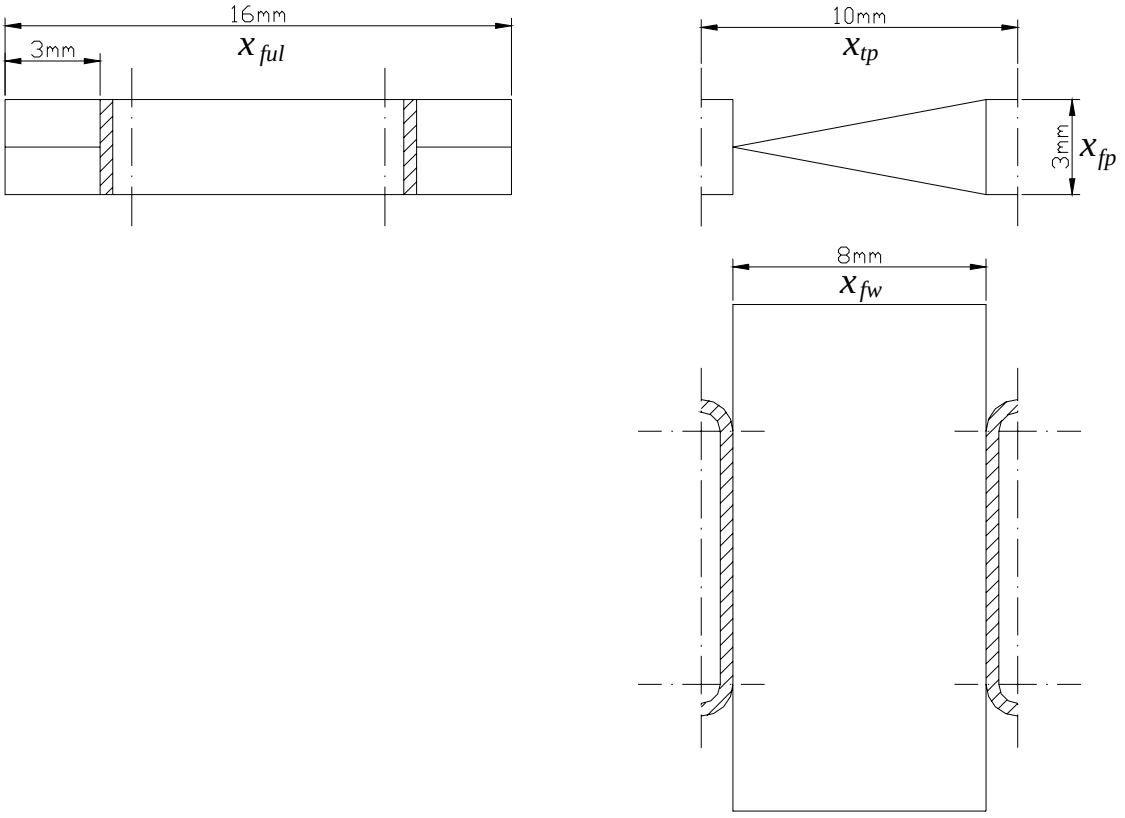

Figure E.2 – Unit cell of the area exposed to the air stream

In order to calculate the total area exposed to the air stream, the number of unit cells in the heat exchanger needs to be established. It is known that the heat exchanger consists out of 216 tubes. The number of unit cells per tube is simply obtained by dividing the fin pitch into the total length of the tube, i.e. 320mm. The resultant area exposed to the air stream for the 3 core 3mm fin pitch heat exchanger is thus:

$$A_a = \frac{320}{3} \times 216 \times \left(A_{au}\right) \tag{E.9}$$

$$= \frac{320}{3} \times 216 \times \left(5.8776 \times 10^{-4}\right) = 13.542 m^2$$

The resulting area for the 3 core 4mm fin pitch heat exchanger is:

$$A_a = \frac{320}{4} \times 216 \times \left(A_{au}\right) \tag{E.10}$$

$$= \frac{320}{4} \times 216 \times \left(5.8876 \times 10^{-4}\right) = 10.660 m^2$$

E.4 Calculating the air stream hydraulic diameter for an air tube

The calculation for the hydraulic diameter of the air channel is done on the same principle as for the water tube. In this case, the wetted perimeter is however defined as given in equation E.11:

$$P_{aw} = x_{fp} + 2\left(\sqrt{\left(\frac{x_{fp}}{2}\right)^2 + \left(x_{fw}\right)^2}\right) \tag{E.11}$$

Through simple trigonometry, the cross section area is defined as:

$$A_{acs} = \frac{x_{fp}}{2} \times x_{fw} \tag{E.12}$$

Using the same basic definition, the hydraulic diameter is defined calculated as:

$$D_{ha} = 4 \times \frac{A_{acs}}{P_{aw}} \tag{E.13}$$

$$= 4 \times \frac{1.2 \times 10^{-5}}{1.92788 \times 10^{-2}} = 2.4898 \times 10^{-3} m$$

for the 3 core 3mm fin pitch heat exchanger, and

$$D_{ha} = 4 \times \frac{A_{acs}}{P_{aw}} \tag{E.14}$$

$$= 4 \times \frac{1.6 \times 10^{-5}}{2.04924 \times 10^{-2}} = 3.1231 \times 10^{-3} m$$

for the 3 core 4mm fin pitch heat exchanger.

E.5 Calculating the nett inlet flow area for the water

Calculating the nett inlet flow area for the water tubes is done by summing the individual cross section inlet area for all the tubes in the inlet header tank. The calculation is as follows for both heat exchangers:

$$A_{caw} = 216 \times A_{tcs} \tag{E.15}$$

$$= 216 \times 1.0731 \times 10^{-5} = 0.00231789 m^2$$

APPENDIX F
COMPARING HEAT TRANSFER PREDICTION WITH ACTUAL RECORDED DATA

F.1 Heat transfer prediction tested against actual measurements

To qualify the model derived from the Wilson plot method, the difference between the actual measured and calculated heat transfer is calculated as a percentage deviation relative to the actual value. Table F.1 gives the actual, calculated and variance for the 3 core 3mm fin pitch heat exchanger, while table F.2 shows the same for the 3 core 4mm fin pitch exchanger. The NTU column is added to show that the maximum NTU of 3 is not exceeded.

Table F.1 - Validation of the experimental data against the characterisation equations for the 3 core 3mm fin pitch heat exchanger

Nr	Actual heat dissipation (kW)	Calculated heat dissipation (W)	Deviation	NTU
1	53.2	52.3	1.77%	1.20
2	48.5	48.2	0.62%	1.19
3	39.9	40.5	1.71%	1.14
4	34.2	34.5	0.99%	1.16
5	42.5	41.5	2.24%	1.68
6	36.0	35.9	0.23%	1.62
7	31.0	31.2	0.63%	1.57
8	26.5	26.2	0.79%	1.62
9	25.0	25.1	0.38%	2.56
10	22.1	22.1	0.27%	2.63
11	18.9	19.0	0.44%	2.55
12	16.3	16.3	0.07%	2.59
13	40.1	40.5	0.82%	0.76
14	46.7	47.2	1.07%	0.92
15	49.5	50.4	1.73%	1.00
16	52.4	53.3	1.71%	1.07
17	34.9	35.3	1.16%	0.76
18	39.5	40.2	1.59%	0.90
19	44.0	44.3	0.83%	1.03
20	47.0	46.7	0.65%	1.13
21	30.4	30.7	0.90%	0.77
22	34.3	34.4	0.14%	0.93
23	36.8	37.7	2.36%	1.00

Table F.1 - Continues

Nr	Actual heat dissipation (kW)	Calculated heat dissipation (W)	Deviation	NTU
24	38.8	39.4	1.53%	1.08
25	24.8	25.1	0.96%	0.77
26	30.0	30.2	0.58%	0.93
27	31.2	30.9	0.68%	1.06
28	33.1	32.9	0.65%	1.13
MAXIMUM			**2.36%**	**2.63**

Table F.2 - Validation of the experimental data against the characterisation equations for the 3 core 4mm fin pitch heat exchanger

Nr	Actual heat dissipation (kW)	Calculated heat dissipation (W)	Deviation	NTU
1	48.5	48.4	0.16%	0.94
2	43.2	43.1	0.18%	0.95
3	37.0	36.9	0.29%	0.96
4	30.6	30.3	0.80%	0.96
5	38.4	38.7	0.83%	1.27
6	34.1	34.0	0.38%	1.30
7	29.5	29.4	0.39%	1.30
8	24.1	24.0	0.21%	1.29
9	24.0	24.1	0.35%	2.10
10	21.3	21.2	0.32%	2.13
11	18.4	18.4	0.51%	2.17
12	14.8	14.8	0.32%	2.10
13	39.0	38.5	1.19%	0.71
14	43.4	43.4	0.01%	0.80
15	45.5	45.8	0.62%	0.85
16	46.6	47.5	1.96%	0.88
17	33.6	34.0	1.20%	0.69
18	37.7	37.7	0.14%	0.80
19	39.1	39.3	0.50%	0.86
20	42.1	41.4	1.58%	0.94
21	28.5	28.8	1.03%	0.69
22	33.4	32.6	2.31%	0.84
23	34.8	34.8	0.15%	0.97
24	36.0	35.2	2.00%	0.94
25	23.9	25.1	4.92%	0.68
26	28.1	27.7	1.21%	0.81
27	29.1	28.5	2.14%	0.88
28	30.1	29.9	0.43%	0.92
MAXIMUM			**4.92%**	**2.17**

APPENDIX G

VEHICLE AND ENGINE SPEED CORRELATION

G.1 Calculating the relationship between vehicle speed and engine speed

To calculate the relationship between the vehicle speed and engine speed for the standard configuration rally car, knowledge on the following is required:

- Transmission ratios
- Final drive ratio
- The rolling circumference of the tyre

The transmission ratios for the 6 speed gearbox, as used in the standard configuration, were obtained from the rally team. These values are presented in table G.1.

Table G.1 Gearbox ratios obtained from rally team

Gear	Ratio
1st gear	2.8462
2nd gear	2.1429
3rd gear	1.8000
4th gear	1.5263
5th gear	1.3158
6th gear	1.1429

The final drive ratio is quoted as 4.5455 for the standard configuration which needs to be included in the overall ratio calculation.

Combining the gear ratios with the final drive ratio through multiplication of each gear ratio with the final drive ratio, the required engine rotations for a single drive shaft rotation is presented in table G.2.

Table G.2 – Final drive ratio combined with the gear ratio

Gear	**Ratio including final drive**
1st gear (n_{gf1})	12.93706
2nd gear (n_{gf2})	9.740260
3rd gear (n_{gf3})	8.181818
4th gear (n_{gf4})	6.937799
5th gear (n_{gf5})	5.980086
6th gear (n_{gf6})	5.194805

The standard configuration vehicle is fitted with tyres which have a circumference of 1.95m. Using the total gear ratios as well as the stated rolling circumference of the tyre, the vehicle speed can be expressed in kilometers per hour using equation G.1 for first gear. By replacing n_{gf1} with n_{gf2}, n_{gf3} etc. the vehicle speed can be calculated for second, third etc. gearbox ratios.

$$V_D = \frac{0.06 \times 1.95}{n_{gf1}} \times v_{engine} \qquad \text{(G.1)}$$

Reducing the equation to the form of equation 3.5, the overall ratios can be calculated for the different gears selected, which is given in table G.3.

Table G.3 – Total ratio relating vehicle speed to engine speed

Gear	**Total ratio**
n_1	0.00904379
n_2	0.012012
n_3	0.0143
n_4	0.01686414
n_5	0.01956494
n_6	0.0225225

APPENDIX H
POWER AND TORQUE AT STANDARD CONDITIONS

H.1 Method of correction outlined

SABS 013: Part 1 – 1988 ("Road vehicle internal combustion engines at sea level) [48] explains the manner in which the measured power of a vehicle at specific ambient conditions can be calculated for standard ambient conditions. The standardised power allows comparison of engines tested at different ambient conditions, and gives us a baseline power from which power changes with ambient changes can be predicted.

A correction factor (α_a) for naturally aspirated spark ignition engines is defined in this document as follows:

$$\alpha_a = \left(\frac{99}{P_s}\right)^{1.2}\left(\frac{T_{amb}}{298}\right)^{0.6} \tag{H.1}$$

P_s is the total dry atmospheric pressure measured during the test and can only be used in equation (H.1) if it complies to the following condition:

$$80kPa \le P_s \le 110kPa \tag{H.2}$$

T_{amb} is the ambient temperature of the air to the engine measured during the test and can only be used in equation (H.1) if it complies with the following condition:

$$288K \le T_{amb} \le 308K \tag{H.3}$$

It should also be noted that equation (H.1) is most accurate in the case where:

$$0.93 \le \alpha_a \le 1.07 \tag{H.4}$$

Should the limits stated in equation (H.4) not be met, it is required that the ambient test conditions be stated in the test report, after which the correction factor can then be used to determine the power at standard conditions.

Using the correction factor, the corrected power is calculated through equation (H.5).

$$P_{cor} = \alpha_a P \tag{H.5}$$

The corrected torque is calculated through equation (H.6).

$$P_{cor} = Torque_{cor}\omega_{eng} \tag{H.6}$$

H.2 Correction of data obtained

The data recorded during the testing of the engine on the dynamometer , ambient conditions, correction factor and corrected data is given in table H.1.

Table H.1 – Measured and corrected power and torque data

	Ambient conditions			
	Ambient temperature (T_{amb})		302 K	
	Dry ambient pressure (P_s)		81.2 kPa	
	Correction factor (α_a)		1.279	
	Measured power and torque		**Corrected power and torque**	
Engine speed (rpm)	**Torque – (*Torque*) in Nm**	**Power – (*P*) in kW**	**Torque – ($Torque_{cor}$) in Nm**	**Power – (P_{cor}) in kW**
2000	126	26.39	161.12	33.74
2500	130	34.03	166.23	43.52
3000	137	43.04	175.18	55.04
3500	144	52.78	184.13	67.49
4000	125	52.36	159.84	66.95
4500	158	74.46	202.03	95.21
5000	176	92.15	225.05	117.84
5500	186	107.13	237.84	136.99
6000	188	118.12	240.40	151.05
6500	189	128.65	241.67	164.50
7000	195	142.94	249.35	182.78
7500	190	149.23	242.95	190.82
8000	182	152.47	232.72	194.97
8500	175	155.77	223.77	199.18

NOMENCLATURE

A

A	Total heat transfer area	(m^2)
A_a	Total heat transfer area on the air side of the heat exchanger	(m^2)
A_{au}	Total surface area of unit cell	(m^2)
A_{acs}	Area of air channel cross section	(m^2)
A_{caw}	Nett inlet flow area for water	(m^2)
A_{feu}	External fin surface area of unit cell	(m^2)
A_{front}	Frontal area of heat exchanger	(m^2)
A_{tcs}	Area of water tube cross section	(m^2)
A_{teu}	External tube surface area of unit cell	(m^2)
A_w	Total heat transfer area on the water side of the heat exchanger	(m^2)
a	Constant associated with the Wilson plot method	

C

C_a	Variable defined in equation 1.16	
C_w	Variable defined in equation 2.3	
$C_{\max}$	Maximum flow stream heat capacity rate	(W/°C)
$C_{\min}$	Minimum flow stream heat capacity rate	(W/°C)
C_1	Constant associated with fully developed turbulent flow	
C_2	Constant defined in equation 1.12	
C_3	Constant defined in equation 1.13	
C_4	Constant associated with equation 1.14	
C_5	Constant associated with equation 1.14	
c_{pa}	Specific heat of air	(J/(kg°C))
c_{pw}	Specific heat of water	(J/(kg°C))
c_{pwg}	Tabled specific heat of water, as per Mills [2], just greater than actual specific heat of water	(J/(kg°C))
c_{pws}	Tabled specific heat of water, as per Mills [2], just smaller than actual specific heat of water	(J/(kg°C))

D		
D_{ha}	Hydraulic diameter of air flow passages	(m)
D_{hw}	Hydraulic diameter of water tubes	(m)
d	Constant associated with the Wilson plot method	
F		
F_d	Depth of fin array in flow direction	(m)
F_l	Fin length	(m)
F_p	Fin pitch	(m)
F_t	Fin thickness	(m)
F_w	Water flow rate	(l/s)
f	Constant associated with equation 3.1	
G		
g	Constant associated with equation 3.1	
H		
$\dot{H}_{e,ic}$	Rate of enthalpy loss through the exhaust system due to incomplete combustion	(W)
h_a	Heat transfer coefficient per unit area for air	(W/(m^2°C))
$h_{e,s}$	Exhaust gas enthalpy	(W/(kg/s))
h_w	Heat transfer coefficient per unit area for water	(W/(m^2°C))
J		
j	Constant associated with equation 3.8	
K		
K	Variable as defined in table 1.1	
k_a	Conductivity of air	(W/(m^2°C))
k_w	Conductivity of water	(W/(m^2°C))
L		
L_p	Louver pitch	(m)

M

$\dot{m}_a$	Mass flow rate of air	(kg/s)
$\dot{m}_e$	Mass flow rate of exhaust gasses	(kg/s)
$\dot{m}_f$	Mass flow rate of fuel	(kg/s)
$\dot{m}_w$	Mass flow rate of water	(kg/s)

N

NTU	Number of transfer units	
n	Engine speed	(Rev./min)
n_{gf1}	Transmission ratio including final drive ratio for first gear	
n_{gf2}	Transmission ratio including final drive ratio for second gear	
n_{gf3}	Transmission ratio including final drive ratio for third gear	
n_{gf4}	Transmission ratio including final drive ratio for fourth gear	
n_{gf5}	Transmission ratio including final drive ratio for fifth gear	
n_{gf6}	Transmission ratio including final drive ratio for sixth gear	
n_o	Maximum engine speed	(Rev./min)
n_1	Ratio of V_D/v_{engine} for first gear	
n_2	Ratio of V_D/v_{engine} for second gear	
n_3	Ratio of V_D/v_{engine} for third gear	
n_4	Ratio of V_D/v_{engine} for fourth gear	
n_5	Ratio of V_D/v_{engine} for fifth gear	
n_6	Ratio of V_D/v_{engine} for sixth gear	

P

P	Measured brake power	(W)
P_{amb}	Ambient air pressure	(kPa)
P_{aw}	Wetted air tube perimeter	(m)
P_b	Brake power of an engine	(W)

P_{cor}	Corrected brake power	(W)
P_s	Ambient pressure – dry	(kPa)
P_{tw}	Wetted tube perimeter	(m)
p	Constant associated with equation 4.2	

Q

$\dot{Q}_{cool}$	Heat transfer rate through cooling system	(W)
$\dot{Q}_{dissp}$	Rate of heat dissipation	(W)
$\dot{Q}_F$	Heat transfer rate through cooling system	(W)
$\dot{Q}_{gen}$	Heat generated by engine	(W)
$\dot{Q}_{gen\_std}$	Heat generated by engine at standard conditions	(W)
Q_{LHV}	Lower heating value of fuel	(W s/kg)
$\dot{Q}_{\max}$	Maximum heat dissipated through heat exchanger	(W)
$\dot{Q}_{misc}$	Heat transfer rate through miscellaneous components	(W)
$\dot{Q}_{scap}$	Cooling system spare capacity	(W)

R

R	Gas constant for air	(kJ/(kg K))
R_c	Capacity ratio	
R_{fa}	Fouling thermal resistance based on the surface area for the air side of the exchanger	(K/W)
R_{fw}	Fouling thermal resistance based on the surface area for the water side of the exchanger	(K/W)
R_h	Hydraulic radius	(m)
R_w	Thermal resistance of wall	(K/W)
r	Constant associated with equation 4.2	
r_t	Tube outer radius	(m)

S

S_1	Length of non-louvered inlet and exit regions	(m)
S_2	Redirection length	(m)

s	Constant associated with equation 4.2	
T		
Theta	Louver angle	(°)
$Torque_{cor}$	Corrected brake torque	(Nm)
$T_{a,in}$	Temperature of air prior to heat transfer in heat exchanger	(°C)
T_{amb}	Ambient temperature	(K)
$T_{a,out}$	Temperature of air after heat transfer in heat exchanger	(°C)
T_{wav}	Average water temperature	(°C)
T_{wg}	Tabled water temperature,as per Mills [2], just greater than average water temperature	(°C)
$T_{w,in}$	Temperature of water prior to heat transfer in heat exchanger	(°C)
T_{win_engine}	Temperature of water measure at inlet of engine	(°C)
$T_{w,out}$	Temperature of water after heat transfer in heat exchanger	(°C)
T_{wout_engine}	Temperature of water after engine and oil-to-water heat exchanger	(°C)
T_{ws}	Tabled water temperature,as per Mills [2], just smaller than average water temperature	(°C)
t	Constant associated with equation 4.2	
t_{FE}	Temperature of cooling fluid in engine	(°C)
U		
U	Overall heat transfer coefficient per unit area	(W/(m^2°C))
V		
$\dot{Vol}_w$	Volume flow rate of water	(m^3/s)
V_a	Air speed	(m/s)
V_D	Vehicle speed	(km/h)
v_{akmh}	Cooling air heat exchanger face velocity	(km/h)

v_{engine}	Engine speed	(rpm)

W

w	Constant associated with equation 4.2	

X

x	Constant associated with equation 4.2	
x_{fp}	Fin pitch	(m)
x_{ful}	Fin unit length	(m)
x_{fw}	Fin width of a unit cell	(m)
x_{tp}	Tube pitch	(m)
x_{tt}	Thickness of tube as shown in figure E.1	(m)
x_{tw}	Width of tube as shown in figure E.1	(m)
x_{twt}	Tube wall thickness as shown in figure E.1	(m)

Y

y_a	Variable defined in equation 2.5	
y_w	Variable defined in equation 1.18	

Greek letters

ΔT_f	Inlet temperature difference between the fluids	(°C)
ΔT_w	Temperature difference between the inlet and outlet water temperatures to the heat exchanger	(°C)
α_a	Brake power correction factor	
ε	Heat exchanger effectiveness	
ζ_t	Pressure loss coefficient	
η_{oa}	Overall surface efficiency of total heat transfer area on air side of the extended heat exchanger surface	
η_{ow}	Overall surface efficiency of total heat transfer area on water side of the heat exchanger	
μ	Fluid dynamic viscosity coefficient	(Pa s)
μ_a	Air dynamic viscosity coefficient	(Pa s)
μ_m	Mean fluid dynamic viscosity coefficient for bulk of the fluid	(Pa s)

μ_w	Fluid dynamic viscosity coefficient for fluids attached to the wall of the tube	(Pa s)
μ_{ma}	Mean fluid dynamic viscosity coefficient for bulk of air	(Pa s)
μ_{mw}	Mean fluid dynamic viscosity coefficient for bulk of water	(Pa s)
μ_{wa}	Air fluid dynamic viscosity coefficient for fluids attached to the wall	(Pa s)
μ_{ww}	Water fluid dynamic viscosity coefficient for fluids attached to the wall	(Pa s)
ρ	Fluid density	(kg/m^3)
ρ_a	Air density	(kg/m^3)
ρ_w	Water density	(kg/m^3)
ρ_{wg}	Tabled density as per Mills [2] just greater than the actual water density	(kg/m^3)
ρ_{ws}	Tabled density as per Mills [2] just smaller than the actual water density	(kg/m^3)
ω_{eng}	Rotational speed of engine	(rad/s)

Dimensionless parameters

N_u	Nussult number
Pr	Prandtl number
Pr_a	Prandtl number for air
Pr_w	Prandtl number for water
Re	Reynolds number of fluid flow
Re_a	Reynolds number of air flow
Re_w	Reynolds number of water flow

REFERENCES

[1] Cowell T.A., May 1990, "A general method for the comparison of compact heat transfer surfaces", Journal of Heat Transfer, Vol. 112.

[2] Van den Bulck E., May 1991, "Optimal design of crossflow heat exchangers", Journal of heat transfer, Vol. 113.

[3] London A.L., 1964, "Compact heat exchangers" Mechanical Engineering, ASME, Vol. 86.

[4] London A.L., Furgeson C.K., 1949, "Test results of high performance heat exchanger surfaces used in aircraft intercoolers and their significance for gas-turbine regenerator design", Trans. ASME, Vol. 71

[5] Chang Y, Wang C, 1997, "A generalized heat transfer correlation for louver fin geometry", International journal for heat and mass transfer, Vol 40 no. 3

[6] Mills A.F., 1995, "Basic Heat and Mass Transfer", 1st edition, Richard D. Irwin Inc., Chicago.

[7] Webb R.L., 1982, "Enhancement of Extended Surface Geometries Used in Air Cooled Heat Exchangers", Kakaq, Shah, Bergles, Low Reynolds Number Heat Exchangers, Hemisphere.

[8] Shah R.K., 1983, " Compact Heat Exchanger Surface Selection, Optimisation, and Computer-aided Thermal Design", Kakaq, Shah, Bergles, Low Reynolds Number Heat exchangers, Hemisphere.

[9] Cowell T.A., Heikal M.R., Achaichia A., 1990, "Flow and heat transfer in compact louver fin surfaces", Expl Thermal Fluid Sci. 10.

[10] Sunden B., Svantesson J., "Thermal hydraulic performance of new multilouvered fins", in proceedings of the 9th International Heat transfer conference., Vol 14-HX-16

[11] Wang C., Chi K., Chang, Y., 1998, "An experimental study of heat transfer and friction characteristics of typical louver fin-and-tube heat exchangers", International journal of heat and mass transfer", Vol. 41.

[12] White F.M., 1974, "Viscous fluid flow" 2nd edition, McGraw-Hill Book Company, New York.

[13] Chang Y.J., Wang C.C., Shyu R.J., Hu Y.Z.R., "Performance comparison between automobile flat tube condenser and round tube condenser" 4th ASME/JSME Thermal engineering joint conference. Vol.4 1995

[14] Webb R.L., Jung S.H., "Air-side performance of enhanced brazed aluminium heat exchangers" ASHRAE Transfer 98 Pt 2

[15] Zhang X., Tafti D.K., "Flow efficiency in multi-louvered fins" International Journal of Heat and Mass Transfer, Volume 46, Issue 10, May 2003.

[16] Rohsenow W.M., Hartnett J.P., Ganić E.N., "Handbook of Heat Transfer Applications", Chapter 4 by Shah R.K., Mueller A.C., "Heat Exchangers",2nd edition, McGraw-Hill Book Company, 1989.

[17] Mills A.F., "Basic Heat and Mass Transfer", 1st edition, Richard D. Irwin Inc., Chicago, 1995.

[18] Kays W.M., London A.L., "Compact heat exchangers", 3rd edition, McGraw-Hill, New York, 1984.

[19] Shanoun A., Webb R.L., November 1992, "Predition of Heat Transfer and Friction for Louver Fin Geometry", Journal of Heat Transfer, Vol. 114.

[20] Kajino M., Hiramatso M., 1987, "Research and Development of Automobile Heat Exchangers", Heat Transfer in High Technology and Power Engineering, W.J. Yang and Y. Mori, eds, Hemisphere Publishing Corporation.

[21] Tafti D.K., Zhang X. "Geometry effects on flow transition in multilouvered fins – onset, propagation, and characteristic frequencies" International Journal of Heat and Mass Transfer, Volume 44, Issue 22, November 2001.

[22] Cui J., Tafti D.K., "Computations of flow and heat transfer in a three-dimensional multilouvered fin geometry" International Journal of Heat and Mass Transfer, Volume 45, Issue 25, December 2002.

[23] Wang C., Webb R., Chi K., "Data reduction for air-side performance of fin-and-tube heat exchangers", Experimental thermal and fluid science Vol. 21, 2000.

[24] ESDU 86018, Effectiveness – NTU relationship for the design and performance evaluation of two-stream heat exchangers (1991), Engineering data unit 86018 with amendment A, July 1991, ESDU International publication, London.

[25] Wang C., Lee C., Chang C., Lin S., "Heat transfer and friction correlation for compact louvered fin-and-tube heat exchangers", International journal of heat and mass transfer, Vol. 42, 1999.

[26] Shah R., "Experimental techniques for obtaining design data of compact heat exchanger surfaces", Proceedings of the international conference on compact heat exchangers for the process industries, 1997.

[27] Briggs D.E., Young E.H., " Modified Wilson plot technique for obtaining heat transfer correlations for shell and tube heat exchangers", Chemical engineering symposium, Serial nr. 92, Vol 65, 1969.

[28] Wilson E., "A basis for rational design of heat transfer apparatus", Trans. ASME, Vol 37, 1915.

[29] Shah R.K., Johnson R.S., "Correlations for fully developed turbulent flow through circular and noncircular channels", Trans. AIChE, Vol. 29, 1993. Reprinted in International journal of heat and mass transfer, Vol. 7, 1981.

[30] Shah R., "Assessment of modified Wilson plot techniques for obtaining heat exchanger design data", Heat transfer 1990, Proceedings of the 9th International Heat Transfer Conference, Vol. 5, 1990.

[31] Yang R., Chiang F.P., "An experimental heat transfer study for periodically varying-curvature curved-pipe", International journal of heat and mass transfer, Vol. 45, 2002.

[32] Yang C., Webb R.L., "Condensation of R-12 in small hydraulic diameter extruded aluminum tubes with and without micro-fins", International journal of heat and mass transfer, Vol. 39, 1996.

[33] Farrell P., Wert K., Webb R.L., "Heat transfer and friction characteristics of turbulent radiator tubes", SAE Trans. Vol. 100, 1991.

[34] Chiou J.P., "Optimization study of liquid-to-air heat exchanger in the cooling system of military combat/tactical vehicle", SAE 760851, November 1976.

[35] Costelli A., Gabriele P., Giordanengo D., "Experimental analysis of the air circuit for engine cooling systems", SAE 800033, 1980.

[36] Ninoyu M., Kameyama J., Doi H., Oka H., "Prediction method of cooling system performance", SAE 930146, 1993.

[37] El-Bourini R., March 1993, "Road Measurements of Front End Components' Effect on Vehicle Engine Compartment Air Flow", SAE Technical Paper Series, International Congress and Exposition: Detroit, Michigan, SAE 930145

[38] Bahnsen U., "Airflow management in future design", International journal of vehicle design, Vol 3, 1982.

[39] Emmenthal K.D., "Automobile Aerodynamics", Chapter 9: "Engine cooling system".

[40] Chiou J.P., February 1982, "The Effect of Nonuniform Inlet Air Temperature Distribution on the sizing of the Engine Radiator", SAE Technical Paper Series, International Congress and Exposition: Detroit, Michigan, SAE 820078.

[41] Enomoto Y., Nagano H., "Measurement of wall surface temperature in a combustion chamber in automobile 4-stroke engines", SAE, 1995 Vehicle thermal management systems conference proceedings, May 1995.

[42] Franco A., Martorano L., "Evaluations on the heat transfer in the small two-stroke engines", SAE 980762, 1998.

[43] Chmela F.G., Orthaber G.C., "Rate of heat release prediction for direct injection diesel engines based on purely mixing controlled combustion", SAE 1999-01-0186, 1999.

[44] Franco A., Martorano L., "Methods to evaluate in-cylinder heat transfer and thermal load in the small internal combustion engines", SAE 1999-01-1252.

[45] Heywood J.B., 1988, "Internal Combustion Engine Fundamentals", 1st Edition, McGraw-Hill Book Company, New York.

[46] Costelli A., Gabriele P., Giordanengo D., March 1979, "Experimental analysis of engine cooling systems", SAE Technical Paper Series, International Congress and Exposition: Detroit, Michigan, SAE 790397.

[47] Costelli A., Gabriele P., Giordanengo D., February 1980, "Experimental analysis of the air circuit of engine cooling systems", SAE Technical Paper Series, International Congress and Exposition: Detroit, Michigan, SAE 800033.

[48] SABS 013: Part 1 -1988 standard, "Road vehicle internal combustion engines at sea level".

[49] White F.M., 1979, "Fluid Mechanics" 3rd edition, McGraw-Hill Book Company, New York.